DOI: 10.1002/anie.201207900

Proteasome Inhibitors

# Synthesis and Pharmacology of Proteasome Inhibitors

*Andreas Rentsch, Dirk Landsberg, Tobias Brodmann, Leila Bülow, Anna-Katharina Girbig, and Markus Kalesse**

**Keywords:**
antitumor agents · clinical development · inhibitors · natural products · proteasome

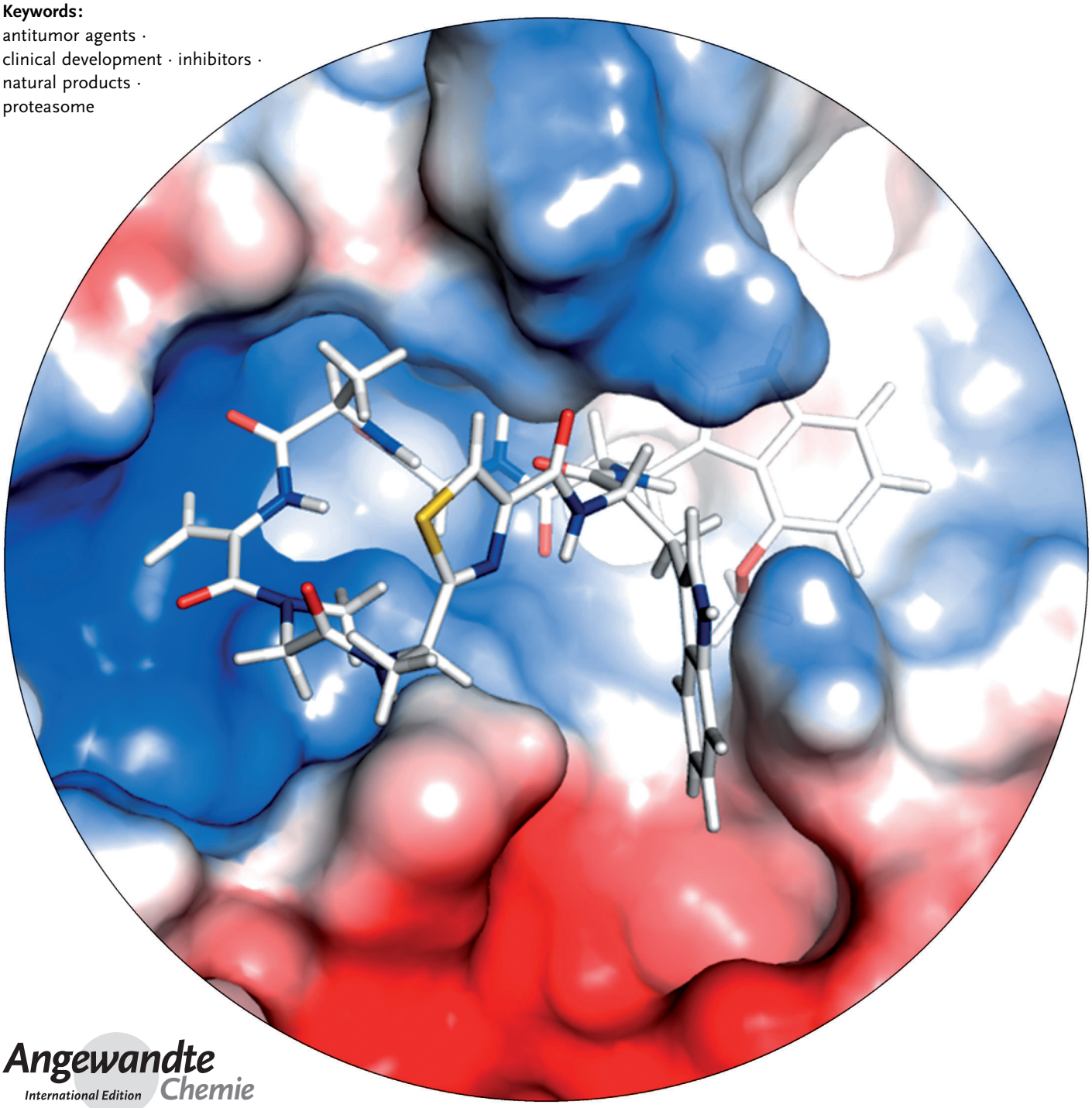



© 2013 Wiley-VCH Verlag GmbH & Co. KGaA, Weinheim

Angewandte International Edition Chemie

*Shortly after the discovery of the proteasome it was proposed that inhibitors could stabilize proteins which ultimately would trigger apoptosis in tumor cells. The essential questions were whether small molecules would be able to inhibit the proteasome without generating prohibitive side effects and how one would derive these compounds. Fortunately, "Mother Nature" has generated a wide variety of natural products that provide distinct selectivities and specificities. The chemical synthesis of these natural products finally provided access to analogues and optimized drugs of which two different classes have been approved for the treatment of malignancies. Despite these achievements, additional lead structures derived from nature are under investigation and will be discussed with regard to their biological potential and chemical challenges.*

**From the Contents**



## 1. Introduction

Owing to the ground-breaking work of Aaron Ciechanover,[1] Avram Hershko, and Irwin Rose on the ubiquitin–proteasome system (UPS)[2] it became evident that protein degradation is a pivotal and highly specific process by which defective proteins are eliminated from the cytosol and endoplasmic reticulum.[3] However, the temporally controlled and highly regulated degradation of key proteins such as cell cycle regulators and transcription factors adds another important aspect to the cellular function of the ubiquitin–proteasome system. Consequently, the body of evidence increased that protein degradation by the ubiquitin–proteasome system controls fundamental processes such as cell cycle regulation,[4] DNA repair,[5] apoptosis,[6] immune and inflammatory responses,[7] as well as hereditary disorders such as cystic fibrosis.[8] Beyond these medical applications, the ubiquitin–proteasome system is one of the most prominent targets to fight malignancies.[9]

The ubiquitin–proteasome system is a nonlysosomal pathway for controlled protein degradation in the cytosol and nucleus of all eukaryotic cells. Its degradation process can be divided into two main steps: The marking of a protein substrate with a polyubiquitin chain and the degradation of the polyubiquitinated substrate by the 26S proteasome.

## 2. The Proteasome–Ubiquitin System

Polyubiquitination, the protein-degradation signal for proteins, is achieved by a series of ligase reactions to attach ubiquitin, a small 76 amino acid containing, highly conserved protein, to the ε-$NH_2$ group of a lysine residue. Recently it was shown that at least four ubiquitins are required to trigger this signal.[10] The commonly accepted mechanism involves subsequent repeated attachment of ubiquitin to the target protein even though the body of evidence increases that other pathways such as attachment of polyubiquitin to the target protein may also occur.[11] During polyubiquitination, ligase E1 activates the C-terminal glycine residue through adenylation which in turn is transformed to a thioester by reaction with a cysteine residue at the active site of E1 (Scheme 1). The subsequent transesterification generates the corresponding

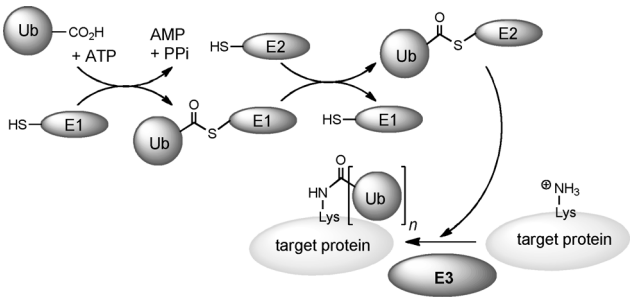


***Scheme 1.*** Mechanism of ubiquitination.

[*] Dr. A. Rentsch, Dr. D. Landsberg, Dr. T. Brodmann, Dr. L. Bülow, Dr. A.-K. Girbig, Prof. Dr. M. Kalesse
Institut für Organische Chemie
and Centre of Biomolecular Drug Research (BMWZ)
Leibniz Universität Hannover
Schneiderberg 1B, 30167 Hannover (Germany)
and
Helmholtz Centre for Infection Research (HZI)
Inhoffenstrasse 7, Braunschweig (Germany)
E-mail: Markus.Kalesse@oci.uni-hannover.de


© 2013 Wiley-VCH Verlag GmbH & Co. KGaA, Weinheim

E2–ubiquitin adduct. Finally, E3 recruits the target protein and transfers the activated ubiquitin from E2 to the substrate, predominantly at the ε-$NH_2$ group of a lysine residue through an isopeptidic linkage. This attachment of ubiquitin is repeated by attaching ubiquitin to the lysine residues (in general Lys48) of the preceding ubiquitin moiety until the required degree of ubiquitination is achieved.

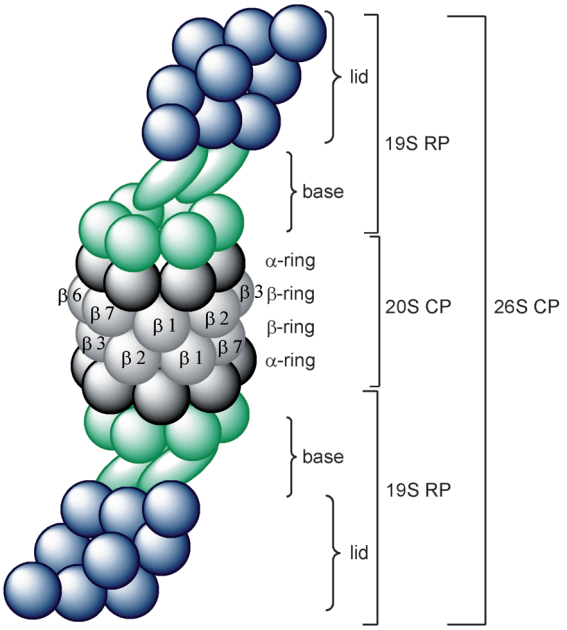


***Figure 1.*** Constitution of the 26S proteasome.

### *2.1 Structure and Biological Function*

The 26S proteasome is the responsible protein complex for the ubiquitin–proteasome degradation.[12] The core structure of the proteasome is a cylindrical 20S particle (Figure 1) that is composed of four stacked rings (α- and β-rings), each consisting of seven different subunits, which host the catalytic centers (Figure 2). Both ends of the 20S segment are capped with 19S regulatory units containing polyubiquitin-binding sites for recognition and isopeptidase activities. Six different

*Markus Kalesse obtained his Dr. rer. nat. in 1991 at the Leibniz University Hannover under the direction of Prof. D. Schinzer. After postdoctoral studies with Prof. S. D. Burke and Prof. L. L. Kiessling at the University Wisconsin/Madison, he completed his habilitation at the University Hannover (1997) under the mentorship of Prof. E. Winterfeldt. He was appointed C3 Professor at the Freie Universität Berlin and was promoted in 2003 to C4 Professor at the University Hannover in 2003. In 2005 he was also appointed Director at the Helmholtz Centre for Infection Research (HZI) in Braunschweig. Prof. Kalesse was awarded the Novartis Lectureship in 2004/2005. His research interests include natural products synthesis, asymmetric catalysis, and medicinal chemistry.*

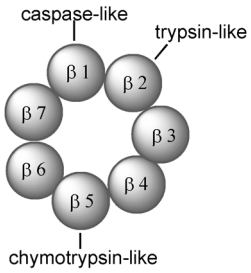


***Figure 2.*** Positioning of active subunits within the β-ring.

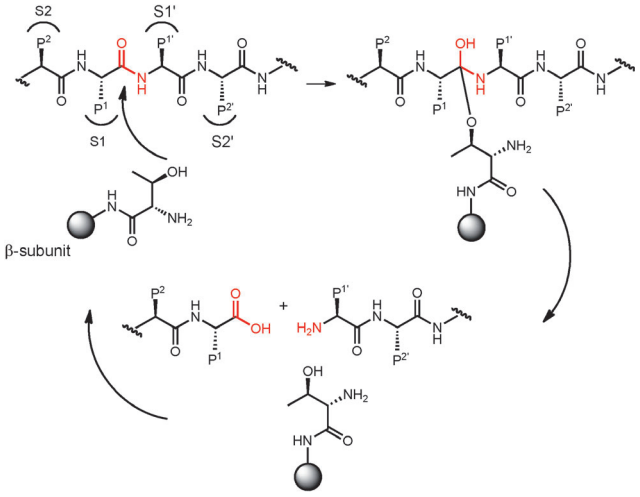


***Figure 3.*** Catalytic mechanism of the proteasome's β-subunits.

ATPases unfold the protein structure and open a channel in the α-ring of the 20S proteasome. Subsequently, denatured and ubiquitinated proteins can access the catalytic pocket for degradation. These active sites include chymotrypsin-like, trypsin-like, and caspase-like proteolytic activities.[13] Before degradation, the polyubiquitin chain is removed at the 19S unit. The catalytic degradation of proteins uses in all three catalytic subunits the hydroxy group of an *N*-terminal threonine as the nucleophile (Figure 3). A more detailed picture of the function of the proteasome as well as of the mode of action of its inhibitors is provided in excellent Reviews put forward by Groll,[14] Kloetzel,[15] Crews,[16] Kisselev,[17] Moroder,[18] and Tsukamoto.[19]

### *2.2. The Proteasome as a Target for Anticancer Drugs*

As the proteasome plays a pivotal role in almost every cellular process (at least indirect), it was questioned if such a pivotal activity would ever become a therapeutic target. However, most cellular processes are highly regulated and minor changes in protein homeostasis result in significant biological changes. Consequently, proteasome inhibition resulting in 40–60% remaining activity would not necessarily unfold unspecific cytotoxic effects but would lead to significant changes in certain protein levels, which results in a specific cellular response. This was demonstrated by the proteasome inhibitor argyrin, which decreases the proteaso-


© 2013 Wiley-VCH Verlag GmbH & Co. KGaA, Weinheim

mal activity without significant cytotoxic side effects in mice but results in significantly higher levels of the cyclin kinase inhibitor p27kip1 and thus induces selectively apoptosis in cancer cells.[20] Additionally, cancer cells generally have higher levels of proteasome activity than nontransformed cells, presumably because of their increased metabolism and higher levels of oxidative stress, cytokines, and growth factors. Therefore, they are more sensitive to proteasome inhibition.[21]

## 3. Natural Products as Proteasome Inhibitors

This Review will cover the synthesis of the most prominent proteasome inhibitors, of which natural products or analogues and derivatives thereof play a pivotal role. Because of the increasing number of newly discovered inhibitors, it will not be possible to cover every synthetic contribution to all proteasome inhibitors. However, in order to provide a comprehensive overview of the different structural motifs found amongst proteasome inhibitors, the families of compounds, for which syntheses are covered, will be presented.[22]

Oxygenated steroids (Figure 4) represent a class of proteasome inhibitors of which the withaferins (**1**, **2**)[23] are the most prominent antitumor compounds. They were

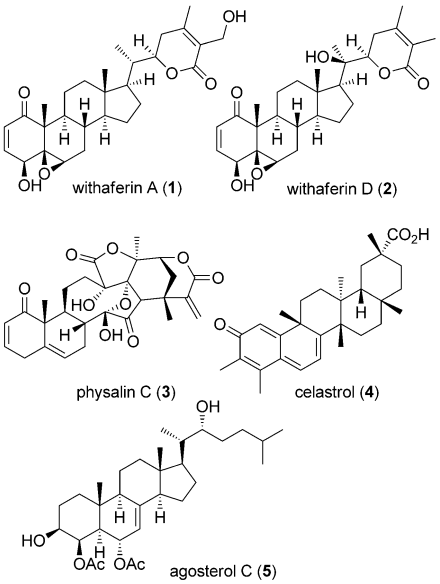


***Figure 4.*** Steroid-derived natural products as proteasome inhibitors.

isolated from the medicinal plant known as "Indian Winter Cherry" or "Indian Ginseng" (*Withania somnifera*), which was used historically in Indian ayurvedic medicine. Their antitumor activity is connected, at least in part, to the inhibition of the chymotrypsin-like activity by nucleophilic attack of the threonine hydroxy group at both Michael acceptor positions.[24] Often mentioned in the context of proteasome inhibition are physalins (**3**),[25] which were identified during a broad screen of 30000 compounds to inhibit the ubiquitin–proteasome pathway, even though they do not inhibit the activity of the purified proteasome. Celastrol (**4**)[26] was isolated as the active compound from the root of the "Thunder of God Vine" (*Tripterygium wilfordii*) used in traditional Chinese medicine (TCM). It inhibits the chymotrypsin-like activity of the purified 20S proteasome at micromolar concentrations ($IC_{50} = 2.5\ \mu mol\,L^{-1}$) and leads to the accumulation of natural proteasome substrates such as IκB-A, Bax, and p27.

The agosterols[27] constitute a group of seven polyhydroxylated sterols, isolated from the marine sponge *Acanthodendrilla* sp. They have been reported to reverse multidrug resistance in tumors. The most active agosterol C (**5**) inhibits the chymotrypsin-like subunit with an $IC_{50}$ value of $10\ \mu g\,mL^{-1}$.

Epigallocatechin gallate (EGCG, **6**), an active ingredient of green tea, is one of the prominent phenolic proteasome inhibitors.[28] Broussonin B (**7**), 7-hydroxy-3-(4-hydroxybenzyl)chroman (**8**), and *cis*-hinokiresinol (**9**) were isolated from extracts of *Anemarrhenae rhizoma* and showed moderate inhibition of the chymotrypsin-like subunit (Figure 5).[29]

Chen et al. examined the plant flavonoids apigenin (**10**), chrysin, and luteolin for their ability to inhibit the proteasome. They found that all three compounds inhibited the chymotrypsin-like and trypsin-like activities specifically.[30] The soy isoflavone genistein (**11**) inhibits the chymotrypsin-like activity which was accompanied by apoptosis of solid tumor cells.[31,32] Dreiseitl et al., who investigated the inhib-

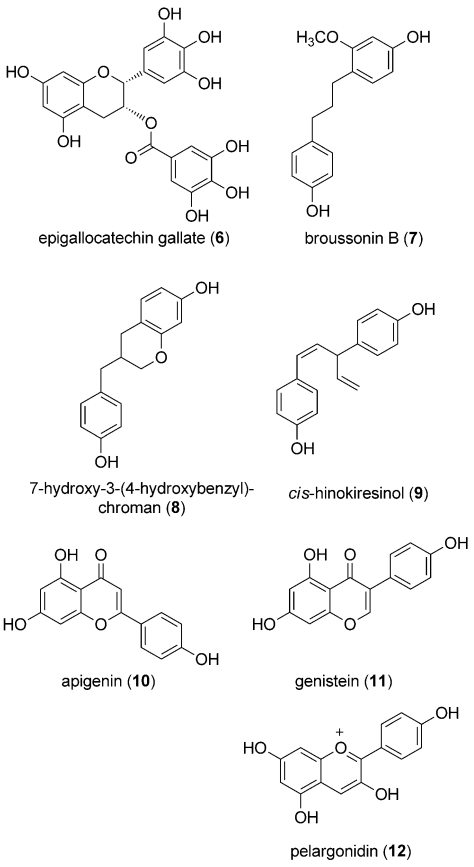


***Figure 5.*** Flavonoids and chromane-type proteasome inhibitors.


© 2013 Wiley-VCH Verlag GmbH & Co. KGaA, Weinheim

ition of the proteasome by anthocyanins and anthocyanidins, found that in particular pelargonidin (**12**) is a specific inhibitor of the CT-L activity with an $IC_{50}$ value of 7.8 μM (Figure 5).[33]

The fungal metabolite gliotoxin (**13**) unfolds its proteasomal activity through its disulfide bridge.[34] This was evidenced by the fact that the noncompetitive inhibition can be reversed by the addition of dithiothreitol. The anthracycline drug aclacinomycin (**14**) (aclarubicin)[35] was the first described nonpeptidic proteasome inhibitor exhibiting discrete specificity for the chymotrypsin-like activity.[36] It was further recognized that both the aglycon and the carbohydrate are essential for its biological activity. The marine natural product petrosaspongiolide M (**15**) inhibits the caspase and chymotrypsin-like activities with $IC_{50}$ values of 0.85 μM and 0.64 μM, respectively.[37] On the other hand, it induces the trypsin-like activity, a phenomenon previously observed for other caspase-like inhibitors.[38] Ajoene (**16**), the major sulfur-containing compound from garlic, inhibits specifically the trypsin-like activity of the proteasome.[39] The epoxyphomalins A (**18**) and B (**17**) were isolated from the marine fungus *Phoma* sp. and unfolded cytotoxic activity at nanomolar concentrations. However, the two compounds differ in their selectivity towards the proteasomal subunits. Epoxyphomalin A (**18**) leads to equally reduced activities, whereas epoxyphomalin B (**17**) preferentially inhibits the chymotrypsin-like subunit.[40] Purrello and Milardi used tetracationic porphyrins such as **19** and their metal derivatives to inhibit the proteasome. The most active derivative (structure shown) exhibits inhibitory activities towards all three subunits comparable to the activity of lactacystin (**160**) (Figure 6).[41] The aaptamines (**20–22**) (Figure 6) were isolated from the marine sponge *Aaptos suberitoides* and inhibit the chymotrypsin-like and caspase-like activities with $IC_{50}$ values of 1.6–4.6 $\mu g\,mL^{-1}$.[42] The cerpegins (**23**, **24**) were isolated from the plant *Ceropegia juncea* and were investigated as potential drugs with anti-inflammatory, anticancer, analgesic, and anti-ulcer properties. The group of Bouvier-Durand et al. studied the proteasome-inhibitory activity of these pyridine alkaloids and identified one derivative that showed selective inhibition of the caspase-like activity at low concentrations (5.2 μM).[43] More recently, Groll and co-workers reported on hydroxyureas as potent inhibitors of the proteasome.[44] During a screening program set up in collaboration with Bayer CropScience for the identification of β5-specific inhibitors, they discovered urea derivative **25** with an $IC_{50}$ value in the upper μM range (no inhibition for the C- and T-like activity). Their crystal structure analysis revealed the specific, noncovalent binding motifs and they consequently initiated the syntheses of optimized variants. During the course of these optimizations, **26** was obtained as a strong and selective inhibitor of the β5 unit and exhibited a novel binding mode.

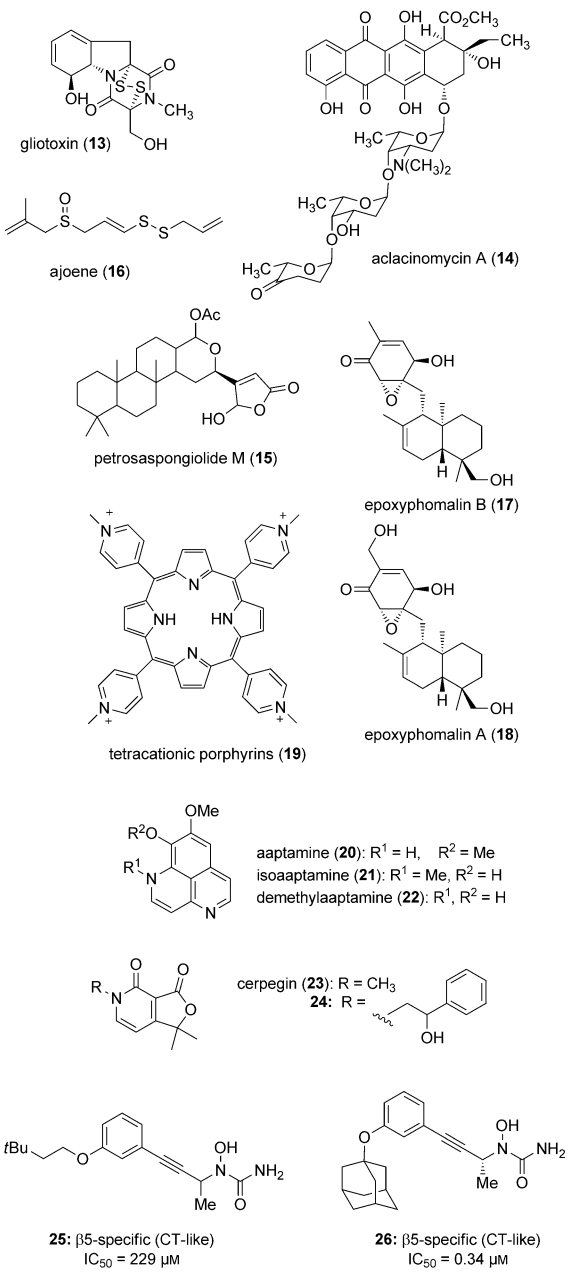


***Figure 6.*** Miscellaneous proteasome inhibitors.

## 4. Proteasome Inhibitors in Clinical Evaluation

Bortezomib (**27**) has become a pivotal drug for the treatment of multiple myeloma (MM) and has consequently initiated a variety of different developments to introduce new proteasome inhibitors to the clinic. Besides bortezomib, four additional drugs representing three distinct classes of compounds are currently in clinical trials. We will briefly discuss their current clinical status and describe potential advantages over existing therapies before we outline their syntheses in detail.[45,46]

Bortezomib (**27**), originally coded as PS-341 and marketed as the first-in-class proteasome inhibitor Velcade by Millennium Pharmaceuticals,[47] was first approved for the U.S. market in 2003 and one year later for the European market.[48] It was approved for the treatment of multiple myeloma and mantle cell lymphoma. More recently it became apparent that combinations with established anticancer agents, in particular lenalidomide and dexamethasone (**34**,


© 2013 Wiley-VCH Verlag GmbH & Co. KGaA, Weinheim

**35**), provide enhanced benefits for frontline patients.[49] Surprisingly, the interaction with epigallocatechin gallate (EGCG, **6**), the previously mentioned proteasomal inhibitor which was expected to have synergistic effects, reduces the activity of bortezomib (**27**).[50] An orally bioavailable, second-generation proteasome inhibitor that features a boronic acid moiety as a reactive group was further developed by Millennium. MLN-9708 (**28**) is an inhibitor of the chymotrypsin-like site with $IC_{50}$ and $K_i$ values of 3.4 nM and 0.93 nM, respectively.[51] In contrast to bortezomib (**27**), which is administered subcutaneously or intravenously, the citrate boronic ester MLN-9708 (**28**) is administered orally as a prodrug. Upon hydrolysis the parent compound MLN-2238 (**30**) is liberated. Currently, 11 clinical trials are in progress. More recently (June 2012), Takeda Pharmaceutical Company has initiated an international phase III clinical trial evaluating MLN-9708 (**28**) in patients with relapsed and/or refractory multiple myeloma. Other trials investigate the combination with established drugs such as dexamethasone (**35**), lenalidomide (**34**), melphalan, and prednisone and combinations thereof (Figure 7).

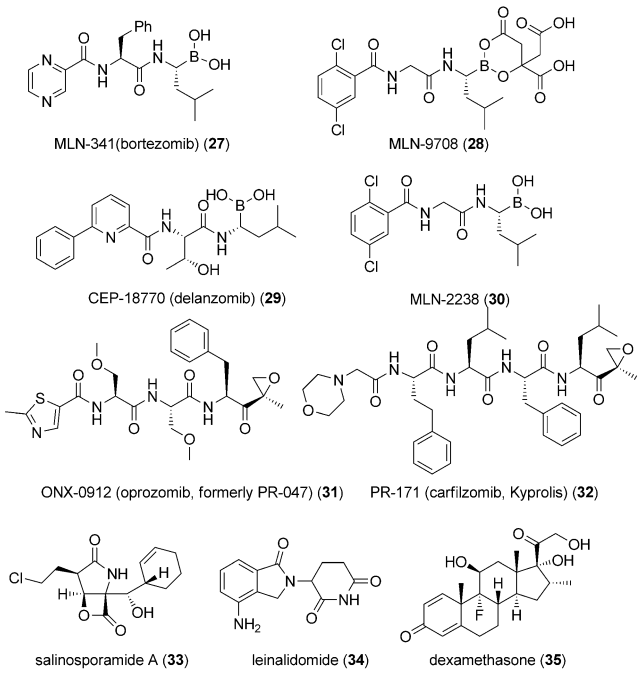


***Figure 7.*** Proteasome inhibitors in clinical use or trial and compounds used in combination therapy (**34**, **35**).

Another peptide boronate-based inhibitor, delanzomib (CEP-18770, **29**), is a potent chymotrypsin-like inhibitor with an $IC_{50}$ of 3.8 nM.[52] CEP-18770 (**29**) was introduced to phase I clinical trials by Ethical Oncology Science. In two ongoing phase I/II studies Cephalon is investigating the overall response rate of CEP-18770 and its maximum tolerated dose as well as safety and efficacy in combination with lenalidomide and dexamethasone in patients with relapsed and/or refractory multiple myeloma.

Carfilzomib (PR-171, **32**),[53] an analogue of epoxomicin (**47**), was developed and clinical trials initiated by Proteolix Inc. which continued under Onyx Pharmaceuticals. Overall, 15 clinical trials are active or recruiting participants, one trial has been completed, and the status of one trial is not known. Carfilzomib (**32**) unfolds its biological activity as an irreversible and specific inhibitor of the chymotrypsin-like activity of the proteasome. At the same time its cytotoxicity against RPMI 8226 cells (multiple myeloma) is higher than that of bortezomib (PR-171 = 71 nmol $L^{-1}$ vs. bortezomib = 303 nmol $L^{-1}$). In January 2011 the U.S. Food and Drug Administration (FDA) granted carfilzomib (**32**) the fast-track status which was changed to standard review designation in December 2011. On June 20, 2012 Onyx Pharmaceuticals announced that the FDA's Oncologic Drugs Advisory Committee (ODAC) had concluded that Kyprolis (proposed brand name for carfilzomib) has a favorable benefit–risk assessment for the use in patients with relapsed and/or refractory multiple myeloma who have received at least two prior lines of therapy (proteasome inhibitor and immunomodulatory agent). Consequently, on July 20, 2012 the FDA approved Kyprolis for people previously treated with bortezomib (**27**) and an immunomodulatory compound such as thalidomide (Figure 7).

Since carfilzomib (**32**) and bortezomib (**27**) are available as intravenous formulations and in order to overcome toxicity and the development of resistance, Onyx initiated clinical studies on the second-generation, orally available epoxyketone proteasome inhibitor ONX-0912 (oprozomib, formerly PR-047, **31**).[54] In two clinical studies solid as well as hematological tumors are addressed.

The natural product salinosporamide A (**33**) inhibits the chymotrypsin-like subunit with an $IC_{50}$ value of 1.3 nM. The compound marizomib (**33**) (NPI-0052, salinosporamide) developed by Nereus is currently undergoing phase I clinical trials for participants with advanced malignancies (Figure 7).

## 5. Peptide Aldehydes

Prior to the discovery of the proteasome–ubiquitin pathway, peptide aldehydes were already well established as inhibitors of serine and cysteine proteases. Consequently, it was not surprising that peptide aldehydes were also described as the first known proteasome inhibitors.[55] Today the most widely employed peptide aldehyde based inhibitors of the proteasome are MG-132 (**36**) (Cbz-Leu-Leu-CHO), MG-115 (**37**) (Cbz-Leu-Leu-Nva-CHO), ALLN (**38**) (*N*-acetyl-Leu-Leu-Nle-CHO), and PSI (**37**) (Figure 8). More recently Kloetzel and Schmidt reported on BSc-2118 (**40**)[56] a peptide aldehyde which unfolds tumor-selective toxicity with a mean therapeutic index of 26.5 (MTT toxicity assays) (Figure 8).

Another group of peptide aldehydes, the fellutamides A and B (**42**, **43**),[57] were isolated from the marine fish associated fungus *Penicillium fellutanum*. Fellutamide B (**43**) inhibits the chymotrypsin-like activity with an $IC_{50}$ of 9.4 nM which is more efficient than that of MG-132 (**34**) (40 nM) and is in the range of epoxomicin (**47**) (5.7 nM). In the structural analysis of fellutamide B (**43**) bound to the yeast 20S

 © 2013 Wiley-VCH Verlag GmbH & Co. KGaA, Weinheim 

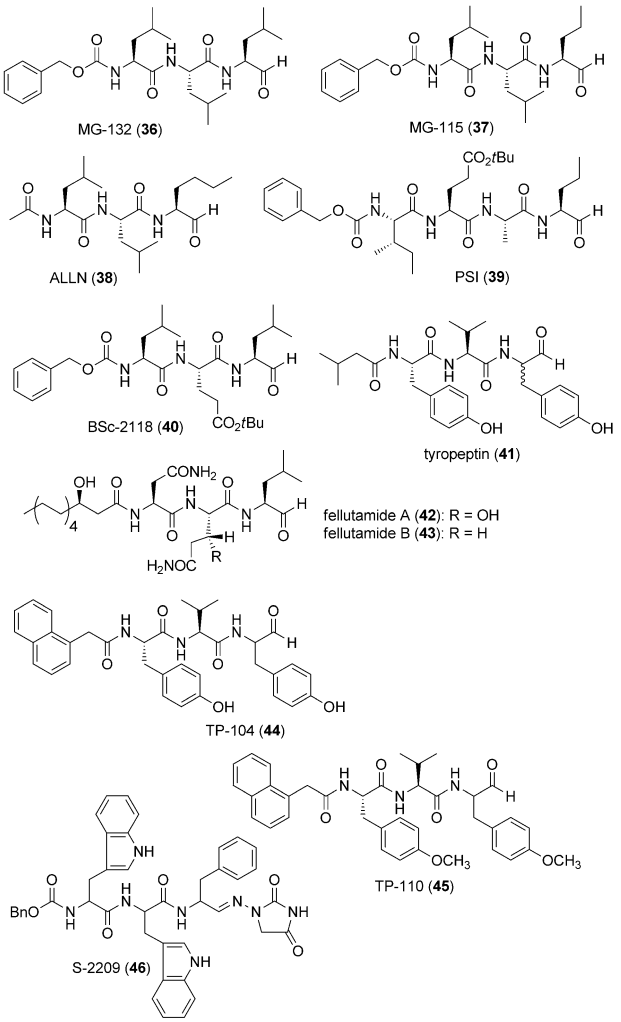


***Figure 8.*** Peptide aldehydes as proteasome inhibitors.

proteasome, it was found that the hydroxy group of the hemiacetal forms a hydrogen bond to the Thr1 N-terminus and thus differs from the established oxyanion pocket stabilization. More recently, tyropeptin A (**41**) was isolated form *Kitasatospora* sp. and shown to inhibit the chymotrypsin and the trypsin-like activity with $IC_{50}$ values of 0.1 and 1.5 $\mu g\,mL^{-1}$, respectively.[58] In an effort to provide larger quantities of optimized compounds Momose et al. synthesized the tyropeptin A analogues[59] TP-104 (**44**) and TP-110 (**45**)[60] (Figure 8). TP-104 (**44**) inhibits the proteasome 20-fold more potently than the parent compound, while TP-110 (**45**) specifically inhibits only the chymotrypsin-like activity. The peptide-semicarbazone S-2209 (**46**) represents a further variation of the peptide aldehyde class of proteasome inhibitors. It induces cell arrest in multiple myeloma cells and inhibits the chymotrypsin-like activity of the proteasome with an $IC_{50}$ value of approximately 220 nM.[61]

All peptide aldehydes exhibit sterically demanding hydrophobic residues at the P1 position and consequently display preferential inhibition of the chymotrypsin-like activity. Their inhibitory effects result from the reversible formation of a hemiacetal (Scheme 2).

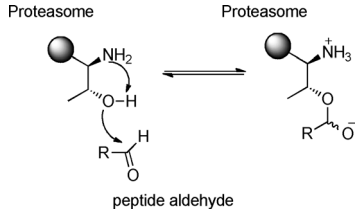


***Scheme 2.*** Proposed mechanism of proteasome inhibition by peptide aldehydes.

An X-ray analysis of ALLN (**38**) bound to the corresponding threonine confirmed the formation of such an intermediate.[62] Additionally, ketoaldehydes that represent a link between simple aldehydes and epoxyketones (e.g. epoxomicin, **47**) selectively inhibit the proteasome (Figure 9).[63]

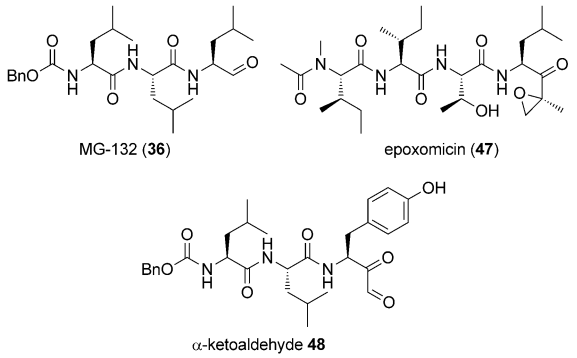


***Figure 9.*** α-Ketoaldehydes as links between peptide aldehydes and epoxy ketones.

### *5.1. Synthesis of Peptide Aldehydes*

Peptide aldehyde derived proteasome inhibitors usually consist of three amino acids. A frequently applied synthesis takes advantage of solution-phase peptide-coupling strategies using reagents such as phosphonium salts (e.g. BOP, PyBrop) or carbodiimides (e.g. DCC, EDC) while formation of the active ester succeeds in the presence of HOBt or PNP.[64] A more challenging task, however, is the synthesis of the enantiomerically pure aldehyde moiety. As α-chiral aldehydes tend to epimerize, mild reaction and workup conditions are essential. Two general strategies have been established.[65] The first strategy resembles classical solid-phase peptide synthesis and the C-terminal carboxylic acid or aldehyde function is replaced by an olefin. Once the first residue is attached to the solid support, the more conventional coupling strategy is followed. Finally, the aldehyde functionality is released after peptide elongation by oxidative processes. An example of this concept is the protection of the aldehyde in the form of an olefin moiety introduced by a Wittig reaction (Scheme 3).[66] After solid-phase peptide coupling, regeneration of the aldehyde is accomplished by ozonolysis and workup using thiourea.


© 2013 Wiley-VCH Verlag GmbH & Co. KGaA, Weinheim

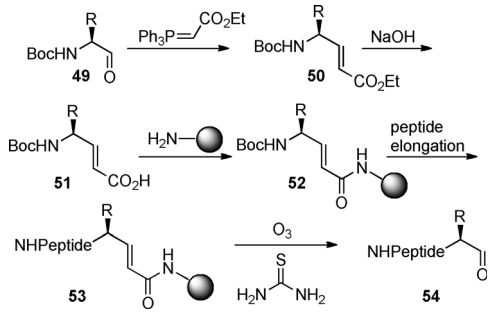

***Scheme 3.*** Solid-phase synthesis of peptide aldehydes.

An alternative protecting-group strategy was used by Crews et al. In their synthesis of fellutamides and analogues they used leucinal-loaded beads, which allowed mild cleavage off the resin to avoid epimerization of the aldehyde (Scheme 4).[67]

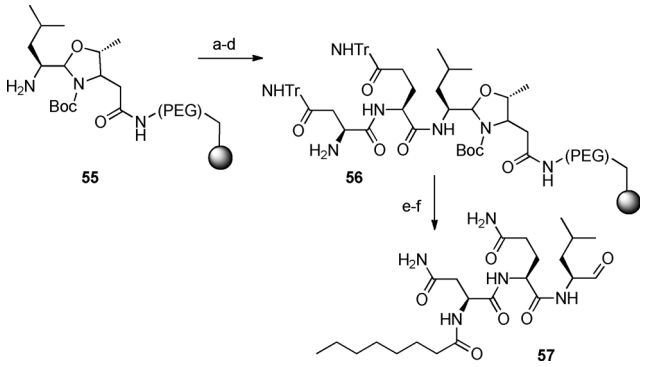

***Scheme 4.*** Aminal protecting-group strategy. Reagents and conditions: a) Fmoc-Gln(Trt)-OH, HBTU, HOBt; b) piperidine, DMF; c) Fmoc-Asn-(Trt)-OH, HBTU, HOBt; d) piperidine, DMF; e) octanoic acid, HBTU, HOBt; f) TFA/MeCN/$H_2O$ = 0.1:40:60. For the definitions of abbreviations please refer to the list provided at the end of the Review.

The second strategy involves peptide coupling beginning from the N-terminus and introduces the aldehyde residue as a final step. Therefore, peptide amides (e.g. Weinreb amides), esters, and alcohols are often utilized precursors that establish the aldehyde through oxidation-state manipulations. Following the latter idea, MG-132 could be synthesized starting with peptide coupling of Cbz-protected leucine (**58**), leucine methyl ester, and finally leucinol (Scheme 5).[68,69] IBX oxidation followed by neutral aqueous workup provided aldehyde **36** without epimerization.

The advantage of peptide aldehydes is certainly their established and at least partially automated synthetic access. This allows for the rapid optimization of lead compounds. An instructive example is the transformation of the calpain inhibitor ALLN (**38**) into a selective proteasome inhibitor (MG-132, **36**). ALLN is one of the early proteasome inhibitors with a preference for calpain. Its inhibition is characterized by a modest dissociation constant ($K_i$ = 140 nM).[70] The selective inhibitor MG-132 in turn inhibits the proteasome with a $K_i$ value of only 4 nM[71] and requires

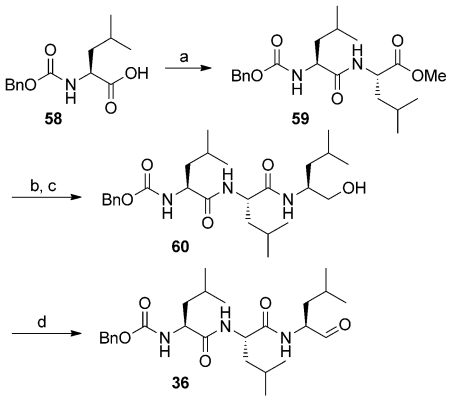

***Scheme 5.*** Synthesis of MG-132 (**36**). Reagents and conditions: a) HCl·Leu-OMe, PyBOP, $iPr_2NEt$, $CH_2Cl_2$, RT, 68%; b) NaOH, $H_2O$/MeOH/dioxane, RT, 92%; c) leucinol, EDAC, HOBt, $Et_3N$, RT, 90%; d) IBX, DMSO, RT, quant.

concentrations more than ten times higher to inhibit calpain.[72] Thanks to their low-cost synthesis, good proteasome inhibition, and reversible binding mode, peptide aldehydes have become widespread research tools for biochemical processes. However, their disadvantages as therapeutic agents are their rather high dissociation rates, low metabolic stability, and poor bioavailability. Also, side reactions with other proteases remain a constant challenge. Consequently, new pharmacophores such as boronic acids were developed.

## 6. Boronic Acids

The replacement of the aldehyde functionality by a boronic acid moiety improves the properties of proteasome inhibitors. This effect is demonstrated by comparing MG-132 (**36**) with its analogue MG-262 (Z-Leu-Leu-Leu-B$(OH)_2$, **61**) (Figure 10). MG-262 (**61**) is more than 100-fold more active in

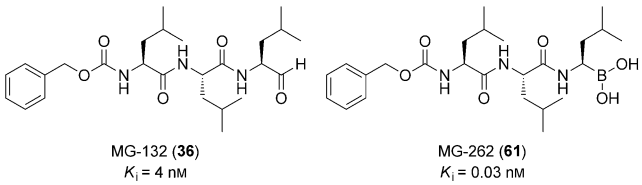


***Figure 10.*** Comparison of MG-132 (**36**) and MG-262 (**61**).

inhibiting the proteasomal degradation of peptides. In general, boronic acids inhibit the 20S proteasome through the formation of a noncovalent, tetrahedral intermediate. It is characterized by the interaction of the p orbital of the Lewis acidic boron atom with an electron pair of the proteasome's N-terminal threonine hydroxy group (Figure 11). Additionally, a salt bridge between the boronic acid and the amine stabilizes this interaction.[73]

Boronic acids are considered to be reversible inhibitors, but unlike peptide aldehydes, their peptide complexes can persist for hours. Additionally, these inhibitors do not

 © 2013 Wiley-VCH Verlag GmbH & Co. KGaA, Weinheim 

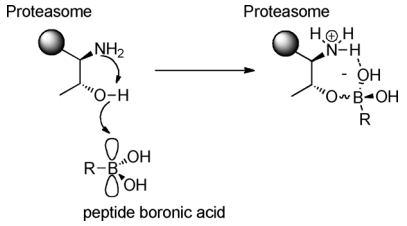


***Figure 11.*** Proposed mechanism of inhibition.

interfere with cysteine proteases owing to only weak thiol–boron interactions. Furthermore, as thoroughly investigated for bortezomib (**27**), the affinity towards the 20S proteasome exceeds that towards most serine proteases significantly. These differences are finally responsible for the success of bortezomib (**27**) as an antitumor drug.

### *6.1. Synthesis of Bortezomib*

During the development of MG-262 (**61**) Adams et al. discovered that excellent activities were obtained with dipeptide derivatives. These studies resulted in the preparation of today's probably best characterized dipeptide boronic acid, bortezomib (**27**) (Velcade). The synthesis takes advantage of rearrangements established by Matteson[74,75] and Shenvi[76] and culminated in Millenium's large-scale production.[77] Recently Janca and Dobrovolny[78] described a slightly modified procedure that provides increased yields and purities (Scheme 6).

Starting with commercially available isobutylboronic acid (**62**), chirality was introduced by esterification with (+)-pinanediol and a subsequent one-carbon homologation by means of a Matteson rearrangement (Scheme 7) led to α-chloroboronic ester **64** in good yields and diastereoselectivity. $S_N2$-

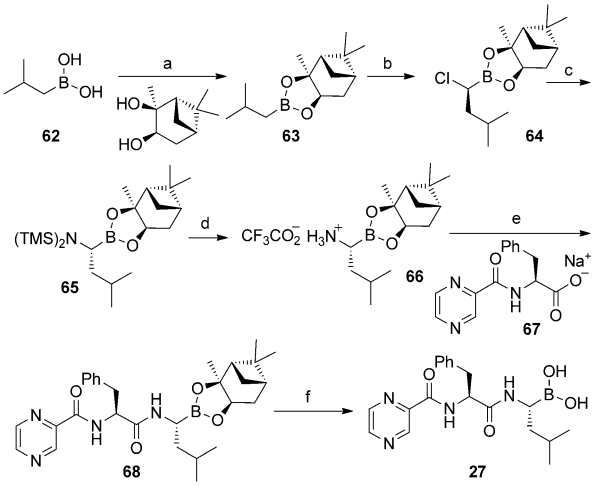


***Scheme 6.*** Synthesis of bortezomib. Reagents and conditions: a) $Et_2O$, RT, 97%; b) 1. $CH_2Cl_2$, THF, LDA, −65 °C; 2. $ZnCl_2$, THF, −65 °C→10 °C, 97%; c) LiHMDS, methylcyclohexane, THF, −20 °C→RT, 92%; d) TFA, $iPr_2O$, methylcyclohexane, −10 °C, 68%; e) TBTU, $CH_2Cl_2$, 0 °C→RT, 87%; f) $iBuB(OH)_2$, HCl (aq), MeOH/hexane, RT, 80%.

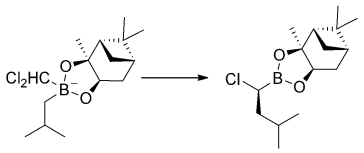

***Scheme 7.*** Matteson homologation.

type displacement of chloride by lithium hexamethyldisilazide yielded **65**, which was hydrolyzed and transformed to the corresponding ammonium salt. The obtained compound **66** is a widely employed intermediate that can be used to synthesize various peptide boronic acids through peptide coupling and subsequent release of the boronic acid functionality.[79] In the case of bortezomib, peptide coupling with **67** was accomplished by treatment with TBTU. Carboxylate **67** in turn was obtained after the coupling of Boc-L-phenylalanine methyl ester with pyrazinoic acid using TBTU and $iPr_2NEt$ followed by ester hydrolysis. The reaction of **68** with isobutyl boronic acid finally liberated the **27**.

An alternative access to bortezomib (**27**) has been put forward by Ellman and co-workers (Scheme 8).[80] They reported on the asymmetric copper-catalyzed diborylation

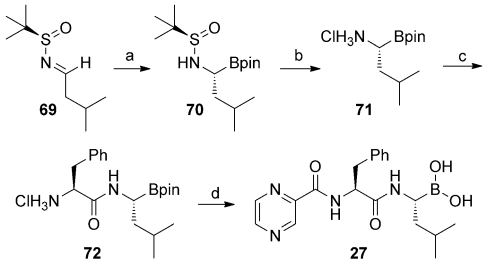


***Scheme 8.*** Ellman synthesis of bortezomib. Reagents and conditions: a) $B_2pin_2$, (Icy)CuO*t*Bu (cat.), benzene, RT, 74%; b) HCl/dioxane, MeOH, dioxane, RT, 93%; c) 1. L-Boc-Phe-OH, TBTU, $iPr_2NEt$, $CH_2Cl_2$, 0 °C; 2. HCl/dioxane, $CH_2Cl_2$, 0 °C→RT; d) 1. pyrazinoic acid, TBTU, $iPr_2NEt$, 0 °C→RT; 2. $iBuB(OH)_2$, HCl (aq), MeOH/pentane, RT; 41% over 4 steps.

of sulfinimine **69** as the key step to establish the chiral α-amino boronic acid moiety. The sulfinyl auxiliary applied is known for its ability to activate C–N double bonds and, if enantiopure, to induce stereocontrol.[81] Addition of $B_2pin_2$ to **69** in the presence of (Icy)CuO*t*Bu follows the pathway displayed in Scheme 8 and provides chiral **71**. From here, established protocols are used to complete the synthesis of bortezomib.

## *7. Epoxyketones*

The epoxyketones represent an important class of proteasome inhibitors. All members contain a peptide consisting of two to four amino acids, one of which is often either threonine or serine, and a C-terminal epoxyketone. As we will point out in Section 7.1, the epoxide configuration is pivotal

 © 2013 Wiley-VCH Verlag GmbH & Co. KGaA, Weinheim 

to the activity of the epoxyketones and consequently conserved throughout all members of this family.[82] The microbial metabolite epoxomicin (**47**) was isolated from the actinomycete strain Q996-17. It shows high in vivo antitumor activity against solid B16 melanoma tumors. Other members of this family include the antitumor agent eponemycin (**73**) and epopromycins A (**74**) and B (**76**), which were identified based on their ability to inhibit plant cell wall synthesis.[83] Gerwick and co-workers recently reported on the carmamycins (**77**, **78**),[84] two epoxyketone proteasome inhibitors isolated from a marine cyanobacterium containing a methionine sulfoxide and a methionine sulfone moiety, respectively (Figure 12).

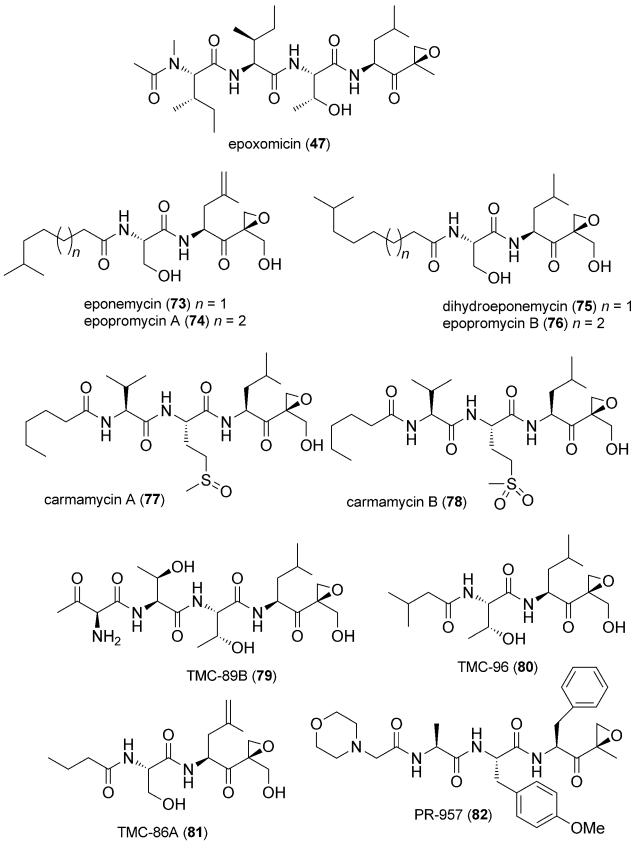


***Figure 12.*** The epoxyketone family of proteasome inhibitors.

The epoxyketones TMC-96 (**80**) and TMC-86A (**81**) were isolated from *Streptomyces* TC 1084 and *Saccharothrix* sp. TC 1094, respectively. They inhibit the chymotrypsin-like and caspase-like activity with $IC_{50}$ values in the low μM range (1.1–31 μM). Recently, Groll and Groettrup used the epoxyketone inhibitor PR-957 (**82**) (ONX 0914) to compare the specificity of the constitutive and the immunoproteasome. Crystal structures of both proteasomes were analyzed in the presence and absence of PR-957 (**82**). These analyses indicated that the S1 pocket of the β5c subunit underwent conformational changes but the S1 pocket of the β5i subunit did not; this finding provides a rational for the observed selectivity towards the immunoproteasome.[85,86] An excellent analysis of proteasome inhibitors' specificity towards different proteasomes is provided by Groll and Huber.[15a]

### *7.1. Epoxomicin*

#### *7.1.1. Epoxomicin's Mode of Action—Formation of a Morpholine Adduct*

The α,β-epoxyketone peptide epoxomicin (**47**) irreversibly inhibits the catalytic activity of the 20S proteasome. More importantly, it does not inhibit several nonproteasomal proteases that are targeted by other proteasome inhibitors. Epoxomicin (**47**) reacts primarily with the chymotrypsin-like site, while the less potent epoxyketone eponemycin (**73**) and its synthetic analogue dihydroeponemycin (**75**) react with the caspase-like and chymotrypsin-like sites at similar rates.[87]

The crystal structure of the yeast *S. cerevisiae* 20S proteasome complexed with epoxomicin (**47**) revealed that the specificity of epoxy pharmacophore is derived from the formation of a morpholine adduct between the terminal threonine and the α,β-epoxyketone.[88]

Two possible pathways were considered for the first step in this reaction. One involves water as a general acid–base catalyst positioned to bridge the Thr1-$O^{\gamma}$ and Thr1-$N^{z}$ atoms. This would lead to activation of the Thr1-$O^{\gamma}$ group and concomitant attack at the carbonyl group of epoxomicin (**47**).[89] Recently, Zhan et al.[90] reported a quantum mechanical calculation that provided evidence that the most favorable reaction pathway for the construction of the morpholine intermediate involves five steps and does not require the assistance of water. According to their results, the first step is a proton transfer from Thr1-$O^{\gamma}$ directly to Thr1-$N^{z}$ to increase the nucleophilicity of the threonine hydroxy group. This zwitterion then attacks the carbonyl group of epoxomicin (**47**) and the resulting negative charge is then neutralized by protonation from Thr1-$N^{z}$. They point out, in contrast to previous perceptions, that Thr1-$O^{\gamma}$ is directly activated by Thr1-$N^{z}$ and water is not involved (Scheme 9). Next Thr1-$N^{z}$ opens the epoxide by means of an intramolecular cyclization with inversion of configuration at the C2 position. The formation of a hydrogen bond between Thr1-$N^{z}$ and the epoxide oxygen activates the epoxide. In addition, Ser129 of the catalytic proteasome subunit is positioned near Thr1-$N^{z}$ and may contribute to nucleophilic activation of Thr1-$N^{z}$. The resulting formation of the morpholine adduct is a six *exo*-tet ring closure, which is favored according to Baldwin's rules, in contrast to the possible seven *endo*-tet ring closure which would result from attack at the less hindered site (Scheme 9).

The major significance of the formation of the morpholine adduct is that it provides the structural basis for epoxomicin's specificity for the inhibition of the proteasome. Other proteases such as cysteine or serine proteases, which are common targets for a variety of other proteasome inhibitors (e.g. peptide aldehydes, vinyl sulfones, boronic acids), do not contain a terminal amino nucleophilic residue as part of their active sites. Consequently, epoxomicin (**47**) would not be able to generate such morpholine adducts. Furthermore, it is noteworthy that changing the epoxide's configuration substantially decreases epoxomicin's activity.


© 2013 Wiley-VCH Verlag GmbH & Co. KGaA, Weinheim

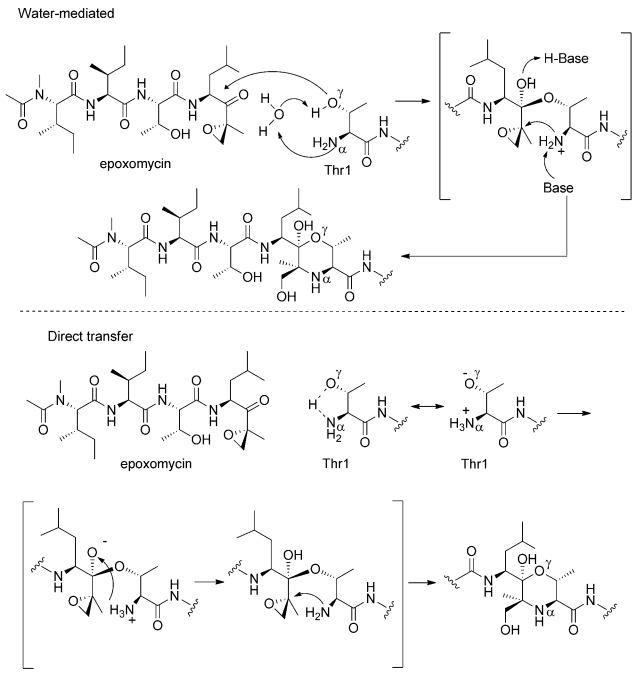


***Scheme 9.*** Formation of the morpholine adduct.

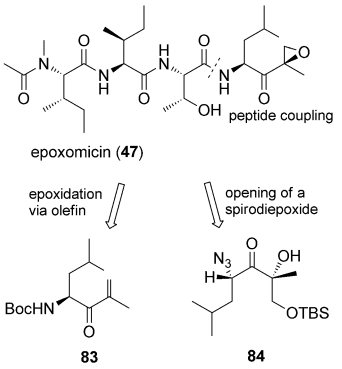


***Scheme 10.*** Retrosynthesis of epoxomicin (**47**).

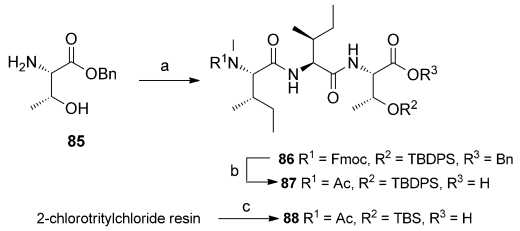


***Scheme 11.*** Synthesis of the western hemisphere of epoxomicin. Reagents and conditions: a) 1. Fmoc-Ile-OH, HBTU, HOBt, *i*$Pr_2$EtN, $CH_2Cl_2$, RT, 23 h, 79%; 2. TBDPSCl, imidazole, THF, RT, 48 h, 64%; 3. piperidine, DMF, RT, 20 min; 4. Fmoc-Melle-OH, HBTU, HOBt, *i*$Pr_2$EtN, $CH_2Cl_2$, RT, 18 h, 99%; b) 1. Piperidine, DMF, RT, 20 min; 2. $Ac_2O$, *i*$Pr_2$EtN, $CH_2Cl_2$, RT, 3.5 h, 99%; 3. 10% Pd/C, $H_2$, MeOH, RT, 1.5 h, 88%; c) 1. Fmoc solid-phase peptide synthesis; 2. acetic acid/trifluoroethanol/$CH_2Cl_2$, 1:1:3, RT, 2 h, 55% based on initial resin capacity.

### *7.2. Total Syntheses of Epoxomicin*

To date two total syntheses of epoxomicin (**47**) have been reported. The first synthesis of racemic epoxomicin by Crews[87b] in 1999 was followed by an enantioselective synthesis in 2004 by the Williams group.[89]

Both total syntheses disconnect epoxomicin (**47**) between the epoxide-containing segment and the peptidic portion. Crews' synthesis takes advantage of established peptide chemistry, generating the epoxide by oxidation of the corresponding olefin. In contrast, the key step of the enantioselective pathway proceeds through the opening of a spirodiepoxide (Scheme 10).

#### *7.2.1. First Total Synthesis of Epoxomicin*

The first total synthesis of epoxomicin (**47**) by Crews et al. is based on the related α,β-epoxyketone-containing natural product eponemycin (**73**) and its derivative dihydroeponemycin (**75**). It relies on the preparation of a stereochemically defined α,β-epoxyleucine fragment which is coupled to the protected *N*-isooctanoylserine fragment to yield the complete backbone of the linear peptides. A similar convergent approach is then applied to the total synthesis of epoxomicin (**47**) (Scheme 11).

The synthesis of the left-hand fragment starts with the coupling of Fmoc-isoleucine to threonine benzyl ester (**85**) with HBTU and HOBt. The threonine hydroxy group of the resulting dipeptide is protected with TBDPSCl. Removal of the Fmoc group followed by coupling with Fmoc-*N*-methyl-isoleucine (HBTU/HOBt) provides the protected left-hand fragment **86**. Removal of the Fmoc group, subsequent acetylation, and finally catalytic hydrogenolysis establishes the left-hand fragment **87**. In addition, the TBS-protected left-hand fragment **88** can also be prepared on solid phase by treatment of commercially available 2-chlorotritylchloride resin with Fmoc-Thr(*O*-TBS)-OH and diisopropylethylamine in dichloromethane followed by standard solid-phase peptide synthesis (Scheme 11).

The synthesis of the right-hand fragment is initiated by the addition of propen-2-yl lithium to Weinreb amide **89** which results in the formation of α,β-unsaturated ketone **83**. Epoxidation with alkaline hydrogen peroxide furnishes a mixture of epoxides **90** and **91** (1.7:1), which are separated by column chromatography and used to generate epoxomicin (**47**) and its epoxide epimer (Scheme 12).

In 2007, researchers at Proteolix Inc. filed a patent on a similar approach for the synthesis of epoxyketones. Their strategy used the Luche reduction and subsequent vanadium-mediated epoxidation for the stereoselective construction of the epoxy alcohol intermediates. Subsequent reoxidation and removal of the Cbz protecting group liberated the corresponding epoxyketone building block, which was used for the assembly of proteasome inhibitors based on established peptide-coupling strategies (Scheme 13).

The final transformations of the Crews synthesis include the removal of the Boc group with TFA and the coupling of

 © 2013 Wiley-VCH Verlag GmbH & Co. KGaA, Weinheim 

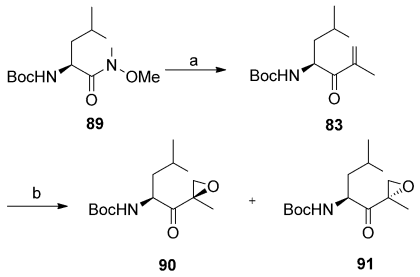


***Scheme 12.*** Synthesis of the epoxyketone subunit. Reagents and conditions: a) 2-bromopropene, *t*BuLi, $Et_2O$, −78 °C, 2.5 h, 92%; b) $H_2O_2$, benzonitrile, $iPr_2EtN$, MeOH, 0→4 °C, 43 h, 76%, **90**/**91** = 1.7:1.

the two fragments using HATU and HOAt to provide TBDPS-protected epoxomicin. In the last step the silyl protecting group was removed with TBAF to complete the synthesis of epoxomicin (**47**) (Scheme 14).

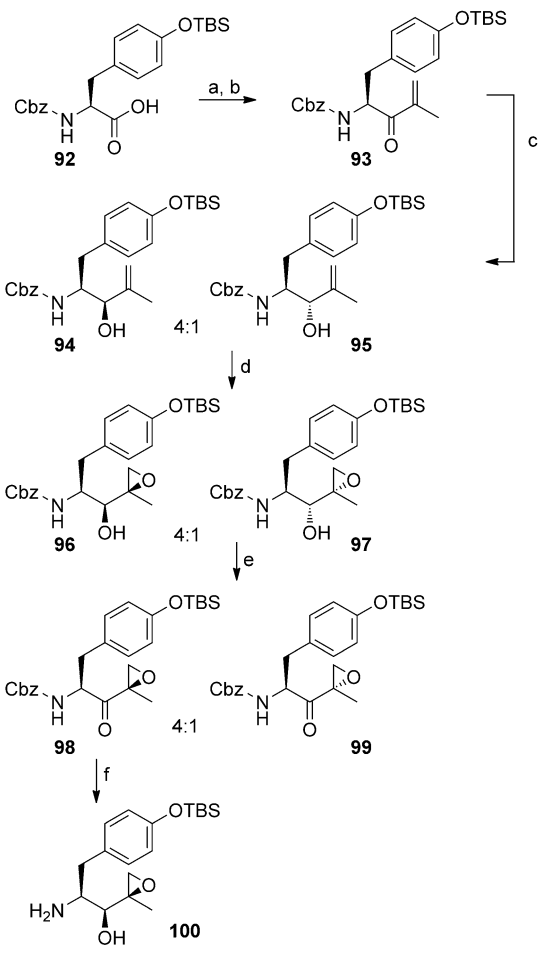


***Scheme 13.*** The Proteolix route towards the epoxyketone subunit. Reagents and conditions: a) Isobutyl chloroformate, $iPr_2NEt$, NMM, $Me(MeO)NH_2Cl$, 0 °C; b) isopropenyl magnesium bromide, THF, −5 °C, 3 h; c) $CeCl_3 \cdot H_2O$, $NaBH_4$, MeOH/THF, 0 °C, 1 h; d) [VO(acac)$_2$], *t*BuOOH, $CH_2Cl_2$, 0 °C, 2 h, e) Dess–Martin periodinane, $CH_2Cl_2$, 0 °C→RT, overnight; f) Pd/C, $H_2$ (1 atm), 2 h, $CH_2Cl_2$, TFA.

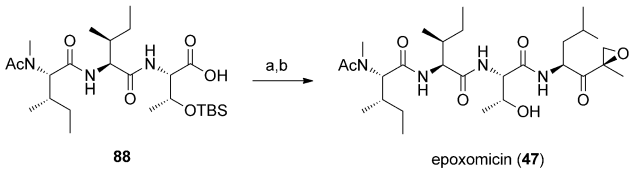


***Scheme 14.*** Synthesis of epoximicin. Reagents and conditions: a) TFA, **90**, HATU, HOAt, $iPr_2EtN$, $CH_2Cl_2$, RT, 18 h, 48%; b) TBAF, THF, RT, 1 h, 96%.

### *7.2.2.* ***Spirodiepoxides in the Total Synthesis of Epoxomicin***

Substrate-directed and reagent-controlled asymmetric epoxidations of alkenes are common strategies for introducing functional groups, whereas the analogous oxidation/nucleophilic opening remains underexploited in synthesis.

Spirodiepoxides provide direct access to highly functionalized and enantiomerically enriched ketones and ketone derivatives. In their total synthesis of epoxomicin (**47**) Williams et al.[91] use spirodiepoxides obtained by oxidation of enantiomerically pure allenes, which in turn were derived from aldehydes, alkynes, and organometallic precursors. Oxidation of the allene, first at the less hindered face of the more substituted π-bond, gave the spirodiepoxide (**102**) as the major isomer (Scheme 15).The azide attacks the spirodiepoxide preferentially at the least hindered epoxide instead of direct attack at the mesylate. The resulting hemiacetal establishes the ketone and oxirane formation results when the mesylate is displaced. Since both the generated epoxyketone (**103**) and its amine derivative were unstable, Williams et al. continued the synthesis with the stable intermediate **108** and established the desired epoxide at the end of their synthesis.

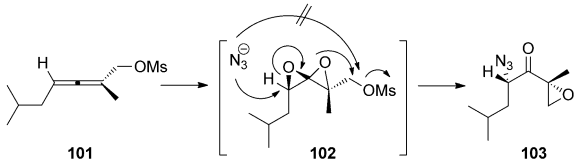


***Scheme 15.*** Mechanism of spirodiepoxide opening.

In the synthetic direction, the hydroxy group of alkyne **105** was converted into the corresponding mesylate and this was subsequently transformed to allene **106**. Treatment of **106** with DMDO followed by exposure to azide produced **107** through the corresponding diepoxide intermediate (> 95% *ee*, d.r. = 3:1). Liberation of the amine establishes **108**, the starting material for the following coupling reactions (Scheme 16).

The synthesis continued with the coupling of **110** to methyl isoleucinate, followed by Boc removal with TFA and subsequent acetylation. Saponification, coupling to threonine (**109**), and hydrogenolysis gave **111**, which was coupled to **97** and provided **112** in 86% yield. The epoxide was synthesized in the endgame of the synthesis, which started with the exposure of **112** to TBAF, cleaving the silyl ether protecting

 © 2013 Wiley-VCH Verlag GmbH & Co. KGaA, Weinheim 

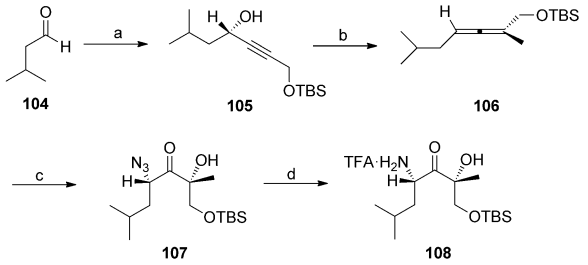


***Scheme 16.*** The spirodiepoxide route. Reagents and conditions: a) (−)-*N*-methylephedrine, $Zn(OTf)_2$, $Et_3N$, toluene, RT, 2 h, $TBSOCH_2CCH$ then **104**, 14 h, 93%, >95% *ee*; b) 1. MsCl, $Et_3N$, $CH_2Cl_2$, −65→23 °C, 2 h; 2. MeMgBr, CuBr, LiBr, THF/MTB ether, −65→23 °C, 2 h, 91%; c) 1. DMDO, −40→23 °C, 1.5 h; 2. $Bu_4NN_3$, $CHCl_3$, −20→23 °C, 1 h, 73% (3:1 d.r.); d) 1. Pd/C, $H_2$, $(Boc)_2O$,·$K_2CO_3$, EtOAc, RT, 12 h, 91%; 2. TFA, 0 °C, 13 min.

group. The resultant primary alcohol was converted to the epoxide via its mesylate. Finally, the *tert*-butyl ether was removed to produce epoxomicin (**47**) (Scheme 17).

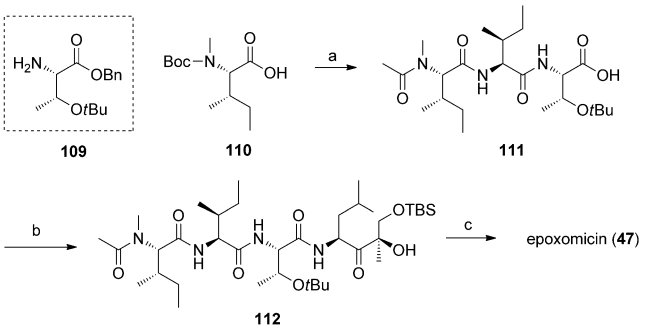


***Scheme 17.*** The Williams synthesis of epoxomicin. Reagents and conditions: a) 1. HCl·Ile-OMe, DCC, HOBt, $Et_3N$, DMF, 0→23 °C, 12 h, 93%; 2. 25% TFA–$CH_2Cl_2$, 10→23 °C, 40 min; 3. $Et_3N$, $Ac_2O$, DMAP, $CH_2Cl_2$, 0→23 °C, 3 h, 95%; 4. 5% NaOH, MeOH-$H_2O$, RT, 2 h, 99%; 5. **109**, DCC, HOBt, $CH_2Cl_2$-DMF, RT, 3 h, 92%; 6. 10% Pd/C, $H_2$; MeOH, RT, 2 h, 100%; b) **108**, $iPr_2EtN$, DCC, HOBt, $CH_2Cl_2$-DMF, RT, 4 h, 86%; c) 1. TBAF, THF, 0→23 °C, 1 h, 89%; 2. MsCl, $iPr_2NEt$, $CH_2Cl_2$, −40→23 °C, 1 h; 3. $K_2CO_3$, THF–$H_2O$, RT, 3 h, 93%; 4. TFA, 0→23 °C, 20 min, 88%.

## 8. Cyclic Peptides

Different cyclic peptides were identified as potent proteasomal inhibitors. The four closely related phepropeptins (**113**–**116**)[92] were isolated from *Streptomyces* sp. and exhibit $IC_{50}$ values between 7.8–21.0 $\mu g\,mL^{-1}$ (Figure 13). They consist of six hydrophobic amino acids with *S* and *R* configuration. Unlike the amino acids in the argyrins, these are not modified by additional transformations and consequently they are more readily available.

Thiostrepton (**117**) belongs to the large family of thiopeptide antibiotics produced by ribosomal peptide biosynthesis.[93] Besides its action as a translation inhibitor and in particular since it showed antiplasmodial activity, which is relevant in the context of antimalarial activity,[94] it also acts as a proteasome inhibitor (Figure 14). Thiostrepton only inhibits

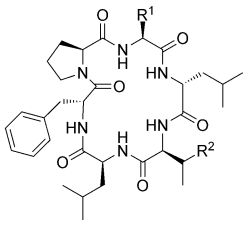

phepropeptin A (**113**): $R^1$ = *i*Pr, $R^2$ = $CH_3$
phepropeptin B (**114**): $R^1$ = Ph, $R^2$ = $CH_3$
phepropeptin C (**115**): $R^1$ = *i*Pr, $R^2$ = $C_2H_5$
phepropeptin D (**116**): $R^1$ = Ph, $R^2$ = $C_2H_5$

***Figure 13.*** The phepropeptins.

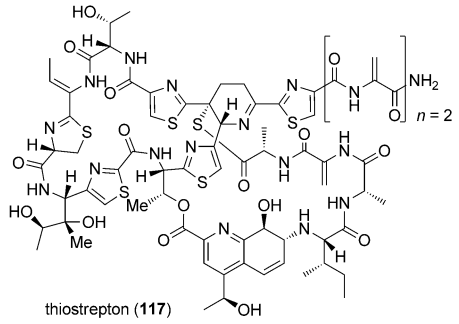


***Figure 14.*** Thiostrepton (**117**).

the caspase- and chymotrypsin-like activities with $IC_{50}$ values in the low μM to nM range. Remarkably, some derivatives were shown to be more active than the parent compound.[95]

### 8.1. Argyrins—A Novel Class of Proteasome Inhibitors

In 2002, Höfle et al. isolated a group of cyclic peptides, argyrins A–H, from the culture broth of strains of the myxobacterium *Archangium gephyra* (Figure 15). These compounds consist of eight amino acids and were shown to be antibiotics against *Pseudomonas* sp., and to inhibit the growth of mammalian cell cultures.

### 8.2. Synthesis of Argyrin B by the Ley Group

Motivated by reports on the immunosuppressive activity of the argyrins and the fact that argyrin B was found to be a potent inhibitor of T-cell independent antibody formation, Ley and co-workers initiated a program for the synthesis of the argyrins. In 2002, this research group reported on the first total synthesis of argyrin B.[96] Subsequent biological evaluations performed at Novartis revealed its immunosuppressive properties and potential as a drug candidate in the field of transplantation. Furthermore, the argyrins display their activity at remarkably low toxicity.

In its retrosynthetic analysis argyrin B (**119**) is disconnected to give thiazole **126** and the two tripeptides **127** and **128** (Scheme 18). The most challenging amino acid in their

 © 2013 Wiley-VCH Verlag GmbH & Co. KGaA, Weinheim 

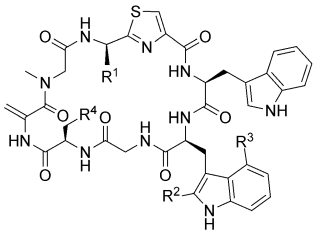

| | $R^1$ | $R^2$ | $R^3$ | $R^4$ |
|---|---|---|---|---|
| argyrin A (**118**) | $CH_3$ | H | $OCH_3$ | H |
| argyrin B (**119**) | $CH_3$ | H | $OCH_3$ | $CH_3$ |
| argyrin C (**120**) | $CH_3$ | $CH_3$ | $OCH_3$ | H |
| argyrin D (**121**) | $CH_3$ | $CH_3$ | $OCH_3$ | $CH_3$ |
| argyrin E (**122**) | $CH_3$ | H | H | H |
| argyrin F (**123**) | $CH_2OH$ | H | $OCH_3$ | H |
| argyrin G (**124**) | $CH_2OH$ | H | $OCH_3$ | $CH_3$ |
| argyrin H (**125**) | H | H | $OCH_3$ | H |

***Figure 15.*** Natural argyrins A–H.

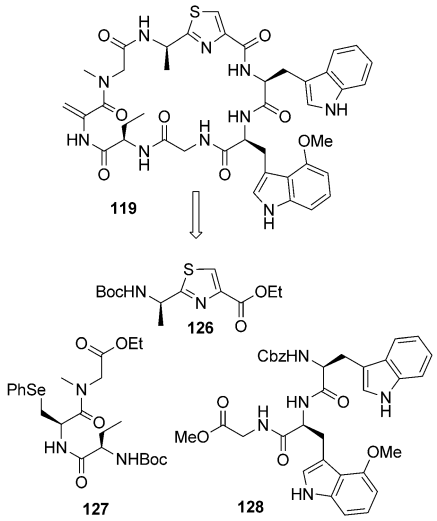

***Scheme 18.*** Ley's retrosynthetic analysis of argyrin B (**119**).

synthesis was the 4-methoxytryptophan building block. Ley and co-workers used an enzymatic kinetic resolution to construct this unusual amino acid. For the preparation of the thiazole moiety **126** *N*-Boc-D-alanine (**129**) was converted into thioamide **130** by amidation and reaction with Belleau's reagent. The thiazole fragment **126** was then established by reaction with ethyl bromopyruvate followed by treatment with trifluoroacetic anhydride and 2,6-lutidine (Scheme 19).

In Ley's synthesis the *exo*-methylene group was established at the end of their synthesis through the elimination of selenium oxide. They constructed the required precursor by introducing the phenylselenyl group through an $S_N2$ displacement at β-lactone **132**, which in turn was generated from **131** by a Mitsunobu reaction (Scheme 20).

For the preparation of the unusual 4-methoxy-L-tryptophan amino acid (**139**) Ley et al. chose immobilized penicillin G acylase for the kinetic resolution of **138** to **139** (Scheme 21).

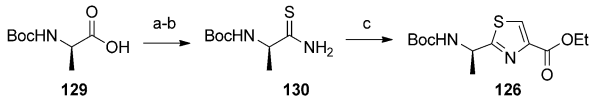

***Scheme 19.*** Synthesis of fragment **126**. Reagents and conditions: a) EDC, HOBt, $NH_3$, $CH_2Cl_2$, 0 °C; b) Belleau's reagent, THF, 0 °C, (quantitative, 2 steps); c) 1. $BrCH_2COCO_2Et$, $KHCO_3$, DME; 2. TFAA, 2,6-lutidine, DME, −15 °C.

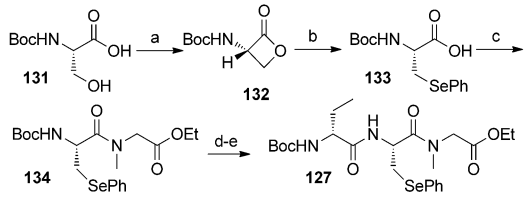

***Scheme 20.*** Synthesis of fragment **127**. Reagents and conditions: a) DEAD, $PPh_3$, THF, −78 °C→RT; b) PhSe-SePh, $NaBH(OMe)_3$, EtOH then **132**, RT, 41 %, 2 steps; c) HCl-Sar-OEt, PyBroP, *i*$Pr_2NEt$, $CH_2Cl_2$, RT, 80 %; d) TFA/$CH_2Cl_2$, RT, e) Boc-D-Abu, EDC, HOBt, *i*$Pr_2NEt$, $CH_2Cl_2$, RT, 71 %, 2 steps.

The assembly of the three major building blocks started with the condensation of **141** and **142**. Saponification of **143** liberated the acid required for the subsequent condensation with fragment **127**. Liberation of both termini and cyclization using TBTU and HOBt established cyclic **145**, which was oxidized; finally, *syn* elimination of selenium oxide completed the first total synthesis of argyrin B (Scheme 22).

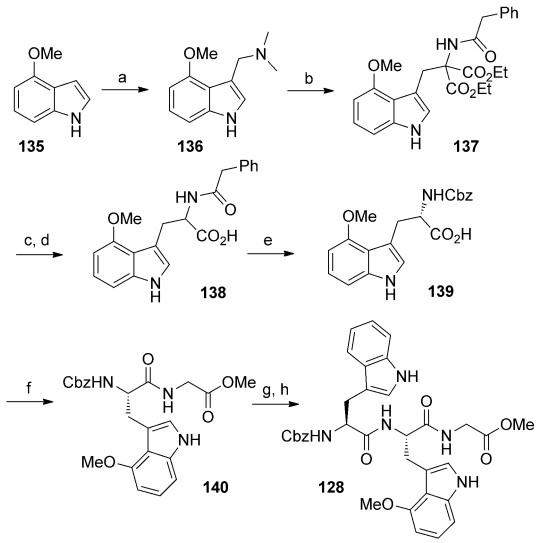

***Scheme 21.*** Synthesis of fragment **128**. Reagents and conditions: a) $CH_2NMe_2^+I^-$, $CH_3CN$, RT, 99 %; b) $(EtO_2C)_2CHNHCOCH_2Ph$, NaOEt, then **136** and $MeSO_4Me$; EtOH, RT, 82 %; c) NaOH, MeOH/dioxane, 50 °C; d) 1. dioxane, 100 °C; 2. NaOH, MeOH/$H_2O$, RT; e) 1. penicillin G acylase immobilized, MeOH/$H_2O$ RT; 2. CbzCl, $NaHCO_3$, THF/$H_2O$, RT, 44 %, 2 steps; f) Gly-OMe, EDC, HOBt, *i*$Pr_2NEt$, $CH_2Cl_2$, RT, 94 %; g) $H_2$, Pd/C, MeOH/aqueous HCl, RT; h) Cbz-L-Trp, EDC, HOBt, *i*$Pr_2NEt$, $CH_2Cl_2$, RT, 81 %, 2 steps.

 © 2013 Wiley-VCH Verlag GmbH & Co. KGaA, Weinheim 

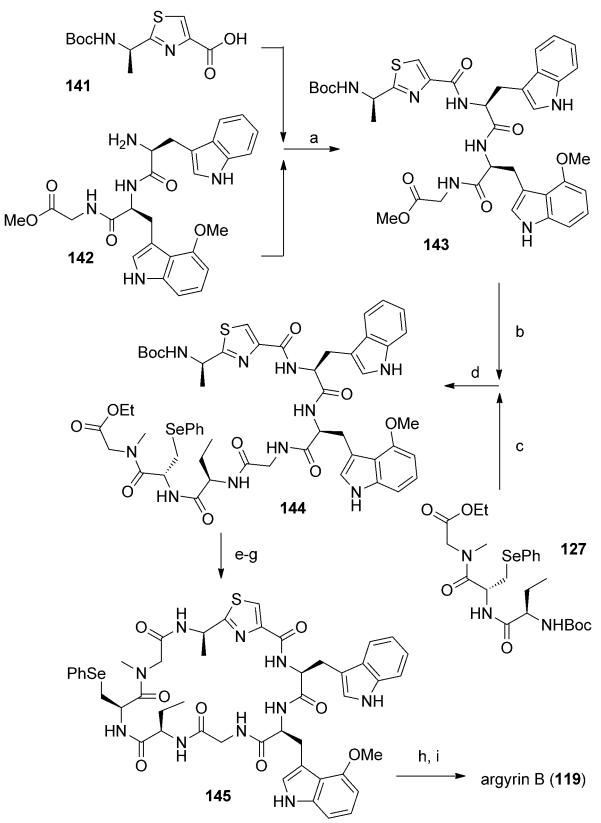


***Scheme 22.*** Synthesis of argyrin B. Reagents and conditions: a) EDC, HOBt, $CH_2Cl_2$, RT, 97%, (2 steps); b) LiOH, THF/MeOH/$H_2O$, RT; c) TFA/$CH_2Cl_2$, RT; d) EDC, HOBt, *i*$Pr_2NEt$, $CH_2Cl_2$, 80%, 2 steps; e) LiOH, THF/MeOH/$H_2O$, RT; f) anisole/TFA, RT; g) TBTU, HOBt, *i*$Pr_2NEt$, $CH_2Cl_2$, RT, 50–60%, (3 steps); h) $NaIO_4$, dioxane/$H_2O$, RT; i) $NaHCO_3$, $CH_3CN/H_2O$, RT, 66%, (2 steps).

### *8.3. Synthesis of Argyrin F by the Kalesse Group*

In 2008, Malek et al. identified argyrin A (**118**) as a potent proteasome inhibitor with high antitumor activity.[20] They reported that argyrin A (**118**) stabilizes the cyclin kinase inhibitor $p27^{kip1}$. Since argyrin A turned out to be a novel highly potent drug candidate, structure–activity relationship (SAR) studies and structural modifications of the lead structure were required for the subsequent translational research. In 2009, Kalesse and co-workers published an optimized route to a library of argyrins and their derivatives providing a detailed picture of the binding modes and structural requirements necessary for further preclinical investigations.[97] The synthesis took advantage of the previously published route by Ley and used their retrosynthetic disconnection (see Section 8.2). Since greater amounts of material were required for clinical evaluations, the route selected did not rely on selenium reagents for constructing the *exo*-methylene group and the tryptophane moiety was generated by enantioselective hydrogenation. The synthesis of argyrin F (**123**) representative for all argyrin derivatives is outlined below. The 4-methoxy-L-tryptophan moiety is generated by asymmetric catalytic hydrogenation with (1*S*,1′*S*,2*R*,2′*R*)-DuanPhos in combination with $[Rh(cod)_2]BF_4$. The substrate for this enantioselective hydrogenation (**147**) was generated by Vilsmeier reaction and Wittig olefination. Standard peptide coupling conditions and removal of the Cbz group followed by reaction with $N^{\alpha}$-Cbz-L-tryptophan afforded the desired building block **128** (Scheme 23).

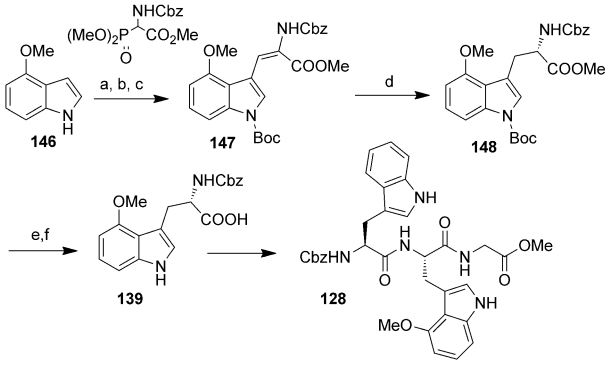


***Scheme 23.*** Synthesis of fragment **128**. Reagents and conditions: a) $POCl_3$, DMF, 75%; b) $(Boc)_2O$/DMAP, $CH_2Cl_2$, 89%; c) phosphonate, DBU, $CH_2Cl_2$, 73%; d) $[Rh(cod)_2]BF_4$/(1*S*,1′*S*,2*R*,2′*R*)-DuanPhos, $H_2$ (6 bar), MeOH, RT, 96 h, 99%, 90% *ee*; e) TFA, $CH_2Cl_2$; f) LiOH, THF/MeOH/$H_2O$, 70% (2 steps).

The synthesis of tripeptide **150** commenced with dipeptide **149**. A copper(I)-catalyzed elimination of the serine hydroxy group from **149** led to the introduction of the *exo*-methylene moiety. Hydrolysis of the ester followed by peptide coupling with sarcosine yielded fragment **150** which contains the dehydroalanine unit. This moiety was remarkably stable as long as the α-amine had an electron-withdrawing substituent and could be carried through the synthesis without decomposition (Scheme 24).[98]

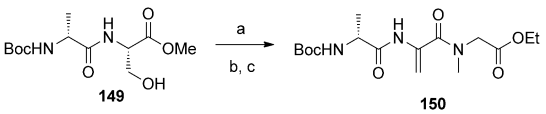


***Scheme 24.*** Synthesis of fragment **150**. Reagents and conditions: a) CuCl, EDC, $CH_2Cl_2$, 96%; b) LiOH,THF/MeOH/$H_2O$; c) HCl-Sar-OEt, PyBroP, *i*$Pr_2NEt$, $CH_2Cl_2$, 0°C→RT, 74%.

The synthesis of the thiazole fragment **153** follows Ley's route but used the *tert*-butyl-protected *N*-Boc-L-serine **151** instead. Transformation into thioamide **152** and reaction with ethyl bromopyruvate and subsequent treatment with trifluoroacetic anhydride and 2,6-lutidine provided thiazole **153** (Scheme 25).

These three segments were joined by established peptide transformations. Hydrolysis of the ester moiety of **154** and the coupling with deprotected dehydroalanine fragment **150** provided the linear peptide **155**. The cyclization was performed with TBTU and HOBt. Finally, deprotection of the *tert*-butyl-protected primary alcohol could be facilitated using TFA without reaction at the *exo*-methylene moiety (Scheme 26).


© 2013 Wiley-VCH Verlag GmbH & Co. KGaA, Weinheim

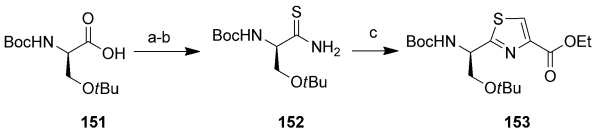


***Scheme 25.*** Synthesis of fragment **153**. Reagents and conditions: a) EDC, HOBt, $NH_3$, $CH_2Cl_2$, 0 °C; b) Belleau's reagent, THF, 0 °C, (quantitative, 2 steps); c) 1. $BrCH_2COCO_2Et$, $KHCO_3$, DME; 2. TFAA, 2,6-lutidine, DME, −15 °C.

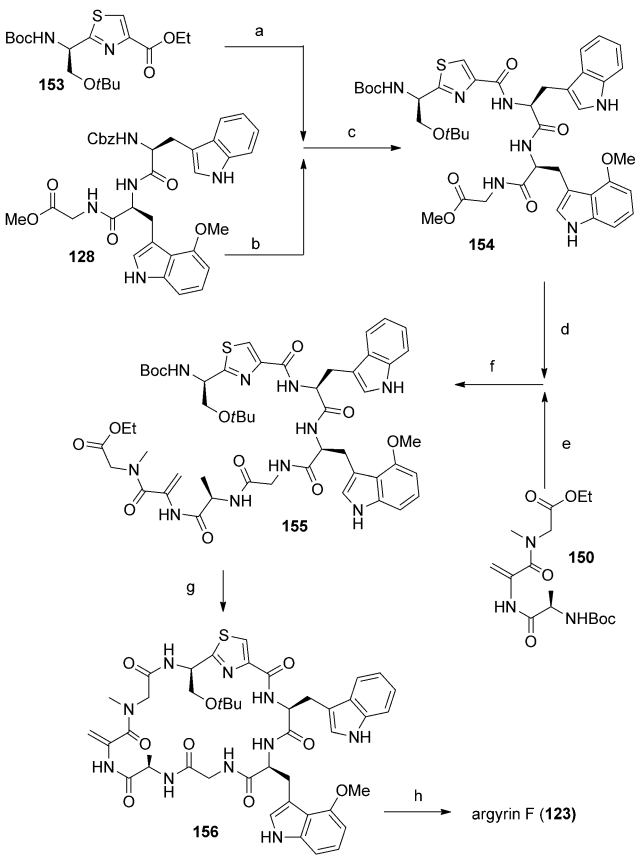


***Scheme 26.*** Synthesis of argyrin F (**123**). Reagents and conditions: a) LiOH, THF/MeOH/$H_2O$; b) $H_2$, Pd/C; c) EDC, HOBt, $iPr_2NEt$, 82% (2 steps); d) LiOH, THF, MeOH/$H_2O$; e) TFA, $CH_2Cl_2$; f) EDC, HOBt, $iPr_2NEt$, 85% (2 steps); g) 1. LiOH, THF/MeOH/$H_2O$; 2. TFA, $CH_2Cl_2$; 3. TBTU, HOBt, $iPr_2NEt$, 88% (3 steps); h) TFA, $CH_2Cl_2$, 83%.

Based on biological evaluations of their library of argyrin derivatives Kalesse et al. identified the methoxy group at tryptophan Trp1, the methyl group at position $R^4$, and the *exo*-methylene group as essential for the biological activity. Additionally, they reported that pharmacokinetic profile of argyrin F (**123**) is even better than that of argyrin A (**118**). It acts as a reversible and competitive inhibitor of the proteasome and is a tumor-specific vascular-damaging substance.

## 9. Beta-Lactones

β-Lactones are among the earliest known proteasome inhibitors. Their mode of action is based on the covalent attachment of the reactive lactone to the N-terminal threonine. Belactosin A (**157**)[99] was isolated from *Streptomyces* sp. UCK14 and, like belactosine C (**158**), shows inhibition of the proteasome (Figure 16).[100]

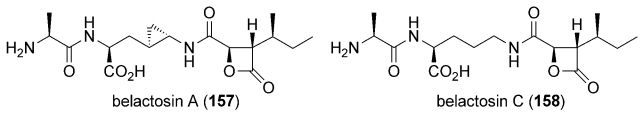


***Figure 16.*** Lactone proteasome inhibitors.

### 9.1. Salinosporamide A

In 2003, Fenical et al.[101] isolated the microbial secondary metabolite salinosporamide A (**33**) from *Salinispora tropica*, a marine actinomycete. This compound is produced by the CNB-392 strain and inhibits all three proteolytic sites of the 20S proteasome without affecting other proteases. Additionally, salinosporamide A (**33**) blocks the cell proliferation of various tumor cell lines (with $IC_{50}$ values as low as 10 nM) including Velcade-resistant myeloma cell lines.[102]

The structure of salinosporamide A (**33**) is analogous to that of omuralide (**159**),[103] another β-lactone–lactam natural product. It is proposed that omuralide is constructed through β-lactonization of the thiol ester of lactacystin (**160**, Figure 17).[104] Both are terrestrial microbial products as

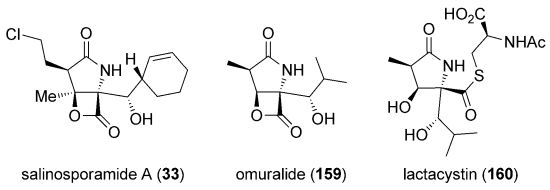


***Figure 17.*** Structures of lactone–lactam proteasome inhibitors.

well as potent useful inhibitors of proteasome activity. Salinosporamide A **33** displays substantially higher inhibitory activities and is approximately 35 times more active than omuralide (**159**). Insights into the mechanism of inhibition were provided from the crystal structure of the yeast 20S proteasome in complex with salinosporamide A (**33**). Based on this crystal structure, Groll et al. proposed an irreversible binding of salinosporamide A. After acylation of the N-terminal Thr1$O^{\gamma}$ group through the opening of the β-lactone in **33**, the chloride on its side chain is displaced by the C6 hydroxy group with concomitant formation of the tetrahydrofuran intermediate. This reaction prevents hydrolysis of the ester linkage to the proteasome (Scheme 27).[105] In contrast, acylation by omuralide (**159**) is reversible and results in the complete recovery of the proteasomal activity within 24 h. Consequently, detailed investigations on the

 © 2013 Wiley-VCH Verlag GmbH & Co. KGaA, Weinheim 

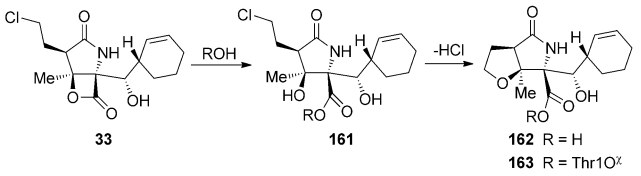


***Scheme 27.*** Mechanism of the irreversible inhibition of salinosporamide.

function of chloride displacement were published[106,107] and provide a complete picture of the unique inhibitory mode of action of salinosporamide A (**33**).[108] This remarkable mechanism as well as its structural complexity earmarked salinosporamide A (**33**) as a challenging target for total synthesis.

### *9.2. Syntheses by the Corey Group*

In 2004, Corey et al. presented the first total synthesis of salinosporamide A (Scheme 28).[109] Their strategy to establish the quarternary carbon made use of the conformational rigidity of oxazolidine **165**. Subsequent removal of the oxazoline was facilitated by $NaBH_3CN$ under acidic conditions and gave *N*-4-methoxybenzylamine **166**. A stereoselective Baylis–Hillman reaction[110] was then used for the conversion of bisketone **167** into **168**. This cyclization proceeded with a diastereomeric ratio of 9:1 and established

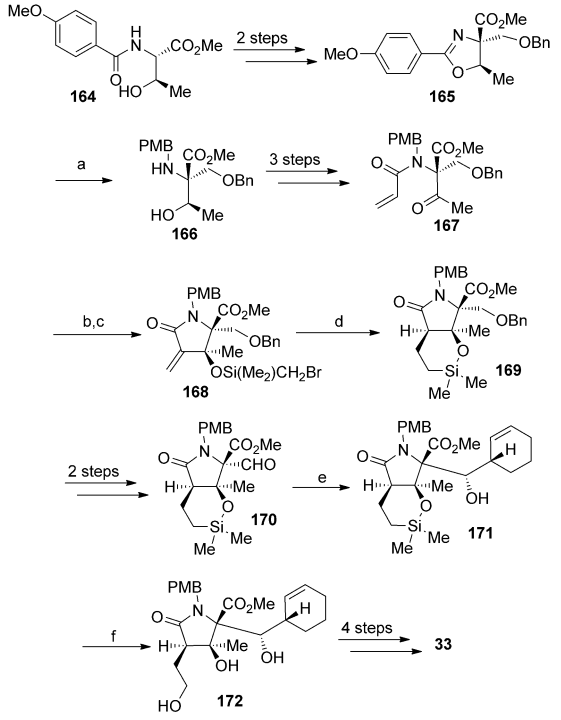


***Scheme 28.*** Reagents and conditions: a) $NaCNBH_3$, AcOH, 40 °C, 12 h, 90%; b) quinuclidine, DME, 0 °C, 7 d, 90%, d.r. = 9:1; c) $BrCH_2Si(CH_3)_2Cl$, $NEt_3$, DMAP, $CH_2Cl_2$, 0 °C, 30 min, 95%; d) $Bu_3SnH$, AIBN, benzene, reflux, 8 h, 89%; e) 2-cyclohexenylzinc chloride, THF, −78 °C, 5 h, 88%; f) KF, $KHCO_3$, $H_2O_2$; THF/MeOH (1:1), 23 °C, 18 h, 92%.

the tertiary alcohol of salinosporamide (**33**). Silylation with bromomethyldimethylsilyl chloride and radical cyclization provided **169** in 88% yield. After hydrogenolytic deprotection with Pd/C and Dess–Martin oxidation, aldehyde **170** was reacted with 2-cyclohexenylzinc chloride. This particular transformation is used in a variety of other syntheses of salinosporamide A (**33**) and provides the desired product **171** stereoselectively (20:1). A Fleming–Tamao oxidation[111] results in triol **172**, which is PMB-deprotected. Finally, hydrolysis with lithium hydroxide, lactonization with BOP-Cl, and chlorination of the ethylhydroxy group provide salinosporamide A (**33**) in 17 steps and an overall yield of 12.4%.

One year later Corey et al. replaced the Baylis–Hillman transformation by the Kulinkovich reaction[112] as the key step (Scheme 29) and improved the diastereomeric ratio of the

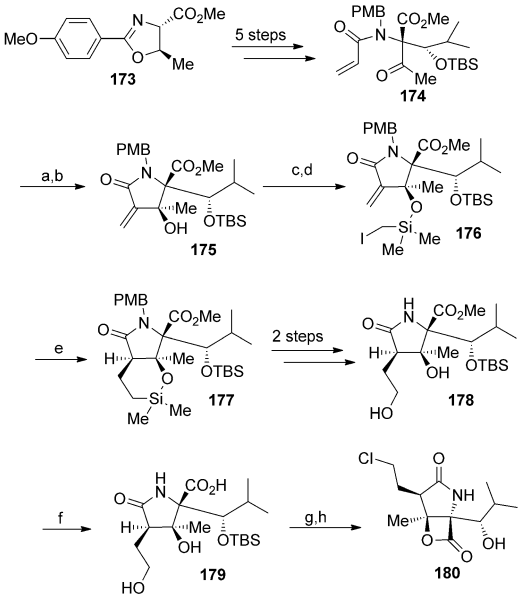


***Scheme 29.*** Reagents and conditions: a) $Ti(OiPr)_4$, $C_5H_9MgCl$, *t*BuOMe, −40 °C, 30 min, $I_2$, −40 °C, 2 h then 0 °C, 2 h; b) $NEt_3$, $CH_2Cl_2$, 23 °C, 30 min, 85% (2 steps); c) $BrCH_2Si(CH_3)_2Cl$, imidazole, DMF, 0 °C, 6 h; d) NaI, acetone, 60 °C, 86% (2 steps); e) $Bu_3SnH$, $Et_2AlCl$, $Et_3B$, toluene, −78 °C, air, 3 h, 93%; f) $[\{MeTeAlMe_2\}_2]$, toluene, 23 °C, 12 h; g) $Ph_3PCl_2$, $CH_3CN$, pyridine, 12 h, 81% (2 steps); h) HF (48%)/$CH_3CN$ (3:1), 23 °C, 3 d, 82%.

tertiary alcohol from 9:1 to 99:1.[113] Starting from oxazoline **173**, they introduced an isopropyl group instead of the cyclohexenyl group. A sequence of transformations involving oxazolidine cleavage, Swern oxidation, and N-acylation then provided keto acrylamide **174**. At this point, the aforementioned Kulinkovich reaction was applied, which used titanium tetrapropyloxide and cyclopentylmagnesium chloride to generate the reagent. The resulting α-titanamethyl-γ-lactam intermediate was quenched with iodine and the resulting α-iodomethyl-γ-lactam, generated by metal–halide exchange, was subjected to elimination. As in their previous synthesis, a radical reaction was employed to establish the chloride-containing side chain stereoselectively. Subsequent removal


© 2013 Wiley-VCH Verlag GmbH & Co. KGaA, Weinheim

of the PMB group on the amide nitrogen and cleavage of the silicon–oxygen bond liberated lactam **178**. In the context of this synthesis, Corey introduced [{MeTeAlMe$_2$}$_2$] as a new reagent for the cleavage of sterically hindered methyl esters under mild conditions (toluene, 23 °C).[114] The subsequent side-chain chlorination and the β-lactonization was performed in a single step with the use of $Ph_3PCl_2$. Finally, desilylation with hydrofluoric acid resulted in the omuralide–salinosporamide A hybrid **180** in 15 steps starting from **173** with an overall yield of 19.7% (Scheme 29).

### 9.3. Synthesis by the Danishefsky Group

At about the same time as Corey's second synthesis Danishefsky et al.[115] published their route to salinosporamide A (**33**). The conformationally restricted pyroglutamate-derived substrate **181** allowed selective addition at C3 from the α-face (Scheme 30).[116] Taking advantage of an *anti* addition led to subsequent α-alkylation at C2 (**182**). A sequence of ozonolysis, reduction, formation of the carbonate ester, and cleavage of the N,O-acetal established **183**, which was converted to its imidate ester **184**. Deprotonation of the imidate with LiHMDS initiated the intramolecular acylation.

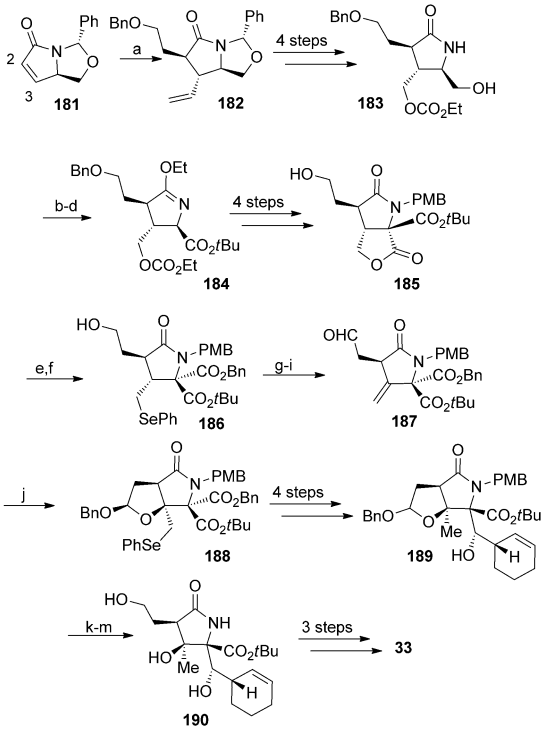


***Scheme 30.*** Reagents and conditions: a) 1. Vinylmagnesium bromide, TMSCl, CuI, THF, −78 °C, 75%, 2. LDA, 1-iodo-2-benzyloxyethane, THF, RT, 77%, 14:1; b) Jones reagent, acetone, RT; c) $Me_2NCH(OtBu)_2$, toluene, reflux, 72%, (2 steps); d) $Et_3OBF_4$, $K_2CO_3$, $CH_2Cl_2$, RT, 88%; e) PhSeSePh, $NaBH_4$, EtOH, 60 °C; f) BnBr, $K_2CO_3$, DMF, RT, 65% (2 steps); g) 30% $H_2O_2$ (aq), THF, RT; h) toluene, 100 °C; i) Dess–Martin periodinane, $CH_2Cl_2$, RT, 89% (3 steps); j) PhSeBr, $AgBF_4$, BnOH, $CH_2Cl_2$, −20 to 0 °C, 74%, d.r. = 12:1; k) CAN, $CH_3CN$–$H_2O$, 0 °C, 90%; l) Na, $NH_3$ (liq), −78 °C; m) $NaBH_4$, THF/$H_2O$ (2:1), RT, 97% (2 steps).

Further protecting-group manipulations set the stage for the pivotal phenylselenium-meditated lactone opening and concomitant benzylation to construct diester **186**. The selenium oxide elimination provided both the expected elimination product and the readily oxidized aldehyde **187**, which cyclized in the presence of phenylselenyl bromide and silver tetrafluoroborate to generate **188**. Cyclohexenylzinc chloride (see Section 9.2) was introduced using Corey's conditions. Consequently, the resulting triol **190** was obtained after PMB removal and reductive cleavage of the benzyl glycosylate. Hydrolysis of the ester, lactonization with BOP-Cl, and chlorination with $Ph_3PCl_2$ provided **33** in 26 linear steps and an overall yield of 1.6%.

### 9.4. Synthesis by Ling, Macherla, and Co-Workers

Macherla and Ling published their synthesis in 2007.[116] Their approach is an educational example of the concept of the "regeneration of chirality" based on oxazolidine **192** (Scheme 31). An intramolecular aldol reaction established cyclic **194** and provided the new quaternary center, a tertiary alcohol, and a stereoselectively attached allylic group at the same time and in a diastereomeric excess of 70%. Conversion

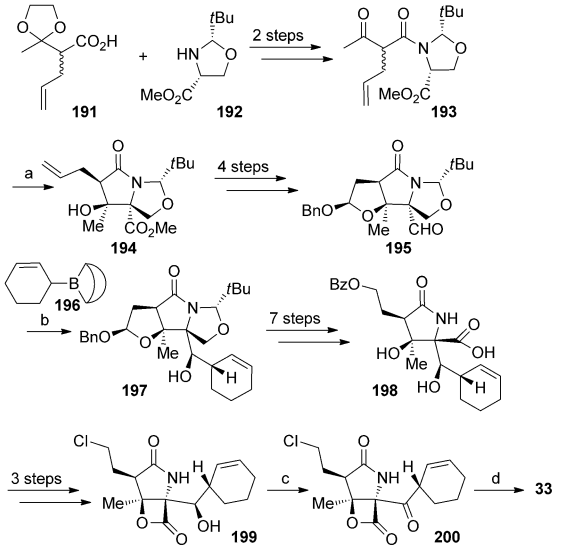


***Scheme 31.*** Reagents and conditions: a) *t*BuOK, THF, RT, 15 min, 64%; b) borane **196**, THF, −78 °C to RT, 11.5 h, 80%; c) Dess–Martin periodinane, $CH_2Cl_2$, 2 h, 60%; d) KRED-EXP-B1Y, $NAD^+$, GDH-103, glucose, pH 6.9, 37–39 °C, 40 min, 56%.

to **195** set the stage for the stereoselective incorporation of the cyclohexenyl moiety. In contrast to the previous syntheses, a cyclohexene borane (**196**) instead of a zinc chloride species was used during this step. Cleavage of both the tetrahydrofuran and the oxazolidine ring and subsequent TMS protection was followed by an oxidation to give carboxylic acid **198** (Dess–Martin–Pinnick sequence). β-Lactonization with BOP-Cl and introduction of the chloroethyl group with $Ph_3PCl_2$ was followed by inversion of the side-chain alcohol by a sequence

 © 2013 Wiley-VCH Verlag GmbH & Co. KGaA, Weinheim 

consisting of Dess–Martin oxidation and reduction using an enzymatic ketoreductase to provide **33** in an overall yield of 0.23% and 20 linear steps.

### 9.5. Synthesis by the Hatakeyama Group

An indium-catalyzed Conia-ene reaction[117] was the key transformation applied by Hatakeyama et al.[118] in their synthesis (Scheme 32). In the first step of the sequence

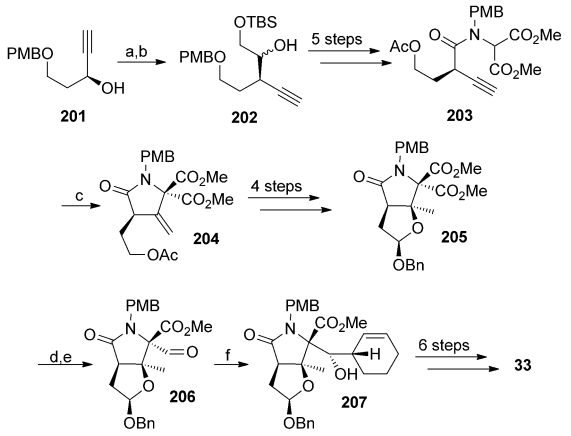


***Scheme 32.*** Reagents and conditions: a) MsCl, $NEt_3$, DMAP, $CH_2Cl_2$, 0 °C, 95%; b) $Pd(OAc)_2$, $PPh_3$, $Et_2Zn$ then $TBSOCH_2CHO$, THF, −78 → −20 °C, 63%; c) $In(OTf)_3$ (5 mol%), toluene, 110 °C, 96%; d) $NaBH_4$, THF/EtOH, 88%; e) Dess–Martin periodinane, $CH_2Cl_2$, 94%; f) cyclohex-2-enylzinc chloride, THF, −78 °C, 88%.

alcohol **201** was transformed to its mesylate. This was subjected to a Marshall reaction using (*tert*-butyldimethylsilyloxy)acetaldehyde and diethyl zinc to provide **202**. Subsequent transformations established the cyclization precursor **203**. The Conia-ene reaction was promoted by $In(OTf)_3$ to give **204**. Several subsequent steps provided lactam **207**, and from this point the synthesis follows the route established by Danishefsky.

### 9.6. Synthesis by Nagamitsu, Omura, and Co-Workers

A new strategy for the installation of the cyclohexene side chain was presented by Nagamitsu and Omura in their total synthesis (Scheme 33).[119] Starting from aldehyde **208**[120] a Wittig olefination followed by enzymatic desymmetrization was chosen to access **210**. A sequence of protecting-group manipulations established a cyclic carbamate, which was protected with a PMB group to yield **212**. An osmium-catalyzed dihydroxylation and periodate cleavage generated aldehyde **213**. The subsequent addition of the lithium enolate of cyclohexanone took advantage of the coordinating properties of the MEM group and thus provided stereoselectively the desired aldol product. Subsequent benzoate protection gave **215**. In order to establish the required double bond at the cyclohexene segment, the cyclohexenone carbonyl group was

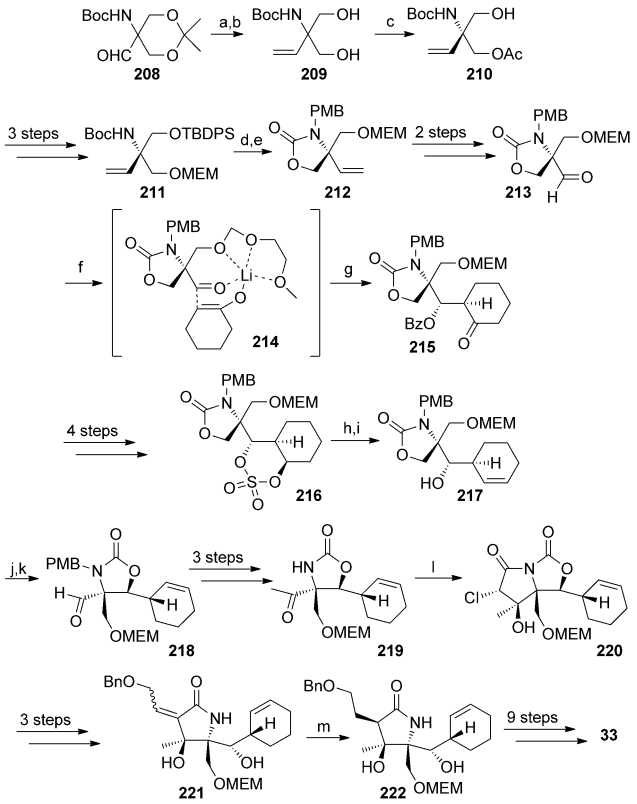


***Scheme 33.*** Reagents and conditions: a) $Ph_3P^+CH_3Br^-$, NaHMDS, THF, RT, 97%; b) *p*-TsOH–$H_2O$, MeOH, RT, 82%; c) lipase, vinyl acetate, *i*$Pr_2O$, RT; d) TBAF, THF, RT; e) NaH, THF–DMF, then PMBCl, RT, 97%, (2 steps); f) LDA, cyclohexanone, THF, −78 °C; g) BzCl, 79%; h) DBU, toluene, 100 °C; i) TsOH·$H_2O$, dioxane, RT, 97%, (2 steps); j) NaH, THF–EtOH, RT; k) $(COCl)_2$, DMSO, $NEt_3$, $CH_2Cl_2$, −78 °C, 92%, (2 steps); l) LiHMDS, THF, −78 °C, then chloroacetyl chloride, 63%; m) $LiEt_3BH$, THF, 0 °C, 77%.

reduced under Luche conditions and the benzoate group was hydrolyzed to give an *anti*-1,3-diol. For the elimination, cyclic sulfate **216** was treated with DBU and TsOH to provide cyclohexene **217**. Intramolecular transcarbamation and Swern oxidation followed by Grignard reaction, Dess–Martin oxidation, and N-deprotection resulted in ketone **219**. The required γ-lactam **220** was established by N-acylation and intramolecular aldol reaction, whereas the side chain could be installed using a $SmI_2$-mediated Reformatsky-type reaction, which after elimination provided lactam **221**. Compound **221** underwent a sequence of deprotection and protection steps followed by final oxidation, Birch reduction, β-lactonization, chlorination, and TES deprotection to afford salinosporamide A (**33**) in an overall yield of 2.1% and 38 linear steps.[120]

### 9.7. Synthesis by the Iwabuchi Group

Starting with Garner's aldehyde (**223**)[121] Iwabuchi et al. introduced an unprecedented strategy to establish the cyclohexenyl moiety.[122] Organocatalytic addition of cyclohexanone to Garner's aldehyde gave β-hydroxy ketone **224**, which was subjected to a reduction–elimination sequence to estab-


© 2013 Wiley-VCH Verlag GmbH & Co. KGaA, Weinheim

lish the double bond stereoselectively. Protecting-group manipulations and oxidation led to methyl ester **226**, which upon treatment with *p*-toluenesulfonic acid generated oxazoline **227**. The tertiary alcohol was formed by the Reformatsky reaction of ketone **229** with α-bromo-γ-butyrolactone. Reductive treatment of the oxazoline generated the required γ-lactam **231**, which was converted to diol **232**. An AZADO-catalyzed oxidative lactonization then furnished the lactone moiety in a one-pot procedure. Deprotection and chlorination completed the synthesis in 26 steps and an overall yield of 2.0% (Scheme 34).

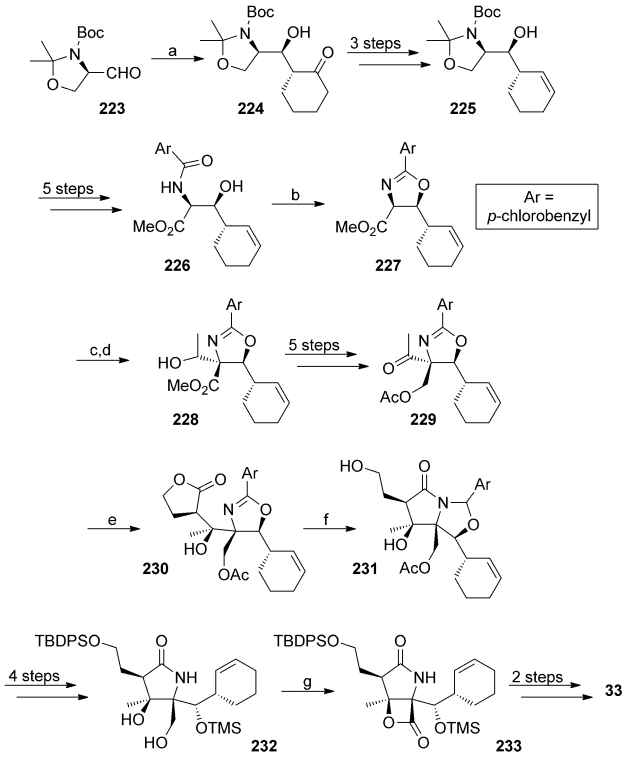


***Scheme 34.*** Reagents and conditions: a) D-proline, cyclohexanone, $CHCl_3$/DMSO, 5 °C, 81%; b) *p*-TsOH, toluene, reflux, 47%; c) LDA, THF, −78 °C, then AcCl, 76%; d) $NaBH_4$, MeOH, −40 °C; e) 1. $(Ph_3P)_3RhCl$, α-bromo-γ-butyrolactone, $Et_2Zn$, THF, −20 °C; 2. DBU, $CH_2Cl_2$, 0 °C, 57%; f) $NaBH_3CN$, AcOH/THF, 0 °C; g) AZADO, $PhI(OAc)_2$, $CH_2Cl_2$, RT, 78%.

### 9.8. Synthesis by Fukuyama

In 2011, Fukuyama et al. published their approach towards salinosporamide A (**33**, Scheme 35).[123] Starting with **235** obtained from 4-pentenoic acid (**234**), acylation to give the oxazolidinethione and subsequent alkylation established the chiral center, which was later the point of attachment for the chlorinated side chain. Cleavage of the auxiliary and reductive amination led to amine **236**. Amine protection and subsequent liberation of the ketone yielded after crystallization enantiomerically pure pyrrolidine **237**. A one-pot procedure including ozonolysis, methylation, and removal of the formyl group followed by oxidation established lactam

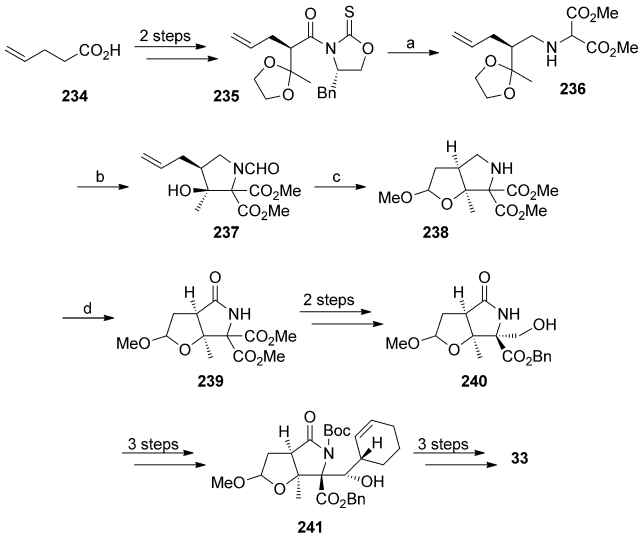


***Scheme 35.*** Reagents and conditions: a) DIBAl-H, toluene, −78 °C, then AcOH, MeOH, −78 °C→RT, then amino dimethylmalonate hydrochloride, NaOAc, 0 °C, then $NaBH_3CN$, −20 °C→RT; b) $HCO_2H$, AcOH, THF, 0 °C, then $HCl_{(aq)}$, acetone, 0 °C→RT, recrystallization from $Et_2O$, 71% (2 steps); c) $O_3$, $MeOH/CH_2Cl_2$, −78 °C, then $Me_2S$, CSA, −78 °C→RT, then AcCl, 0 °C→RT, 99%, (d.r. = 2:1); d) $RuO_2$, $NaIO_4$, *n*-PrOAc–MeCN phosphate buffer, 0 °C, 85%.

**239**. Intermediate conversion to its dibenzyl ester and selective reduction led to alcohol **240**, which was further transformed under established conditions. Finally, salinosporamide A (**33**) was obtained in 14 steps and 19% overall yield.

### 9.9. Syntheses of Racemic Salinosporamide

A synthesis of (±)-**33** was published by Pattenden and coworkers.[124] Starting with β-ketoester **242** (Scheme 36)[125] protection of the ketone allowed the ester moiety to be hydrolyzed and converted to amide **243**. The key step in their synthesis is the acid-catalyzed intramolecular formation of racemic lactam **244**. Protection of both the hydroxy group and the amide followed by selective reduction gave aldehyde **245.** The cyclohexenyl side chain was installed using the protocol developed by Corey. Finally, following Corey's route (±)-**33** was obtained in 14 steps and 12% overall yield.

Romo et al. published a second approach in 2007 (Scheme 37).[126] Commencing with serine derivative **246**,

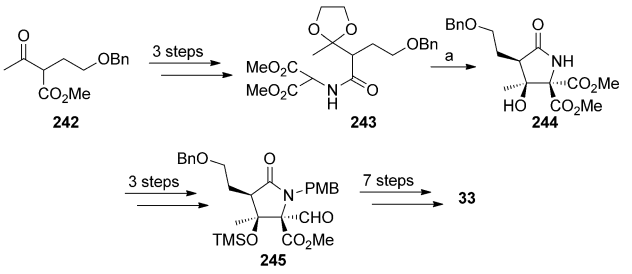


***Scheme 36.*** Reagents and conditions: a) $AcOH/H_2O$ (4:1), 65 °C, 4 d, 71%.

 © 2013 Wiley-VCH Verlag GmbH & Co. KGaA, Weinheim 

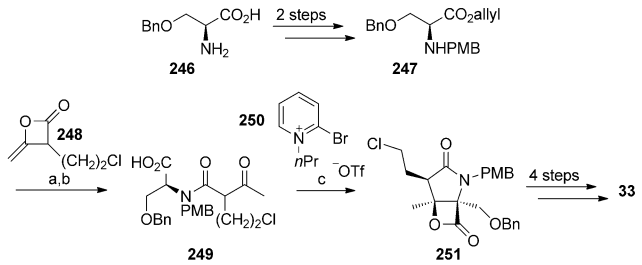

***Scheme 37.*** Reagents and conditions: a) Diketene **248**, 1-hydroxypyridine, THF, 60 °C, 36 h, 80%; b) $[Pd(PPh_3)_4]$, morpholine, 75%; c) modified Mukaiyama reagent **250**, $iPr_2NEt$, 4-PPY, $CH_2Cl_2$, −10 °C, 6 h, 25–35%, d.r. = 2:1 to 3:1.

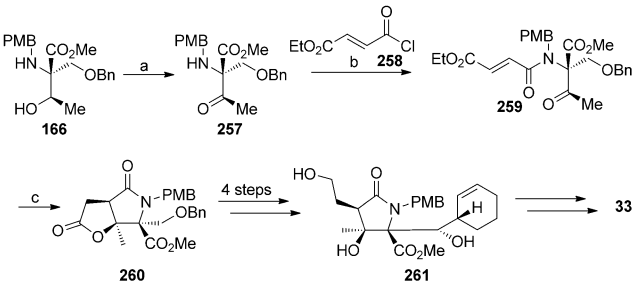

***Scheme 39.*** Reagents and conditions: a) $(COCl)_2$, DMSO, $NEt_3$, $CH_2Cl_2$, −78→−40 °C, 72%; b) **258**, $iPr_2NEt$, $CH_2Cl_2$, 0 °C→RT, quant.; c) $[(Me_3P)_2NiCl_2]$, $Et_2Zn$, THF, 0 °C→RT, 42%.

which was esterified and N-protected, coupling with ketene dimer **248** followed by saponification provided **249**. Bis-cyclization with the modified Mukaiyama reagent (**250**), PPY, and $iPr_2NEt$ gave **251** (d.r. = 2:1–3:1). The desired product **251** was benzyl-deprotected and oxidized. Reaction with cyclohexenylzinc chloride and PMB removal provided (±)-**33** in 9 steps and an overall yield of 2.5%.

### 9.10. Formal Syntheses

An alternative route to Corey's pivotal intermediate **256** was presented by Langlois et al. in 2006 (Scheme 38).[127] Lactam **252** was methylated by Michael addition followed

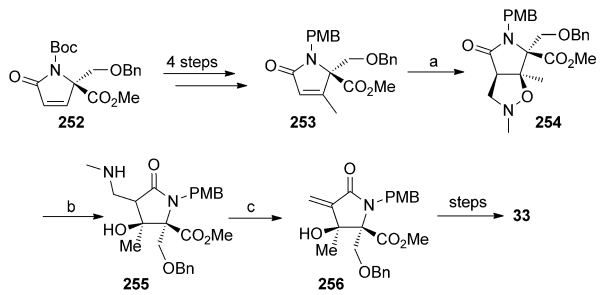

***Scheme 38.*** Reagents and conditions: a) *N*-methylnitrone, toluene, heat, 68%; b) $H_2$, $Pd(OH)_2$, EtOAc–MeOH, 64%; c) MeI, MeOH, then $Na_2CO_3$, $CH_2Cl_2$, 90%.

by elimination of the previous installed α-selenyl species. Exchange of protecting groups gave **253**, which underwent cycloaddition with *N*-methylnitrone to provide pyrrolinone **254** as the major product. Cleavage of the isoxazolidine ring and elimination of the amino group afforded **256**. The subsequent transformations followed Corey's procedure.

Lam et al.[128] reported on the synthesis of an alternative to Corey's intermediate **168** in which the chloroethyl side chain was accessible in a more convenient way (Scheme 39). With Corey's amino alcohol **166**, Swern oxidation was performed followed by acylation with **258**. A cyclization step with a nickel–phosphine complex gave γ-lactone γ-lactam **260** as the major product. Deprotection of the hydroxy group and Swern oxidation were followed by the introduction of the cyclohexenyl substituent according to Corey's protocol. Finally, reductive opening of the lactone gave triol **261**, which could be subjected to Corey's and Pattenden's synthetic routes to afford salinosporamide A (**33**).

A formal synthesis based on Corey's intermediate **165** was published by Tepe et al.[129] Using an oxazolone-mediated ene-type reaction **262** was converted to intermediate **263** which was reduced to ester **264**. Dehydrative cyclization with MsCl and oxazoline reduction generated the chiral amino alcohol **266**. Concluding Bn protection and cleavage of the *tert*-butyl ether[130] provided Corey's intermediate **166** (Scheme 40).

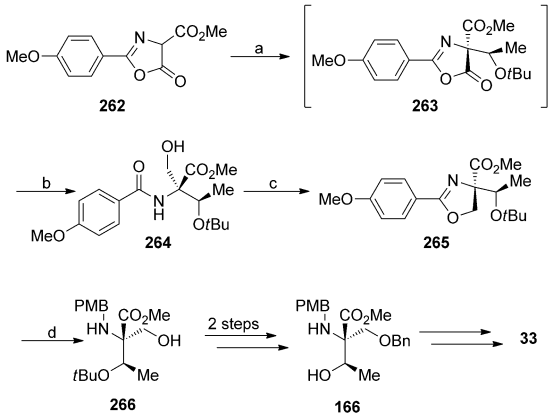

***Scheme 40.*** Reagents and conditions: a) Vinyl *tert*-butyl ether, $(PhO)_2PO_2H$ (10%), benzene, RT (d.r. = 3:1); b) $NaBH_4$, 88% (2 steps); c) MsCl, $NEt_3$, $Cl(CH_2)_2Cl$, reflux, 4 h, 92%; d) $NaCNBH_3$, AcOH, RT, 40 h, 73%.

Bode et al. presented an N-heterocyclic carbene (NHC)-catalyzed approach to Lam's **260**.[131] Amine **267** was converted into aldehyde **268**. The NHC-catalyzed intramolecular cyclization–lactonization process proceeded in 88% yield and the desired diastereomer **260** was obtained in a 1:1.1 ratio in its favor (Scheme 41).

A formal synthesis leading to Corey's compound **172** was reported by Sato and Chida et al. (Scheme 42).[132] Starting from diacetone D-glucose four known steps led to **271**,[133] which was benzyl protected followed by selective cleavage of


© 2013 Wiley-VCH Verlag GmbH & Co. KGaA, Weinheim

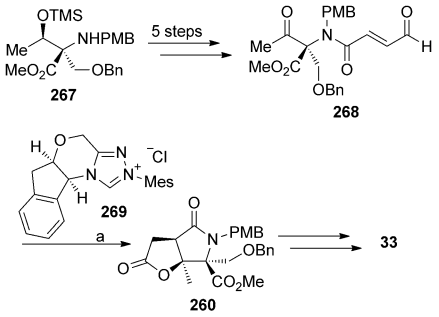

***Scheme 41.*** Reagents and conditions: a) **269**, DBU, THF/*t*BuOH (10:1), 40 °C, 3 h, 88 %, d.r. = 1:1.1.

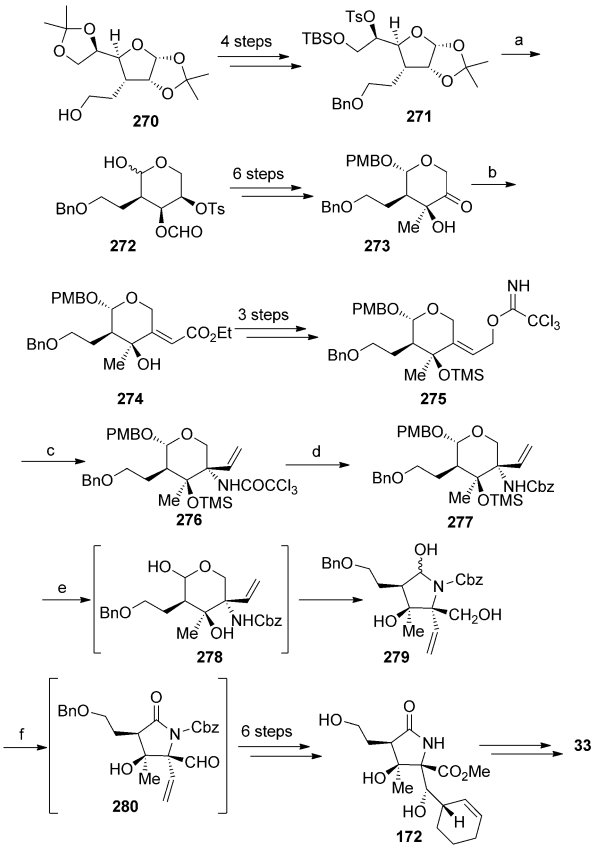

***Scheme 42.*** Reagents and conditions: a) 6 M HCl, THF, then $NaIO_4$, $THF_{(aq)}$; b) $(EtO)_2P(O)CH_2CO_2Et$, NaH, THF, 96 %; c) $Na_2CO_3$, *tert*-butylbenzene, 150 °C, sealed tube, 2 d, 85 % (2 steps), d.r. = 4.3:1; d) DIBAL-H, toluene, −78 °C, then CbzCl, EtOAc, 0.5 M $NaOH_{(aq)}$ quant.; e) TFA/$H_2O$ (4:1), $CH_2Cl_2$, 0 °C; f) Jones reagent, $acetone_{(aq)}$, 0 °C.

one acetonide and protection of both alcohols. Hydrolysis of the remaining acetonide and glycol cleavage with $NaIO_4$ gave pyranose derivative **272**, which was PMB protected and the formyl group removed. Oxidation of the free alcohol and alkylation with $AlMe_3$ gave **273**. After tosyl removal and further oxidation a Horner–Wadsworth–Emmons reaction and TMS protection were applied. Reduction of the ester followed by conversion to its trichloroacetimidate **275** paved the way to the pivotal Overman rearrangement (**276**, 69 %). Removal of the trichloroacetyl group and subsequent N-protection gave **277**, which was treated with TFA to removal the PMB and TMS protecting groups in a single step. The resulting diol **278** transforms spontaneously to hemiaminal **279**. Subsequent Jones oxidation, ester formation, TMS protection, and oxidative cleavage were used to install the cyclohexenyl side chain according to Corey's procedure. Finally, overall deprotection with $BCl_3$ gave **172**.

Ling et al. presented two approaches in 2010.[134] In their first approach, the equivalent of Corey's key intermediate **170** was prepared starting from L-serine hydrochloride (**281**, Scheme 43). N,O-protection and conversion provided the β-keto amide **282** which underwent cyclization and dehydration to give **283**. After alcohol **284** had been established, the double bond was transformed into an epoxide using a customized protocol with concentrated *t*BuOOH and Triton B. Reductive cleavage of the resulting oxirane **285**, oxidative formation of the side-chain lactone **286**, and removal of the chiral auxiliary concluded the synthesis of **287**.

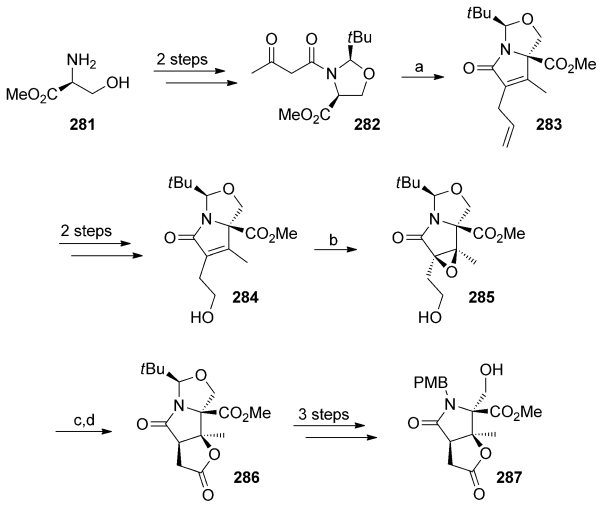

***Scheme 43.*** Reagents and conditions: a) Allylbromide, $K_2CO_3$, DMF, 25 °C, then DBU, toluene, 110 °C, 80 %; b) Triton B (80 wt % in MeOH), *t*BuOOH solution (conc. in decane), THF, 25 °C, 10 min, then **284**, THF, 25 °C, 40 h, 71 %; c) $SmI_2$, THF/MeOH, −80 °C, 100 %; d) PCC, dry 4 Å molecular sieves, $CH_2Cl_2$, 25 °C, 84 %.

In their second approach, **288** was transformed to the triol **290** by side-chain manipulation and dihydroxylation (on the *exo* face). Epoxidation and $SmI_2$-promoted regio- and stereoselective reductive cleavage of the oxirane resulted in diol **291**, which after dehydration served as the direct precursor for Corey's intermediate **168** (Scheme 44).

A formal approach towards the core structure of salinosporamide A (**33**) was presented by Takemoto et al. using an intramolecular hydroamidation reaction (Scheme 45).[135] L-serine (**294**) was PMB protected and cyclized, the resulting oxazoline **295** alkylated, and the imidate hydrolyzed. Conversion into the alkynyl formamide **297** allowed the hydroamidation to take place and subsequent protecting-group manipulations furnished the γ-lactam moiety of **33**.

 © 2013 Wiley-VCH Verlag GmbH & Co. KGaA, Weinheim 

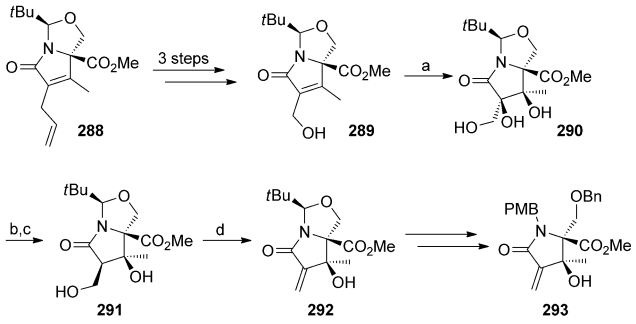

***Scheme 44.*** Reagents and conditions: a) Citric acid, NMO, $K_2OsO_4 \cdot 2H_2O$, THF/$H_2O$, 25 °C; b) $Et_3N$, TsCl, $CH_2Cl_2$, 25 °C, 77% (2 steps); c) $SmI_2$, THF/MeOH, −80 °C, 87%; d) $PPh_3$, imidazole, $I_2$, benzene, 80 °C, 90%.

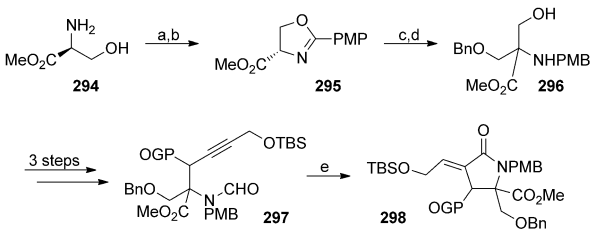

***Scheme 45.*** Reagents and conditions: a) PMPCOCl, *i*$Pr_2NEt$; b) $SOCl_2$, 70%, (2 steps); c) LDA, $BnOCH_2Cl$, HMPA, THF; d) $NaBH_4$, AcOH, 43%, (2 steps); e) $[Rh_4(CO)_{12}]$, xylene, 130 °C.

Kazmaier et al.[136] presented a formal biomimetic approach using amino acid **304**, which was proposed by Moore as an intermediate in salinosporamide's biosynthesis[137] (Scheme 46). The propargylic alcohol **299** was deuter-

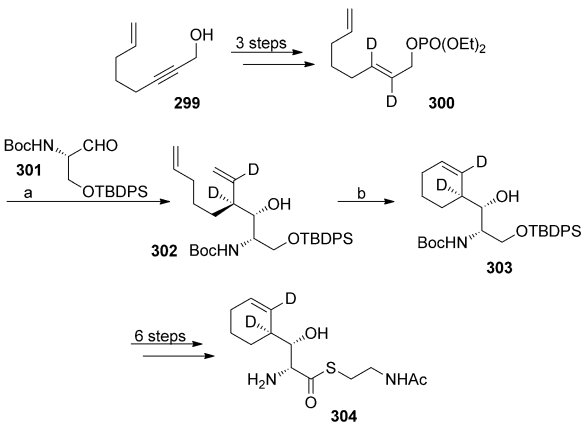

***Scheme 46.*** Reagents and conditions: a) **300**, $CrCl_2$, NaI, THF, RT, 86%; b) Grubbs I catalyst, $CH_2Cl_2$, RT, 96%.

ated in order to achieve a mechanistic picture of the biosynthetic pathway. Transformation to phosphate **300** followed by a substrate-controlled Nozaki–Hiyama–Kishi reaction with aldehyde **301** gave **302**. Ring-closing metathesis generated **303**, and oxidation-state changes established thioester **304**.

Lannou and Ardisson (Scheme 47) published a stereoselective functionalization of the pyrrolidinone moiety.[138] Triol **307** was protected and oxidized to give the aldehyde **309**. Hoppe allylation using the titanium species **310** yielded

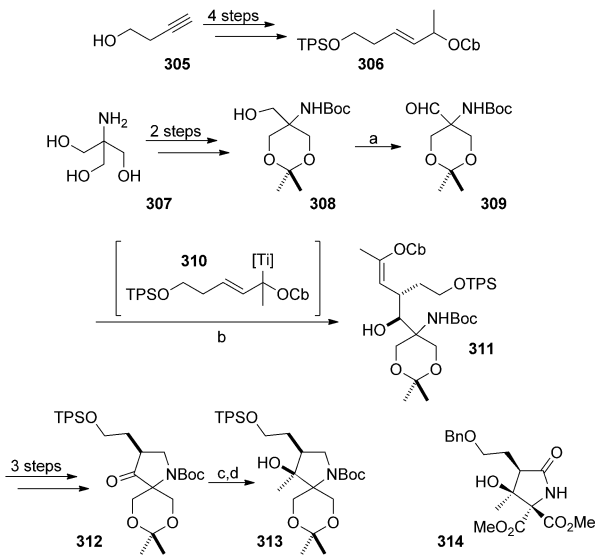

***Scheme 47.*** Reagents and conditions: a) Oxalyl chloride, DMSO, $CH_2Cl_2$, RT, then **308**, $CH_2Cl_2$, RT, 97%; b) (±)-**310**, TMEDA, *n*BuLi in hexanes, $Et_2O$, −78 °C, $Ti(OiPr)_4$, then **309**, THF, −78 °C, 76%; c) $Me_3SOI$, NaH, DMSO, RT, then (±)-**312**, 60 °C; d) $LiAlH_4$, $Et_2O$, 0 °C→RT, 52% (2 steps).

compound **311**, which was cyclized by means of ozonolysis and reductive amination. The required configuration of the tertiary alcohol was achieved by Corey–Chaykovsky epoxidation and reductive opening of the epoxide. The resulting alcohol **313** corresponds to Pattenden's advanced intermediate **314**.

## 10. Vinyl Sulfones

In 1997, Ploegh et al. reported on the covalent modification of the active-site threonine of the proteasomes β-subunits by peptide vinyl sulfones.[139] The synthesis of the vinyl sulfones involves the transformation of protected amino acids to their corresponding aldehydes through the corresponding Weinreb amide. A subsequent Wittig olefination generates vinyl sulfone **317**, which was deprotected to generate building block **318**. With **318** in hand several peptide vinyl sulfones can be accessed as tools and leads for proteasomal research (Scheme 48).

Biological studies revealed that peptide vinyl sulfones interact with the proteasome by Michael addition of the N-terminal threonine to the unsaturated sulfone moiety (Figure 18). The inhibitory potential is comparable to that of peptide aldehydes and it could be shown that peptide vinyl sulfones are less toxic than the peptide aldehyde Z-L3H, for instance.


© 2013 Wiley-VCH Verlag GmbH & Co. KGaA, Weinheim

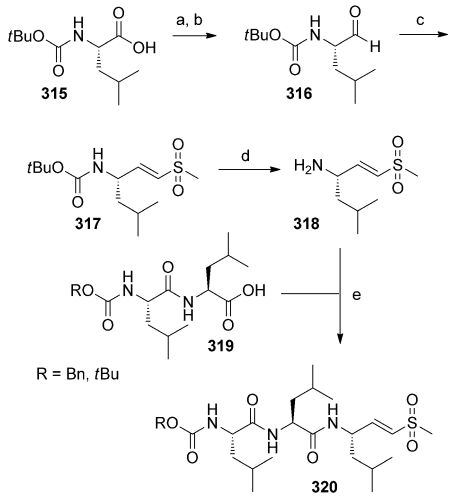


***Scheme 48.*** Synthesis of peptide vinyl sulfones according to Ploegh. Reagents and conditions: a) PyBOP, $i$Pr$_2$NEt, $CH_3NHOCH_3$, $CH_2Cl_2$; b) $LiAlH_4$, $Et_2O$; c) $(EtO)_2P(O)CH_2S(O)_2CH_3$, NaH; TsOH, $Et_2O$; d) Boc removal; e) PyBOP, $i$Pr$_2$NEt, $CH_2Cl_2$.

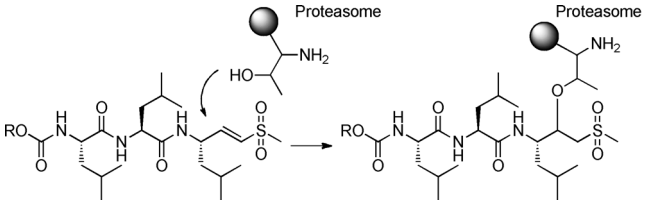


***Figure 18.*** Inhibition of the proteasomal subunits by peptide vinyl sulfones.

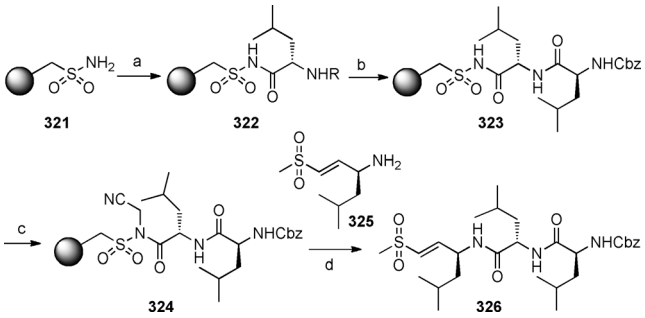


***Scheme 49.*** Solid-phase synthesis of peptide vinyl sulfones using Kenner's safety-catch protocol. Reagents and conditions: a) Fmoc-LeuOH, PyBOP, $i$Pr$_2$NEt, DMF; b) Cbz-LeuOH, PyBOP, $i$Pr$_2$NEt, DMF; c) $ICH_2CN$, $i$Pr$_2$NEt, NMP; d) $i$Pr$_2$NEt, THF.

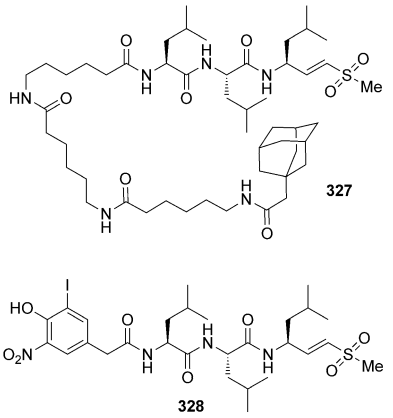


***Figure 19.*** Variations on the peptide vinyl sulfone concept.

Overkleeft and Ploegh[140] subsequently transformed their solution syntheses of peptide vinyl sulfones into a solid-phase protocol using Kenner's safety-catch protocol. Ultimately, this methodology was extended to the synthesis of novel peptide vinyl sulfones as well as to epoxyketones. The synthesis uses the 4-sulfamylbutyrylaminomethyl polystyrene resin, onto which the first Fmoc-protected amino acid was loaded. Established peptide-coupling protocols were applied and the resulting dipeptide was treated with iodoacetonitrile to provide activated **324**. Treatment of the activated resin with **325** then liberated peptide vinyl sulfone **326** (Scheme 49).

Overkleeft used the vinyl sulfone motif in combination with various peptide segments as probes for the proteasomal subunits' specificity.[68] They hypothesized that elongation of a given proteasome inhibitor with the adamantyl N-terminal cap as shown in structure **327** would lead to more potent compounds (Figure 19). At least for compound **327** it became apparent that this concept holds true. The major focus of Overkleeft's proteasome research is to develop inhibitors that can distinguish between the constitutive proteasome and the immunoproteasome which is in particular important from an immunology point of view.[141]

## 11. Macrolactones and Cyclic Amides

Three oxazole-containing macrolides were identified as proteasome inhibitors. They were isolated from marine sponges of the genus *Mycale* and inhibit the chymotrypsin-like activity of the proteasome (Figure 20). The most active metabolite, secomycalolide A (**331**), exhibits an $IC_{50}$ value of 11 $\mu g\,mL^{-1}$.

### 11.1. Syringolin A and Glidobactin A

The syrbactins[142] are a class of natural products that consist of syringolins, glidobactins, and cepafungins (Figure 21). They have been in the focus of biological research for over twenty years and it was finally recognized that the basis for all their activity was the inhibition of the proteasome.[143] The mechanism behind their activity is the nucleophilic attack of the threonine hydroxy group at the Michael acceptor position (Figure 22). The syringolins[144] were isolated as a virulence factors from the plant pathogen *Pseudomonas syringae pv. syringae* (Pss) and they inhibit the proteasome of host plants. The glidobactins A, B, and C were isolated from the gliding bacterium, *Polyangium brachysporum* sp. *nov.* No. K481-B101 and were immediately recog-

 © 2013 Wiley-VCH Verlag GmbH & Co. KGaA, Weinheim 

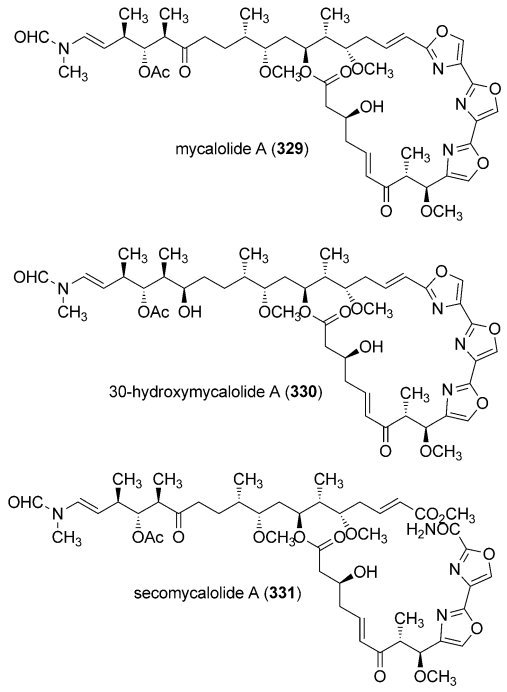


***Figure 20.*** Macrolactones as proteasome inhibitors.

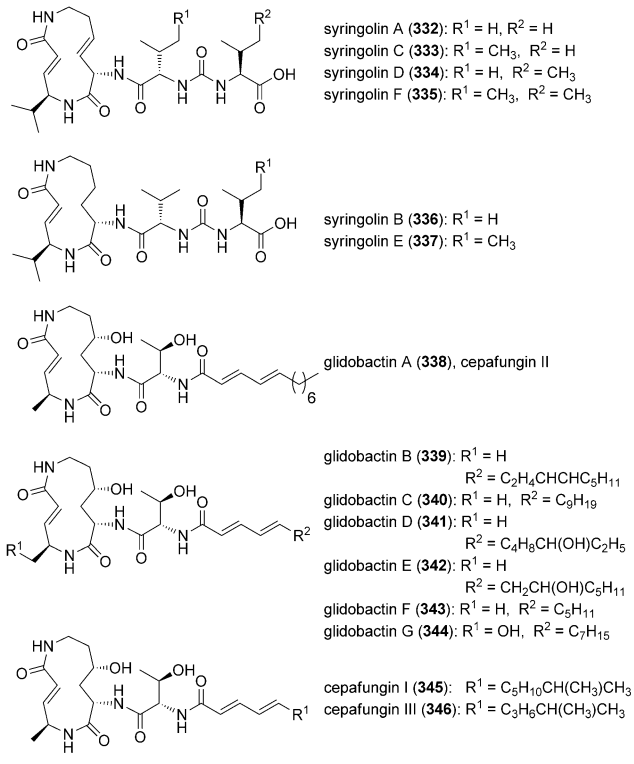


***Figure 21.*** The family of syrbactins natural products.

nized as new antitumor compounds.[145] The cepafungins were isolated from *Pseudomonas* species.[146]

In detailed investigations, Groll and Kaiser could demonstrate that syringolin A (**332**) inhibits preferentially the chymotrypsin unit with an apparent $K_i$ value of 843 nM.

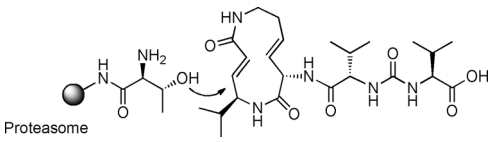


***Figure 22.*** The syrbactins act as a Michael acceptor on the proteasome.

Syringolin B, on the other hand, which lacks only the second double bond, was significantly less potent in inhibiting the β5-subunit ($K_i = 7.78$ μM).[147] Glidobactin A (**338**) exhibited an even more pronounced inhibitory activity ($K_i = 49$ nM).

Owing to their inhibitory activity, the syrbactins were the target molecules in syntheses conducted in various groups. First synthetic contributions were provided by Oka et al.,[148] who used the linear precursor obtained from the hydrolysis of glidobactin A (**338**) as the starting point for synthetic investigations towards ring closure. They were able to perform a macrolactamization using DCC and HOBt. The Schmidt group used a slightly different approach. They performed the macrolactamization on a substrate without the side chain attached, which was introduced at a later point (Scheme 50).[149] For their synthesis of syringolin B (**336**) Kaiser et al. employed a strategy that parallels Oka's approach. Their linear precursor was equipped with the appropriate protecting groups and after liberation of both the amino and the carboxyl group, PyBOP-mediated macrolactamization established syringolin B (**336**, Scheme 50).[148]

The Stephenson group also established a macrolactamization approach for syringolin A (**332**).[150] They started from Garner's aldehyde and employed a Johnson–Claisen rearrangement to obtain acid **353**. A Curtius rearrangement established amine **354** and condensation with **356** provided the linear intermediate **357**. Liberation of the terminal functionalities followed by amide formation with BOP and HOAt finalized their total synthesis of syringolin A (**332**, Scheme 51).

Two syntheses of syringolin A (**332**) using a metathesis approach were published by Kaiser et al.[149,151] Their strategy was to transform the second double bond into a diol and to re-establish that double bond after ring-closing metathesis. Treatment of the acetonide under acidic conditions and formation of the thiocarbonate with thiocarbonyl diimidazole generated the starting material for the subsequent Corey–Winter elimination. While in their first synthesis the Corey–Winter elimination was executed after introduction of the peptide side chain (Scheme 52), in their advanced second synthesis, elimination prior to introduction of the side chain provided an advanced intermediate that allows more convergent approaches and potentially the synthesis of various analogues (Scheme 53).

Pirrung and co-workers reported on a Wittig–Horner approach towards syringolin A (**332**).[152] Introduction of valinol and the phosphonate set the stage for a ring-closing olefination. As in the previously mentioned Kaiser synthesis, this strategy is convergent and allows for the synthesis of small libraries (Scheme 54).

 © 2013 Wiley-VCH Verlag GmbH & Co. KGaA, Weinheim 

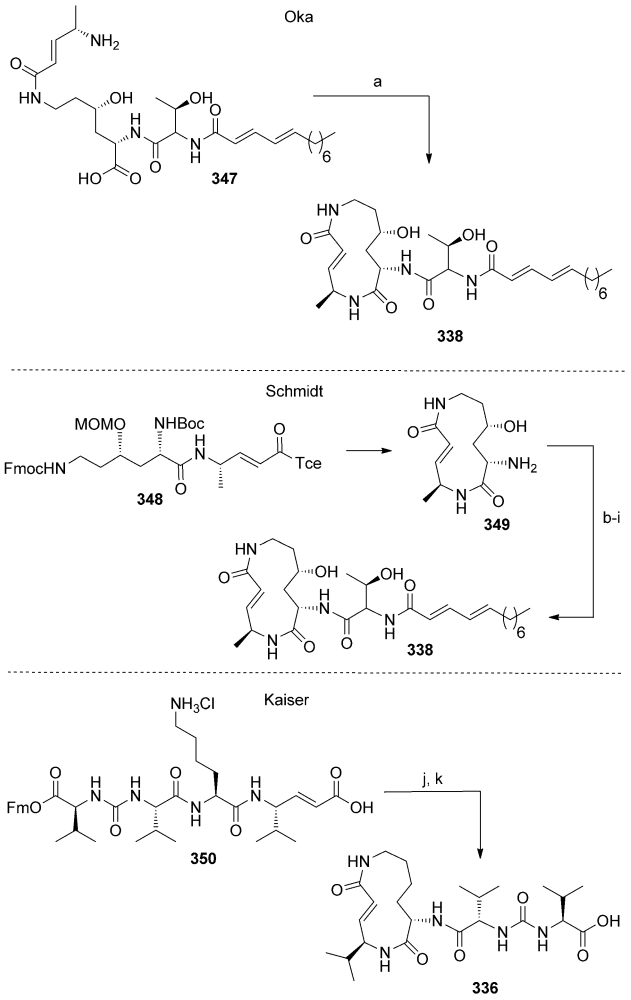


***Scheme 50.*** Macrolactamization strategies towards the syrbactins. Reagents and conditions: a) DCC, HOBt, DMF, 23%; b) AcOH, Zn, quant.; c) $CF_3CO_2C_6F_5$, pyr.; d) DBU, 4-pyrrolidinylpyridine, 20%, (2 steps); e) TFA, THF; f) Boc-Thr-Suc, DMAP, DMF, 72%, (2 steps; g) TFA, THF; h) (2*E*,4*E*)-dodecadienoic acid succinimido ester, *N*-methylmorpholine, DMF, 41 + 26%, (2 steps; i) TFA, THF, quant. j) PyBOP, HOAt, $iPr_2NEt$, DMF, 30%; k) piperidine, DMF, 73%.

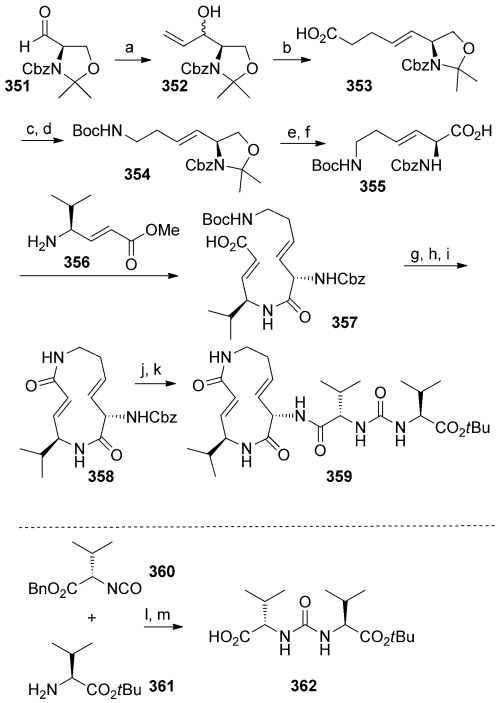


***Scheme 51.*** The Stepenson synthesis of syringolin A. Reagents and conditions: a) Vinylmagnesium bromide, THF, 86%; b) $CH_3C(OMe)_3$, propionic acid, xylene, 93%; c) LiOH, THF/$H_2O$, 96%; d) DPPA, TEA, toluene, *t*BuOH, 81%; e) *p*-TsOH, MeOH, 94%; f) $CrO_3$, aq. $H_2SO_4$, acetone, 78%; g) EDC, HOBt, $iPr_2NEt$, $CH_2Cl_2$, 70%; h) LiOH, THF/$H_2O$, 91%; i) TFA, $CH_2Cl_2$; j) BOP, HOAt, $iPr_2NEt$, DMF, 15%; k) $iPr_2NEt$, $CH_2Cl_2$, 97%; Pd/C, $H_2$, MeOH, 97%; l) HBr, acetic acid, quant.; m) BOP, HOAt, $iPr_2NEt$,DMF, $CH_2Cl_2$, 85%.

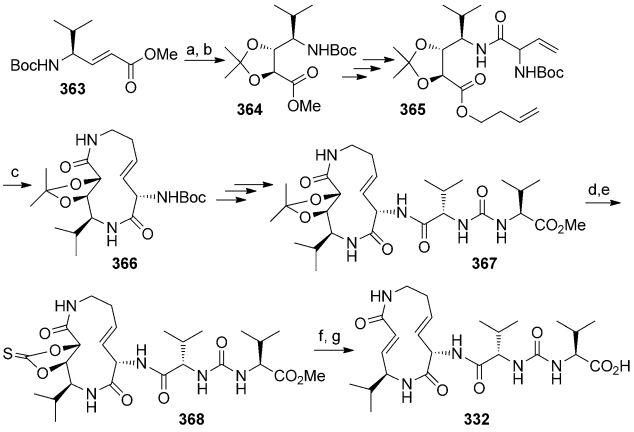


***Scheme 52.*** Kaiser's first metathesis approach towards the syringolins. Reagents and conditions: a) $OsO_4$, NMO, acetone/$H_2O$, 85%; b) 2,2-dimethoxypropane, PPTS, $CH_2Cl_2$, 98%; c) $H_2O_2$, $iPr_2NEt$, $CH_2Cl_2$, 93%; d) Grubbs II catalyst, toluene, 49%; e) $HCO_2H$/MeOH, 98%; f) thiocarbonyl diimidazole DMAP, THF, 89%; g) $P(OMe)_3$, 76%; $AlCl_3$, methylethylsulfide, 92%.

Using a slightly modified strategy, they were also able to complete the synthesis of syringolin B (**336**) by an olefination approach (Scheme 55).

These synthetic contributions set the stage for more detailed investigations on structure–activity relationship based on analogues and hybrid structures. In this context, Pirrung et al.[153] synthesized the oxa analogue **379** (TIR-203), SylB-LIP (**380**), and dGlbA-LIP (**383**). These compounds were compared to each other and to Kaiser's syringolin A analogue SylA-Lip[154] (**382**). In biological assays investigating the proliferation of SK-*N*-As and MYCN-2 neuroblastoma cell lines they found that oxa-SylA-Lip is the most active compound with **380** and **383** equally active and comparable to SylA-Lip (**382**). All of these compounds provide better activities than syringolin A (**332**), which has an activity of about 20 μM. Recently, Ibarra-Rivera and Pirrung[155] reported that the oxa analogue TIR-203 inhibits all three catalytic subunits in multiple myeloma cell lines in a dose-dependent manner (Figure 23).

In an additional effort to provide a more thorough understanding of the structure–activity relationship, the

 © 2013 Wiley-VCH Verlag GmbH & Co. KGaA, Weinheim 

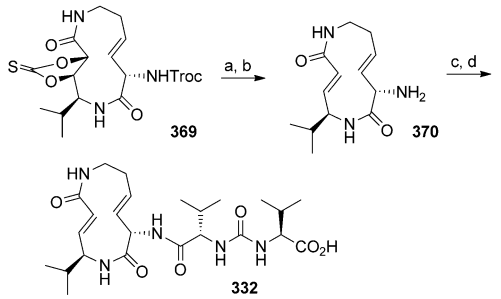

***Scheme 53.*** Kaiser's second metathesis approach towards the syringolins. Reagents and conditions: a) $P(OMe)_3$, 88%; b) Zn, AcOH, THF, 98%; c) urea, PyBOP, HOAt, $iPr_2NEt$, DMF, 95%; d) $AlBr_3$, tetrahydrothiophene, 84%.

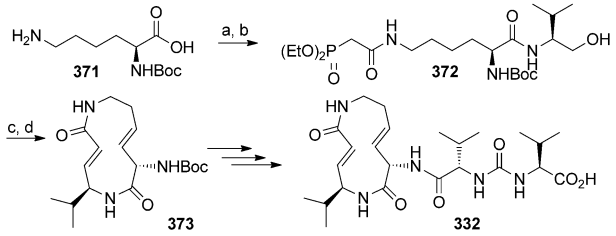

***Scheme 54.*** Pirrung's first Wittig–Horner approach. Reagents and conditions: a) $Na_2CO_3$, dioxane/$H_2O$; b) valinol, DCC, NHS, $CH_2Cl_2$, 75%; c) Dess–Martin periodinane, $CH_2Cl_2$; d) $Zn(OTf)_2$, TMEDA, THF, 65%.

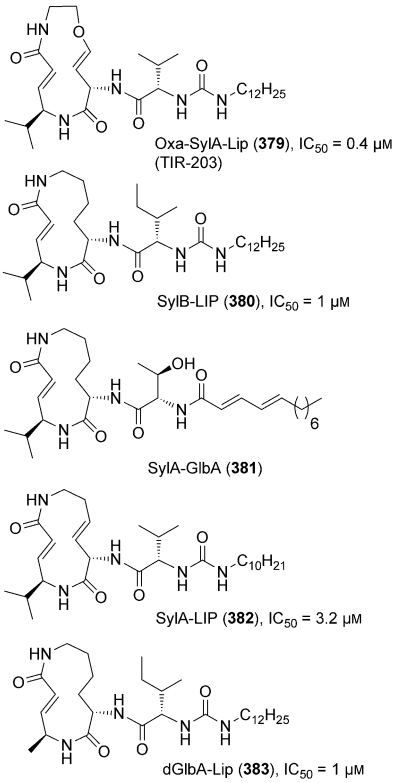

***Figure 23.*** Syringolin analogues.

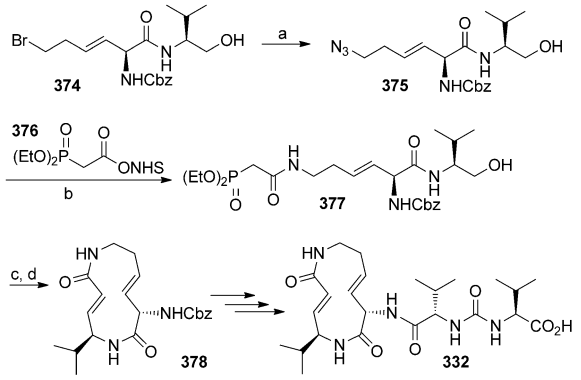

***Scheme 55.*** Pirrung's second olefination approach. Reagents and conditions. a) $NaN_3$, DMF, 100%; b) $PPh_3$, MeOH, c) $CH_2Cl_2$; d) Dess–Martin periodinane, $CH_2Cl_2$, e) $Zn(OTf)_2$, TMEDA, THF, 81%.

Kaiser and the Overkleeft groups joined to investigate hybrid molecules of the syringolins, epoxyketones, and vinyl sulfones.[155] Figure 24 shows the five most active compounds that feature the pharmacophoric groups of either the epoxyketones or the vinylsulfones in combination with side chains derived from syringolins. It should be mentioned that these epoxyketones exhibit additional activities at both the β1- and β2-subunits. In particular, compound **388** displays an unexpected, yet remarkable selectivity towards the β1-subunit.[156]

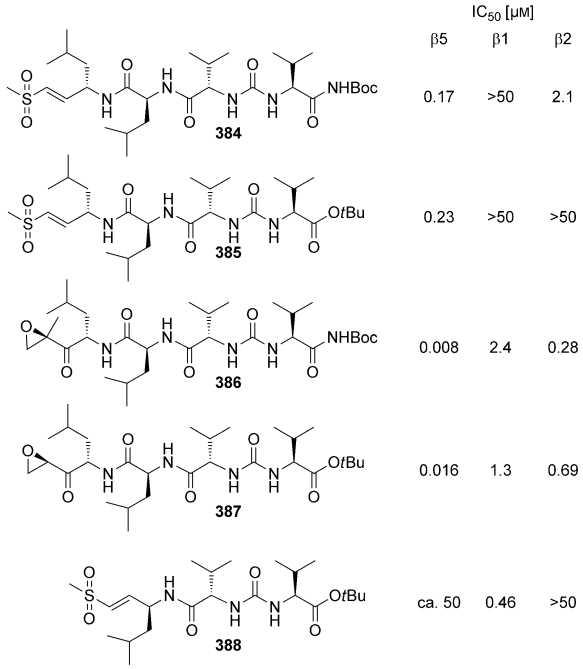


***Figure 24.*** Hybride compounds derived form epoxyketones, vinylsulfones, and syringolines.


© 2013 Wiley-VCH Verlag GmbH & Co. KGaA, Weinheim

## 12. TMC-95 A/B

### 12.1. Biological Activity

TMC-95 A–D (**389**–**392**; Figure 25) are four diastereomers of a new class of natural cyclic peptides. They have been recently isolated from the fermentation broth of *Apiospora montagnei* Sacc TC 1093 derived from soil samples.[157] TMC-

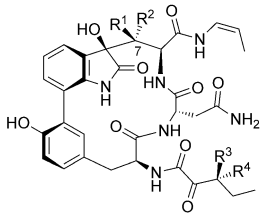

TMC-95 A (**389**): $R^1$ = H, $R^2$ = OH, $R^3$ = $CH_3$, $R^4$ = H
TMC-95 B (**390**): $R^1$ = H, $R^2$ = OH, $R^3$ = $CH_3$, $R^4$ = $CH_3$
TMC-95 C (**391**): $R^1$ = OH, $R^2$ = H, $R^3$ = $CH_3$, $R^4$ = H
TMC-95 D (**392**): $R^1$ = OH, $R^2$ = H, $R^3$ = H, $R^4$ = $CH_3$

***Figure 25.*** The family of TMC-95 compounds.

95 A (**389**) is the most potent proteasome inhibitor in this family of natural products. It inhibits the chymotrypsin-like (ChT-L), trypsin-like (T-L), and peptidoglutamyl-hydrolyzing (caspase-like, PGPH) activities of the 20S proteasome with $IC_{50}$ values of 5.4, 200, and 60 nmol, respectively. Inversion of the stereocenter at C7 has a dramatic effect on the $IC_{50}$ value of the inhibitors. While TMC-95 B (**390**) shows similar inhibition activities in the nanomolar range, the activities of the diastereomers TMC-95 C and D (**391**, **392**) are 20 to 150 times weaker. Therefore, the *S* configuration at this position is essential for inhibitory activities.

All of the proteasome inhibitors—the synthetic peptide aldehydes, boronates, and vinyl sulfones and also natural lactacystin and epoxomicin—lead to the covalent binding of the N-terminal threonine of the β-subunits.[158] TMC-95 A is one of the first examples of a proteasome inhibitor that functions through a noncovalent and reversible interaction. Even more importantly, the TMC-95 compounds inhibit the 20S proteasome specifically without inhibiting other proteases such as *m*-calpain, cathepsin L, and trypsin, as confirmed by NMR studies. Bonding interactions were revealed by crystal structures of TMC-95 A bound to the yeast 20S proteasome. Groll et al. thus confirmed that TMC-95 A is bound to all three active subunits of 20S proteasome through a tight network of hydrogen bonds.[159] The crystal structure also confirmed the significance of the C7 hydroxy group. The *S* configuration is present in the active inhibitors TMC-95 A and B, while the *R* configuration explains the weaker inhibition because of steric hindrance with the carbonyl oxygen of residue 21 in subunit β2. The orientation of TMC-95 A in the proteasome complex corresponds to that of epoxomicin. The *n*-propylene side chain binds to the proteasomal S1 pocket, while the asparagine side chain inserts into the S3 pocket. The ketoamide side chain is only weakly involved in protein interactions. Consequently, the stereocenter at C36 has only little influence on the biological activity.

The high biological activity and the molecular complexity attracted the attention of synthetic chemists. The interesting structural features of these inhibitors include the highly oxidized L-tryptophan and the aryl-oxindol ring attachment combined with the (*Z*)-1-propenyl amide and the 3-methyl-2-oxopentanoate side chain.

### 12.2. First Total Syntheses of TMC-95 A/B by Danishefsky

The first total syntheses of TMC-95 inhibitors were published by Lin and Danishefsky in 2002.[160] The retrosynthetic analysis by Danishefsky et al. utilizes a macrolactamization to establish the 17-membered macrocyclic core of TMC-95 A/B[161] with the bisaryl domain to be installed by a Suzuki-type coupling (Figure 26). The formation of the *cis*-propenyl amide side chain was one of the key challenges in the synthesis of TMC-95 A/B. The chemical instability of this moiety in acidic and basic media inspired Danishefsky et al. to develop a new method to generate *cis*-propenyl amides through the rearrangement–hydrolysis of α-silylallyl amides (Scheme 56).

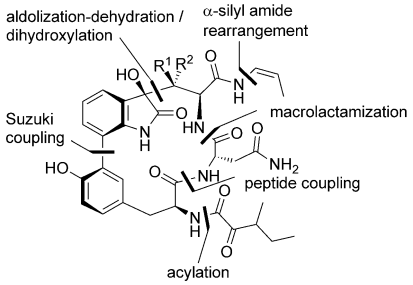


***Figure 26.*** Retrosynthetic analysis of the Danishefsky synthesis.

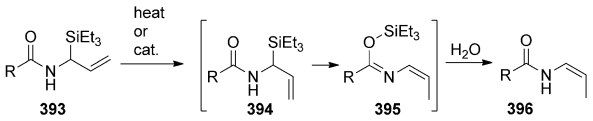


***Scheme 56.*** Synthesis of the *cis*-propenyl amide.

Remarkably, at 110 °C substrates like **393** undergo a concurrent ene and silatropic bond reorganization leading to **395**. Aqueous hydrolysis of these compounds afforded enamides **396** in good yields and with the *cis* product as the only observed isomer.

The synthesis of the biaryl fragment **403** of TMC-95 A and TMC-95 B started with iodooxindole **397**. Cross-aldol addition to Garner's aldehyde (**223**), followed by β-elimination of the derived mesylate afforded a 1:1.3 mixture of α,β-unsaturated lactams (*Z*)-**398** and (*E*)-**399**. An iodine-mediated isomerization converted the *Z* alkene to the desired *E* isomer. Boronic acid **402** was synthesized starting from L-tyrosine. A five-step procedure afforded the desired boronic

 © 2013 Wiley-VCH Verlag GmbH & Co. KGaA, Weinheim 

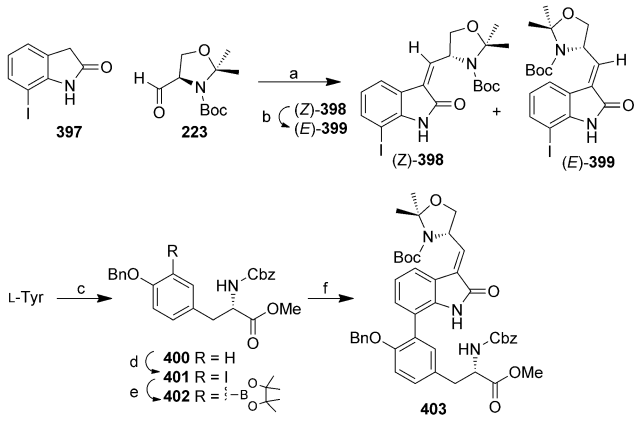


***Scheme 57.*** Synthesis of biaryl compound **403**. Reagents and conditions: a) LDA, THF, −78 °C, 1.5 h; $NEt_3$, MsCl, $CH_2Cl_2$, −70 °C→ −50 °C, 1.5 h; 81 % (*E*/*Z* = 1.3:1); b) $I_2$ (cat.), benzene, 80 °C, 26 h; DMP/PPTS, toluene, 65 °C, 5 h; 85 %; c) 1. MeOH/$SOCl_2$, 2. CbzCl/$K_2CO_3$; 3. BnBr, $Cs_2CO_3$, acetone, reflux; 88 %, 3 steps; d) $Ag_2SO_4/I_2$, MeOH, RT, 1 h; 99 %; e) pinacolatodiborane, $[PdCl_2(dppf)]\cdot CH_2Cl_2$, KOAc, DMSO, 80 °C, 10 h, 91 %; f) (*E*)-**399**, $[PdCl_2(dppf)]\cdot CH_2Cl_2$, $K_2CO_3$, DME, 80 °C, 2 h; 75 %.

acid in very good yields. Finally, fragments **400** and **402** were joined using a palladium-mediated Suzuki reaction (Scheme 57).[162]

The synthesis continued with hydrolysis of methyl ester **403** and peptide coupling with H-Asp-O*t*Bu. Subsequent Sharpless dihydroxylation introduced the hydroxy groups at C6 and C7 in a diastereomeric ratio of 5:1 relative to the 6*R*,7*S* stereoisomer (Scheme 58).

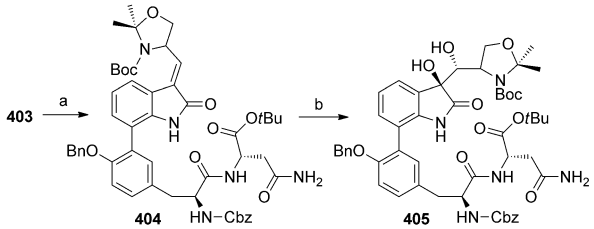


***Scheme 58.*** Synthesis of diol **405**. Reagents and conditions: a) 1) LiOH, THF/$H_2O$, 0 °C, 1.5 h; 2) H-Asn-O*t*Bu, EDC/HOAT, THF, RT, 2 h; 85 % (2 steps); b) $OsO_4$/NMO, $(DHQD)_2$-PHAL, *t*BuOH/$H_2O$, RT, 12 h; 88 % (d.r. = 5:1).

Starting from compound **405**, deprotection of the N,O-acetonide linkage and protection of the primary hydroxy group at C15 as a TIPS ether followed by hydrolysis of the *tert*-butyl ester with TFA afforded the precursor for the pivotal macrolactamization. Using standard peptide-coupling reagents (EDC, HOAT) the fully functionalized macrocyclic core **408** of TMC-95A/B was obtained. Finally, the 3-methyl-2-oxopentanoic acid side chain was introduced to establish **409a** and **409b** as a 1:1 mixture of diastereomers (Scheme 59).

Removal of the TIPS ether followed by protection of all four hydroxy groups as TES ethers led to compound **410**. The primary hydroxy group was selectively deprotected and

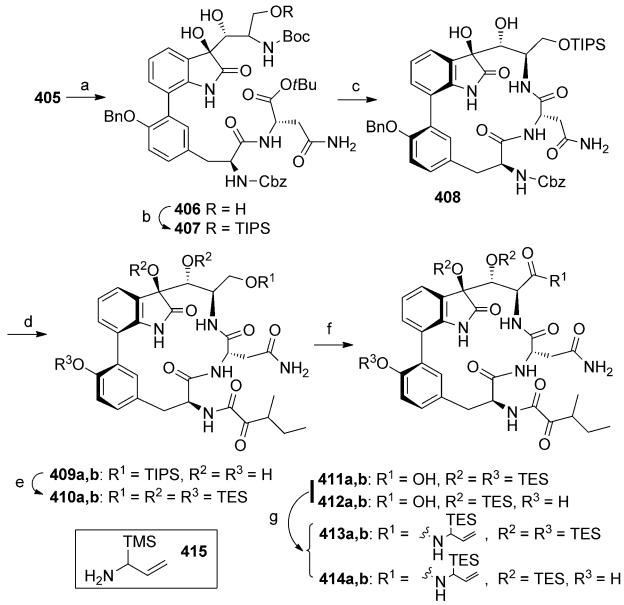


***Scheme 59.*** Synthesis of α-silylallyl amides **413a**,**b** and **414a**,**b**. Reagents and conditions: a) PPTS/MeOH, reflux, 2 h; b) TIPSCl, imidazole/DMAP, $CH_2Cl_2$, RT, 5 h; 88 % (2 steps); c) 1. TFA/$CH_2Cl_2$ (4:1), RT, 2 h; 2. EDC/HOAT/$iPr_2NEt$ , $CH_2Cl_2$/DMF(2 mM), RT, 24 h; 52 % (2 steps); d) 1. Pd/C, $H_2$, EtOH, RT, 19 h; 2. (±)-3-methyl-2-oxopentanoic acid, EDC/HOAT, $CH_2Cl_2$/DMF, RT, 2 h; 85 % (2 steps); e) 1. HF/Py; 2. TESOTf, 2,6-lutidine, $CH_2Cl_2$, 0 °C→RT, 15 h; 3. $NaHCO_3$; 4. citric acid, EtOAc/$H_2O$; 73 %; f) Jones reagent, acetone, 0 °C, 2 h; g) **415**, EDC/HOAT, $CH_2Cl_2$/DMF, RT, 13 h; 45 % (2 steps).

oxidized using Jones reagent which led to a mixture of **411a**,**b** and **412a**,**b** as a result of partial deprotection of the phenol moiety. Condensation with amine **415** generated the precursor for the construction of the (*Z*)-1-propenylamide unit.

The α-silylallyl amide was converted into the (*Z*)-1-propenyl amide by means of the previous described thermal rearrangement (Scheme 60). The crude mixture of these compounds was deprotected with HF/pyridine to afford a 1:1 mixture of TMC-95 A and B, which could be separated by reverse-phase HPLC. Thus, the first total synthesis of TMC-95 A (**389**) and TMC-95 B (**390**) was completed in 25 steps.

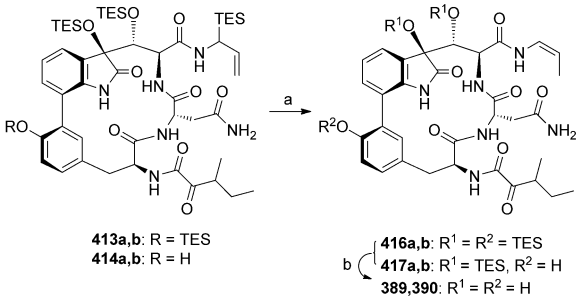


***Scheme 60.*** Synthesis of TMC-95A and TMC-95B. Reagents and conditions: a) 1. *o*-xylene, 140 °C, 3 d; 2. $H_2O$; b) HF/Py, THF/Py; then $Me_3SiOMe$; 49 % (2 steps).


© 2013 Wiley-VCH Verlag GmbH & Co. KGaA, Weinheim

### 12.3. Total Synthesis of TMC-95 A by Inoue and Hirama

Hirama, Inoue, and co-workers reported the stereoselective construction of TMC-95A (**389**) in 2003.[163] A first approach to the "northern" segment failed because of unsuccessful deprotection of the carbamate in presence of the labile propenylamide.[164] The modified route started with indole **418**. The important synthesis features are a stereoselective Mizoroki–Heck reaction and a diastereoselective oxidation/intramolecular epoxide reaction sequence (Figure 27). An advanced intermediate of their synthesis was obtained by a three-step procedure to convert oxindole **418** into iodide **419** (Scheme 61).

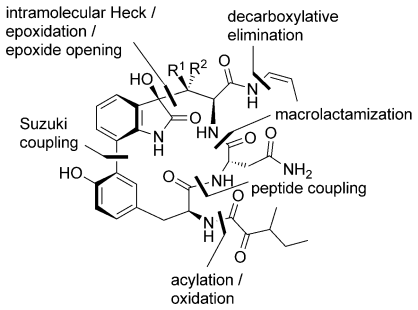


***Figure 27.*** Retrosynthetic disconnection according to Hirama.

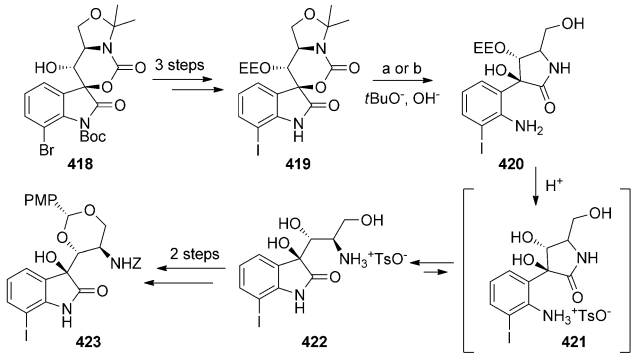


***Scheme 61.*** Synthesis of compound **423**. Reagents and conditions: a) KO*t*Bu (15 equiv), $H_2O$ (10 equiv), $Et_2O$, RT, 74%; b) KO*t*Bu (15 equiv), $H_2O$ (10 equiv), $Et_2O$, RT; then $H_2O$, TsOH, MeOH, RT.

The key step in the synthesis of the northern part was the removal of the unusually resistant carbamate group. Substantial experimentation identified conditions developed by Gassman et al.[165] as optimal. A combination of $OH^-$ and KO*t*Bu hydrolyzed both the carbamate and the acetonide with concomitant transamidation to provide aniline **420** in excellent yields (74%).

For the construction of the bisaryl moiety, aryl boronate **427** was synthesized from iodotyrosine derivative **424** and α-hydroxycarboxylic acid **425** using standard conditions. Two protection steps and the conversion of the iodide into the aryl boronate established **427** in 81% yield over three steps (Scheme 62).

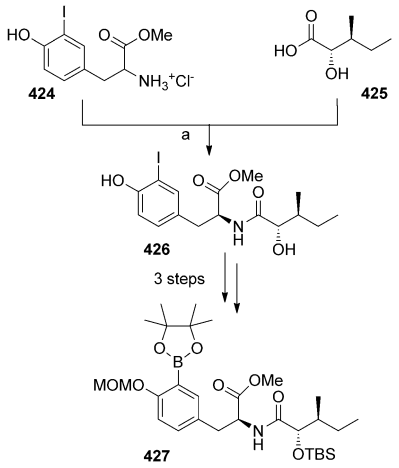


***Scheme 62.*** Synthesis of aryl boronate **427**. Reagents and conditions: a) **425** (2 equiv), EDC HCl, HOBt, 4-methylmorpholine, DMF, 0°C, 56%.

The biaryl domain was installed by a Suzuki reaction between aryl boronate **427** and iodide **423** in excellent yields (84%). Hydrolysis of methyl ester **428** and coupling with L-asparagine benzyl ester resulted in the fully functionalized acyclic TMC-95 core **430** (Scheme 63).

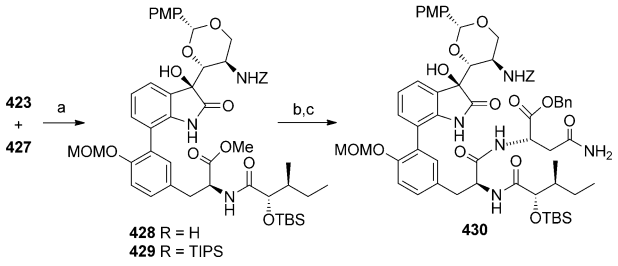


***Scheme 63.*** Synthesis of compound **430.** Reagents and conditions: a) **427** (1.5 equiv), $[Pd(PPh_3)_4]$, $Na_2CO_3$, DME/$H_2O$ (4:1), 95°C, 84%; b) LiOH, THF/$H_2O$ (1:1), 0°C; c) H-Asn-OBn TFA, EDC HCl, HOBt, DMF, 0°C, 75%.

Simultaneous cleavage of the benzyloxycarbonyl and the benzyl ester gave the seco acid, which could be cyclized to give macrolactam **431**. The introduction of the (*Z*)-propenylamide side chain required first the replacement of the TBS ether by the more labile TES ether and removal of the PMP acetal using buffered zinc triflate and ethanethiol. The primary hydroxy group of the resulting triol was selectively oxidized using the Parikh–Doering protocol followed by Pinnick oxidation. Final coupling with L-allothreonine benzyl ester followed by hydrogenolysis afforded β-hydroxycarboxylic acid **436**. Treatment with DEAD and triphenylphosphine induced a dehydrative decarboxylation to install the (*Z*)-propenylamide **437** as a single diastereoisomer through Grob-type *anti* elimination (Scheme 64).

Cleavage of the TES ether at C35 followed by Dess–Martin oxidation provided MOM-protected TMC-95 A in excellent yields. However, final removal of the MOM group proved to be problematic due the aforementioned reactivity

 © 2013 Wiley-VCH Verlag GmbH & Co. KGaA, Weinheim 

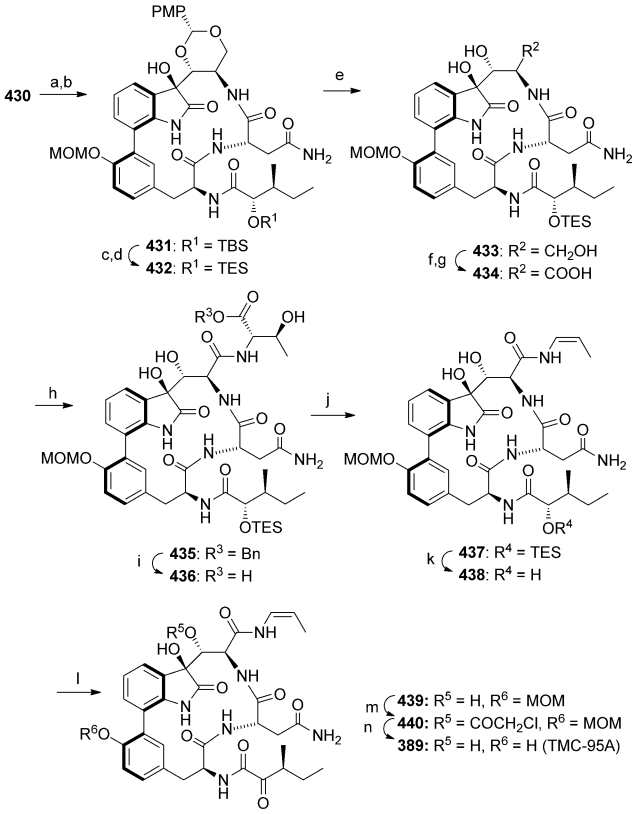


***Scheme 64.*** The Hirama synthesis. Reagents and conditions: a) $H_2$, $Pd(OH)_2$/C, THF/$H_2O$ (1:1); b) EDC·HCl, HOAt, DMF, 0 °C, 78 %.; c) TBAF, 4 Å MS, THF, 86 %; d) TESCl, imidazole, DMF, 85 %; e) Zn-$(OTf)_2$, EtSH, $NaHCO_3$, $CH_2Cl_2$, 100 %; f) $SO_3$·pyr, $Et_3N$, $CH_2Cl_2$/DMSO (3:1), RT; g) $NaClO_2$, $NaH_2PO_4$, 2-methyl-2-butene, *t*BuOH/$H_2O$ (5:1), RT; h) L-allo-Thr-OBn·TFA, EDC·HCl, HOBt, DMF, 0 °C, 67 %; i) $H_2$, $Pd(OH)_2$/C, THF/$H_2O$ (1:2); j) DEAD, $PPh_3$, 4 Å-MS, 0 °C→RT, 59 %; k) HF·pyridine, THF, 79 %; l) Dess–Martin periodinane, $CH_2Cl_2$, 80 %; m) $(ClCH_2CO)O$, pyridine, $CH_2Cl_2$, 0 °C; n) aqueous HCl (1 N)/THF (3:1), RT; then sat. aqueous $NaHCO_3$, 64 %.

of the propenyl amide moiety under acidic conditions. Therefore, temporary protection of the free hydroxy group at C7 as its chloroacetyl ester was necessary to avoid undesired side reactions. A one-pot protocol using acidic and basic conditions finally established TMC-95 A (**389**).

### *12.4. Total Synthesis by the Williams Group*

In 2003 Albrecht and Williams reported a concise formal synthesis of TMC-95 A (**389**) and B (**390**) by formation of a late-stage intermediate of the Danishefsky synthesis.[166] One year later, they reported their concise total synthesis using a strategy similar to that of the Hirama synthesis albeit with an optimized protecting-group strategy.[167] In analogy to the previously presented approaches, Williams et al. used a Suzuki coupling for formation of the bisaryl domain, a decarboxylation/elimination strategy to install the *cis*-propenyl amide, and a macrolactamization (Figure 28).

A remarkable feature of this synthesis is the formation of the highly oxidized tryptophan by a modified Julia coupling

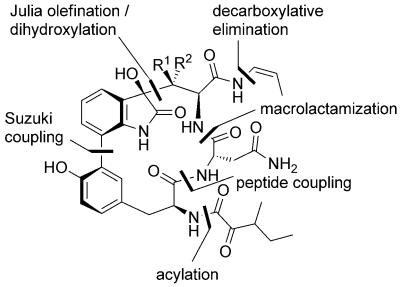


***Figure 28.*** The Williams retrosynthetic analysis of TMC-95 A/B.

followed by dihydroxylation of the double bond. The heteroaromatic sulfone was prepared by standard chemical transformations in four steps starting from *N*-Cbz-L-serine methyl ester. Julia olefination of **441** with 7-iodoisatin (**443**) provided the best results under conditions reported by Jacobsen et al.[168] and the the desired oxindole was obtained with an *E*/*Z* ratio of 5:1 (**444**/**445**) in 79 % yield (Scheme 65).

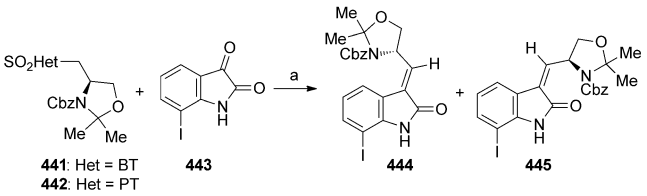


***Scheme 65.*** Modified Julia olefination. Reaction conditions: a) DMF, DMPU, LiHMDS, 0 °C, 79 % (*E*/*Z* = 5:1). Het = benzothiazolyl (BT) or 1-phenyl-1*H*-tetrazol-5-yl (PT).

The synthesis of the boronic ester **448**, required for the Suzuki reaction, started from commercially available 3-iodo-L-tyrosine (**446**) which was converted in three steps into the fully protected tyrosine derivative **447** and then to boronic ester **448** using the Miyaura protocol.[169] Suzuki coupling between fragment **448** and **444** with $K_2CO_3$ in refluxing aqueous dimethoxyethane catalyzed by dichloro[1,1′-bis-(diphenylphosphino)ferrocene]palladium generated the bisaryl unit **449** in 90 % yield (Scheme 66).

Saponification of methyl ester **449** followed by formation of the asparagine residue by peptide coupling with $NH_2$-Asn-OBn ester led to alkene **450**. The key dihydroxylation was mediated by $OsO_4$ in aqueous pyridine and afforded diol **451** as a single isomer in excellent yields (87 %).

To avoid problems in the last deprotection step (removal of the MOM group), Williams et al. decided to remove all acid-labile protecting groups with trifluoroacetic acid. The endgame of the synthesis of TMC-95 A/B parallels Danishefsky's synthesis including formation of the D,L-3-methyl-2-oxo-pentanoic acid side chain, macrolactamization, and the preparation of the enamide group (Scheme 67).

In summary this synthesis contains a minimum of protecting-group manipulations and provides TMC-95 A (**389**) and B (**390**) as a 1:1 mixture in 18 steps and in 4 % overall yield.


© 2013 Wiley-VCH Verlag GmbH & Co. KGaA, Weinheim

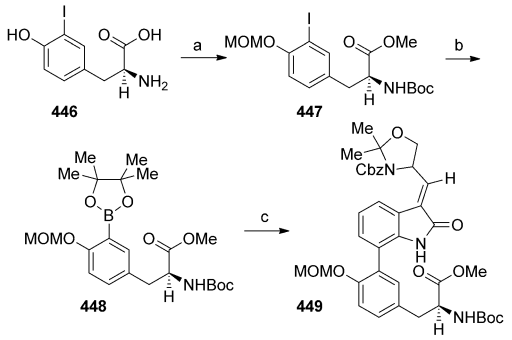

***Scheme 66.*** Suzuki biaryl formation. Reagents and conditions: a) 1. $SOCl_2$, MeOH, RT, 18 h; 2. di-*tert*-butyldicarbonate, saturated $NaHCO_3$, $CH_2Cl_2$, 0 °C→RT, 12 h; 3. chloromethyl methyl ether, diisopropylethylamine, $CH_2Cl_2$, 0 °C, 3 h, 95%, 3 steps; b) bis(pinacolato)diboron, KOAc, dichloro[1,1′-bis(diphenylphosphino)ferrocene]palladium, DMSO, 80 °C, 4 h, 80–89%; c) **444**, $K_2CO_3$, dichloro[1,1′-bis(diphenylphosphino)ferrocene]palladium, aqueous dimethoxyethane, reflux, 90%.

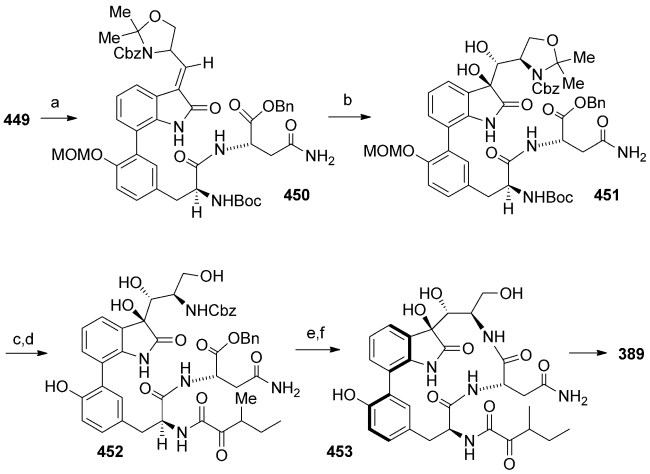

***Scheme 67.*** Preparation of the macrocyclic core. Reagents and conditions: a) 1. LiOH, THF, $H_2O$, 0 °C; 2. $H_2N$-Asn-OBn, HOAt, EDCl, diisopropylethylamine, $CH_2Cl_2$, 0 °C, 4 h, 98% (2 steps); b) $OsO_4$, pyridine, 0 °C, 1 h, and then saturated $NaHSO_3$, 87%; c) TFA/$H_2O$ (1:1), RT, 4 h; d) 3-methyl-2-oxopentanoic acid sodium salt, HOAt, EDC, THF, 0 °C, 98% (2 steps); e) Pd black, $H_2$, MeOH, RT, 6 h; f) EDC, HOAt, $CH_2Cl_2$, DMF (1:1), RT, 1 mM, 49%, 2 steps.

### 12.5. *Derivatives of TMC-95 A*

Owing to its excellent biological profile TMC-95 is an interesting lead structure for the synthesis of derivatives. While the TMC-95 A analogues developed by Danishefsky et al. retain the highly oxidized oxindol moiety, Moroder et al. synthesized analogues with a simplified TMC-95 core structure. Vidal et al. designed linear based TMC-95 proteasome inhibitors. However, these analogues differ substantially from the original natural products.

#### 12.5.1. *Moroder's Derivatives of TMC-95 A*

Inspired by the X-ray structure of TMC-95 A (**389**) as a complex with the 20S proteasome and in combination with molecular modeling studies, Moroder et al. identified the minimum structural binding motif of TMC-95A (**389**). Consequently, the TMC-95 A analogue **454** was chosen as the first synthetic target (Figure 29).[170]

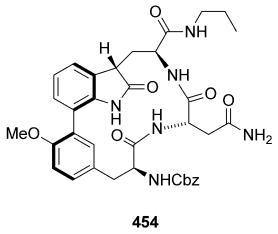

***Figure 29.*** Minimum binding motif of TMC-95 A.

The key key transformations in the synthesis are shown in Scheme 68. Aryl boronate **456** and the $N^{\alpha}$-Boc-propylamide derivative **455** were joined using standard Suzuki cross-coupling conditions. The peptide chain was extended with the

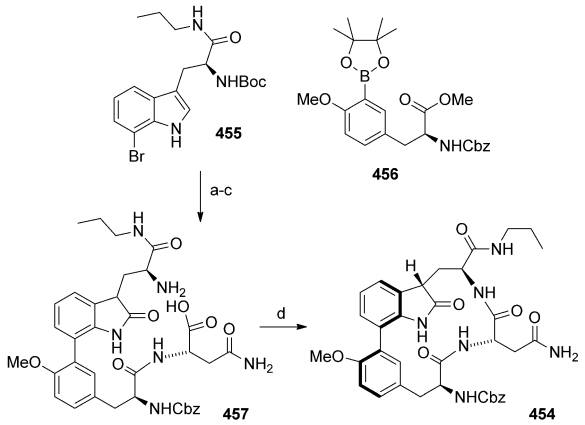

***Scheme 68.*** Reagents and conditions: a) $[Pd(dppf)Cl_2]\cdot CH_2Cl_2$ (5 mol%), $K_2CO_3$ (3 equiv), DME/$H_2O$ (7:1), 70 °C; b) H-Asn-*Ot*Bu, EDC, HOBt; c) DMSO (20 equiv), AcOH/HCl (4:1); d) PyBOP (4 equiv), HOBt (4 equiv), $iPr_2NEt$ (6 equiv).

asparagine *tert*-butyl ester by peptide coupling followed by a DMSO/HCl-mediated oxidation of the indole moiety to give the linear precursor **457**. Cyclization to the constrained ring structure was successfully performed using PyBOP/HOBt/$iPr_2NEt$ to afford macrolactam **454** as a single diastereoisomer.

Gratifyingly, only the isomer with correct configuration at the C3 stereocenter could be cyclized. Comparison of the $IC_{50}$ values of **454** to those of TMC-95 A (**389**) showed that it has similar activity against TL and PGPH but it is approximately 100 times less potent as an inhibitor of the chymotrypsin-like activity. This substantial decrease of inhibition was attributed

 © 2013 Wiley-VCH Verlag GmbH & Co. KGaA, Weinheim 

to exchanging the (*Z*)-1-propenylamide with the more flexible propylamide side chain.

Derivative **458**, which exhibits an extended side chain, was synthesized to analyze the substrate-binding mode. The more flexible biaryl ether derivatives **459** and **460** were accessed by an intramolecular aromatic nucleophilic displacement.[171] Compound **459** was in particular valuable since it was possible to get a crystal structure analysis of this compound bound to the yeast 20S proteasome (Figure 30).

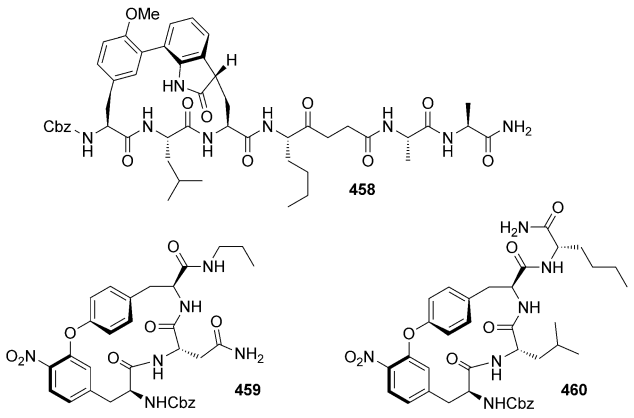


***Figure 30.*** Simplified TMC-95 analogues.

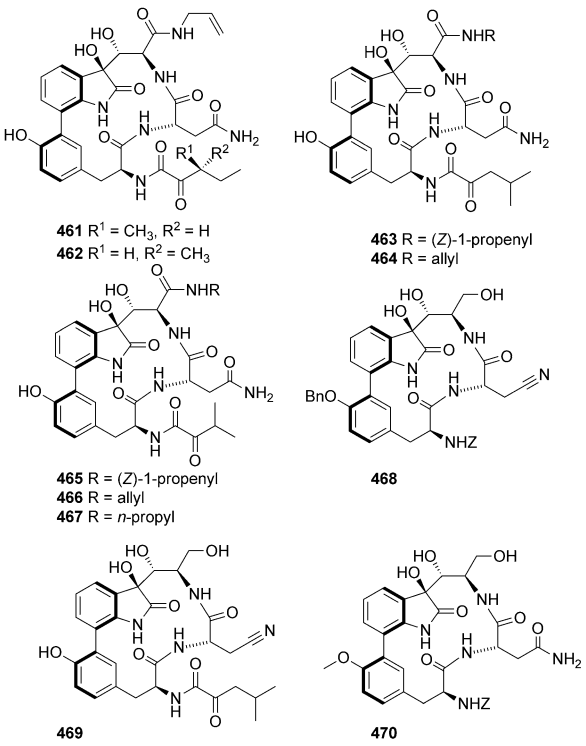


***Figure 31.*** Danishefsky's analogues of TMC-95 A.

### *12.5.2.* ***Danishefsky's Derivatives of TMC-95 A***

Their approach towards the first total synthesis of TMC-9 5A/B allowed Danishefsky and co-workers to synthesize late-stage derivatives of TMC-95 A. In order to explore first structure–activity relationships and to reduce the number of impractical synthetic steps Danishefsky et al. designed the TMC-95 analogues **461**–**470**.[172] When the enamide function was replaced with a less labile allylamide and the C36 stereocenter was eliminated the resulting derivative still displayed biological activity. On the other hand, the *n*-propylamide analogue **467** was 10 times less active than TMC-95 A and B as well as **465**.[173] Also, triols **469** and **470** showed a lower activity than compounds exhibiting the enamide or allylamide side chain (Figure 31).

### *12.5.3.* ***Vidal's Derivatives of TMC-95 A***

In 2003, Vidal and co-workers reported the synthesis of three cyclic TMC-95 A derivatives (**471**; Figure 32).[174] The key step of their synthesis contained an intramolecular Ullmann-type reaction to form the macrocycle. These simplified analogues contain simplified peptide side chains and the highly oxidized oxindol was replaced by simple indole moieties. Recently, another publication described the design of over 45 linear TMC-95-based proteasome inhibitors.[175]

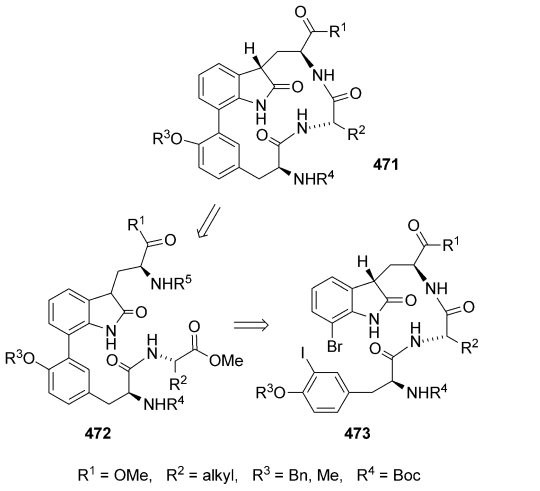


***Figure 32.*** Vidal's derivatives of TMC-95 A.

## *13. Conclusion*

Proteasome inhibitors have emerged as promising compounds for the treatment of malignancies. Even though one had expected that a pivotal target such as the proteasome would never lead to specific inhibitors, it was shown that certain small molecules are able to selectively increase the cellular level of cell cycle regulators such as p27. Starting out from peptide aldehydes and boronates, other natural products have served as the starting point for a thorough drug-development process which has culminated in the introduction of new drugs. Since even at the present stage of research


© 2013 Wiley-VCH Verlag GmbH & Co. KGaA, Weinheim

the reactive groups among these natural products as well as their overall structure differ substantially, they may act as starting points for inhibitors for more specific antitumor treatment. To harvest their potential and fulfill the expectations of society, the joint efforts of synthetic and medicinal groups as well as cooperation between academia and industry are essential.

## Abbreviations

| | |
|---|---|
| (1*S*,1′*S*,2*R*,2′*R*)-DuanPhos | (1*S*,1′*S*,2*R*,2′*R*)-2,2′-di-*tert*-butyl-2,3,2′,3′-tetrahydro-1*H*,1′*H*(1,1′)biisophosphindolyl |
| $(Boc)_2O$ | di-*tert*-butyldicarbonate |
| $(DHQD)_2$-PHAL | 1,4-bis(9-*O*-dihydroquinidine)phthalazine |
| (Icy)CuO*t*Bu | (1,3-dicyclohexylimidazol-2-ylidene)copper(I)-*tert*-butoxide |
| 4-PPY | 4-pyrrolidinopyridine |
| Abu | aminobutyric acid |
| AIBN | azobisisobutyronitrile |
| Asn | asparagine |
| AZADO | 2-azaadamantane-*N*-oxyl |
| $B_2pin_2$ | bis(pinacolato)diborane |
| Belleau's reagent | 2,4-bis(4-phenoxyphenyl)-1,3-dithia-2,4-diphosphetane-2,4-disulfide |
| Bn | benzyl |
| Boc | *tert*-butoxycarbonyl |
| BOP | benzotriazol-1-yloxytris(dimethylamino)-phosphonium hexafluorophosphate |
| CAN | ceric ammonium nitrate |
| Cbz | benzyloxycarbonyl |
| CbzCl | benzyl chloroformate |
| CSA | camphor sulfonic acid |
| DBU | 1,8-diazabicyclo[5.4.0]undec-7-ene |
| DCC | *N*,*N*′-dicyclohexylcarbodiimide |
| DEAD | diethyl azodicarboxylate |
| DIBAL-H | diisobutylaluminum hydride |
| DMAP | 4-dimethylaminopyridine |
| DMDO | dimethyldioxirane |
| DME | 1,2-dimethoxyethane |
| DME | dimethoxyethane |
| DMF | *N*,*N*-dimethylformamide |
| DMP | 2,2-dimethoxypropane |
| DMPU | *N*,*N*-dimethylpropylene urea |
| DPPA | diphenylphosphoryl azide |
| dppf | bis(diphenylphosphanyl)ferrocene |
| EDC | *N*-(3-dimethylaminopropyl)-*N*′-ethylcarbodiimide hydrochloride |
| Fmoc | fluorenylmethoxycarbonyl |
| GDH | glucose dehydrogenase |
| HATU | *O*-(7-azabenzotriazol-1-yl)-*N*,*N*,*N*′,*N*′-tetramethyluronium hexafluorophosphate |
| HBTU | *O*-(benzotriazol-1-yl)-*N*,*N*,*N*′,*N*′-tetramethyluronium hexafluorophosphate |
| HMPA | hexamethylphosphoramide |
| HOAt | 1-hydroxy-7-azabenzotriazole |
| HOBt | 1-hydroxy-1*H*-benzotriazole |
| IBX | 2-iodoxybenzoic acid |
| KRED-EXP-B1Y | ketoreductase |
| LDA | lithium diisopropylamide |
| LiHMDS | lithium hexamethyldisilazide |
| MOM | methoxymethyl |
| MS | molecular sieves |
| MsCl | methanesulfonyl chloride |
| $NAD^+$ | nicotinamide adenine dinucleotide |
| NHS | *N*-hydroxysuccinimide |
| NMM | *N*-methylmorpholine |
| NMO | 4-methylmorpholine *N*-oxide |
| NMP | 1-methyl-2-pyrrolidinone |
| PCC | pyridinium chlorochromate |
| PMBCl | 4-methoxybenzyl chloride |
| PMP | 4-methoxyphenyl |
| PPTS | pyridinium *p*-toluenesulfonate |
| *p*-TsOH | *p*-toluenesulfonic acid |
| PyBOP | benzotriazol-1-yloxytris(pyrrolidino)phosphonium hexafluorophosphate |
| PyBroP | bromotris(pyrrolidino)phosphonium hexafluorophosphate |
| pyr | pyridine |
| Suc | succinimido |
| TBAF | tetrabutylammonium fluoride |
| TBDPSCl | *tert*-butylchlorodiphenylsilane |
| TBTU | *O*-(benzotriazol-1-yl)-*N*,*N*,*N*′,*N*′-tetramethyluronium tetrafluoroborate |
| Tce | 2,2,2-trichlorethyl |
| TEA | triethylamine |
| TES | triethylsilyl |
| TFA | trifluoroacetic acid |
| TFAA | trifluoroacetic anhydride |
| TMEDA | *N*,*N*,*N*′,*N*′-tetramethylethylenediamine |
| TsCl | *p*-toluenesulfonyl chloride |
| TsOH | *p*-toluenesulfonic acid |

*We acknowledge valuable input from Prof. Dr. M. Kaiser and Prof. Dr. H. Overkleeft during the preparation of this review.*

Received: September 30, 2012
Published online: March 25, 2013

[1] a) A. Ciechanover, H. Heller, S. Elias, A. L. Haas, A. Hershko, *Proc. Natl. Acad. Sci. USA* **1980**, *77*, 1365–1368; b) A. Ciechanover, *Angew. Chem.* **2005**, *117*, 6095–6119; *Angew. Chem. Int. Ed.* **2005**, *44*, 5944–5967.

[2] P. M. Kloetzel, E. Krüger, U. Seifert, F. Ebstein, *FEBS J.* **2011**, *278*, 12–13.

[3] a) A. Ciechanover, A. L. Schwartz, *Proc. Natl. Acad. Sci. USA* **1998**, *95*, 2727–2730; b) A. Ciechanover, *Biochem. Soc. Trans.* **2003**, *31*, 474–481; c) A. L. Goldberg, K. Rock, *Nat. Med.* **2002**, *8*, 338–340; d) C. M. Pickart, *Cell* **2004**, *116*, 181–190; e) A. Navon, A. Ciechanover, *J. Biol. Chem.* **2009**, *284*, 33713–33718.

[4] a) K. Nasmyth, *Annu. Rev. Genet.* **2001**, *35*, 673–745; b) M. G. Goebl, J. Yochem, S. Jentsch, J. P. McGrath, A. Varshavsky, B. Byers, *Science* **1988**, *241*, 1331–1335; c) M. Glotzer, A. W. Murray, M. W. Kirschner, *Nature* **1991**, *349*, 132–138.

[5] M. Scheffner, J. M. Huibregtse, R. D. Vierstra, P. M. Howley, *Cell* **1993**, *75*, 495–505.

[6] R. Honda, H. Tanaka, H. Yasuda, *FEBS Lett.* **1997**, *420*, 25–27.

 © 2013 Wiley-VCH Verlag GmbH & Co. KGaA, Weinheim 

[7] a) E. Krüger, P. M. Kloetzel, *Curr. Opin. Immunol.* **2012**, *24*, 77 – 83; b) U. Seifert, L. P. Bialy, F. Ebstein, D. Bech-Otschir, A. Voigt, F. Schroter, T. Prozorovski, N. Lange, J. Steffen, M. Rieger, U. Kuckelkorn, O. Aktas, P. M. Kloetzel, E. Kruger, *Cell* **2010**, *142*, 613 – 624; c) E. Sijts, P. M. Kloetzel, *Cell. Mol. Life Sci.* **2011**, *68*, 1491 – 1502; d) Z. J. Chen, J. Hagler, V. J. Palombella, F. Melandri, D. Scherer, D. Ballard, T. Maniatis, *Genes Dev.* **1995**, *9*, 1586 – 1597.

[8] C. L. Ward, S. Omura, R. R. Kopito, *Cell* **1995**, *83*, 121 – 127.

[9] a) P. M. Voorhees, R. Z. Orlowski, *Annu. Rev. Pharmacol. Toxicol.* **2006**, *46*, 189 – 213; b) U. Testa, *Curr. Drug Targets* **2009**, *10*, 968 – 981; c) J. Sterz, I. von Metzler, J. C. Hahne, B. Lamottke, J. Rademacher, U. Heider, E. Terpos, O. Sezer, *Expert Opin. Invest. Drugs* **2008**, *17*, 879 – 895; d) P. M. Kloetzel, *Gene Ther.* **1998**, *5*, 1297 – 1298.

[10] a) J. Piotrowski, R. Beal, L. Hoffman, K. D. Wilkinson, R. E. Cohen, C. M. Pickart, *J. Biol. Chem.* **1997**, *272*, 23712 – 23721; b) C. M. Pickart, D. Fushman, *Curr. Opin. Chem. Biol.* **2004**, *8*, 610 – 616.

[11] a) M. Hochstrasser, *Cell* **2006**, *124*, 27 – 34; b) T. Ravid, M. Hochstrasser, *Nat. Cell Biol.* **2007**, *9*, 422 – U109; c) W. Li, D. Q. Tu, A. T. Brunger, Y. H. Ye, *Nature* **2007**, *446*, 333 – 337.

[12] a) D. Finley, *Annu. Rev. Biochem.* **2009**, *78*, 477 – 513; b) E. Genin, M. Reboud-Ravaux, J. Vidal, *Curr. Top. Med. Chem.* **2010**, *10*, 232 – 256.

[13] a) L. Huang, D. Yu, K. Ho, K. Qian, K.-H. Lee, C.-H. Chen, *Bioorg. Med. Chem.* **2008**, *16*, 6696 – 6701; b) M. Rechsteiner, C. P. Hill, *Trends Cell Biol.* **2005**, *15*, 27 – 33; c) W. Baumeister, J. Walz, F. Zühl, E. Seemüller, *Cell* **1998**, *92*, 367 – 380; d) M. Groll, W. Heinemeyer, S. Jager, T. Ullrich, M. Bochtler, D. H. Wolf, R. Huber, *Proc. Natl. Acad. Sci. USA* **1999**, *96*, 10976 – 10983.

[14] a) E. M. Huber, M. Groll, *Angew. Chem.* **2012**, *124*, 8838 – 8850; *Angew. Chem. Int. Ed.* **2012**, *51*, 8708 – 8720; b) L. Borissenko, M. Groll, *Chem. Rev.* **2007**, *107*, 687 – 717; c) M. A. Gräwert, M. Groll, *Chem. Commun.* **2012**, *48*, 1364 – 1378.

[15] M. A. Gräwert, N. Gallastegui, M. Stein, B. Schmidt, P. M. Kloetzel, R. Huber, M. Groll, *Angew. Chem.* **2011**, *123*, 563 – 566; *Angew. Chem. Int. Ed.* **2011**, *50*, 542 – 544.

[16] a) J. S. Schneekloth, C. M. Crews, *Curr. Drug Targets* **2011**, *12*, 1581 – 1594; b) K. B. Kim, C. M. Crews, *J. Med. Chem.* **2008**, *51*, 2600 – 2605.

[17] A. F. Kisselev, W. A. van der Linden, H. S. Overkleeft, *Chem. Biol.* **2012**, *19*, 99 – 15.

[18] M. Groll, R. Huber, L. Moroder, *J. Pept. Sci.* **2009**, *15*, 58 – 66.

[19] S. Tsukamoto, H. Yokosawa, *Curr. Med. Chem.* **2007**, *13*, 745 – 754.

[20] I. Nickeleit, S. Zender, F. Sasse, R. Geffers, G. Brandes, I. Sorensen, H. Steinmetz, S. Kubicka, T. Carlomagno, D. Menche, I. Gutgemann, J. Buer, A. Gossler, M. P. Manns, M. Kalesse, R. Frank, N. P. Malek, *Cancer Cell* **2008**, *14*, 23 – 35.

[21] A. Arlt, I. Bauer, C. Schafmayer, J. Tepel, S. S. Muerkoster, M. Brosch, C. Roder, H. Kalthoff, J. Hampe, M. P. Moyer, U. R. Folsch, H. Schafer, *Oncogene* **2009**, *28*, 3983 – 3996 and references therein.

[22] S. Tsukamoto, H. Yokosawa, *Expert Opin. Ther. Targets* **2009**, *13*, 605 – 621.

[23] H. J. Yang, G. Q. Shi, Q. P. Dou, *Mol. Pharmacol.* **2007**, *71*, 426 – 437.

[24] P. Bargagna-Mohan, P. P. Ravindranath, R. Mohan, *Invest. Ophthalmol. Visual Sci.* **2006**, *47*, 4138 – 4145.

[25] a) I. Vandenberghe, L. Creancier, S. Vispe, J. P. Annereau, J. M. Barret, I. Pouny, A. Samson, Y. Aussagues, G. Massiot, F. Ausseil, C. Bailly, A. Kruczynski, *Biochem. Pharmacol.* **2008**, *76*, 453 – 462; b) M. Kawai, T. Matsuura, *Tetrahedron* **1970**, *26*, 1743 – 1745.

[26] a) Y. Dai, J. DeSano, W. H. Tang, X. J. Meng, Y. Meng, E. Burstein, T. S. Lawrence, L. A. Xu, *Plos One* **2010**, *5*, e14153; b) T. Lenda, J. Konieczny, D. Jantas, M. Zapala, E. Lorenc-Koci, *Pharmacol. Rep.* **2009**, *61*, 359 – 360; c) S. Walcott, J. J. Heikkila, *Biochem. Cell Biol.* **2010**, *88*, 417 – 417; d) S. E. Walcott, J. J. Heikkila, *Comp. Biochem. Physiol. Part A* **2010**, *156*, 285 – 293; e) W. B. Wang, L. X. Feng, Q. X. Yue, W. Y. Wu, S. H. Guan, B. H. Jiang, M. Yang, X. Liu, D. A. Guo, *J. Cell. Physiol.* **2012**, *227*, 2196 – 2206; f) H. J. Yang, D. Chen, Q. Z. C. Cui, X. Yuan, Q. P. Dou, *Cancer Res.* **2006**, *66*, 4758 – 4765.

[27] S. Tsukamoto, M. Tatsuno, R. W. M. van Soest, H. Yokosawa, T. Ohta, *J. Nat. Prod.* **2003**, *66*, 1181 – 1185.

[28] a) K. Osanai, V. Milacic, Q. P. Dou, T. H. Chan, *Heterocycles* **2008**, *76*, 485 – 505; b) S. R. Choudhury, S. Balasubramanian, Y. C. Chew, B. S. Han, V. E. Marquez, R. L. Eckert, *Carcinogenesis* **2011**, *32*, 1525 – 1532; c) B. Bannerman, L. Xu, M. Jones, C. Tsu, J. Yu, P. Hales, J. Monbaliu, P. Fleming, L. Dick, M. Manfredi, C. Claiborne, J. Bolen, E. Kupperman, A. Berger, *Cancer Chemother. Pharmacol.* **2011**, *68*, 1145 – 1154.

[29] S. Tsukamoto, T. Wakana, K. Koimaru, T. Yoshida, M. Sato, T. Ohta, *Biol. Pharm. Bull.* **2005**, *28*, 1798 – 1800.

[30] a) D. Chen, K. R. Landis-Piwowar, M. S. Chen, Q. P. Dou, *Breast Cancer Res.* **2007**, *9*, R80; b) Y. X. Wu, X. Fang, *Planta Med.* **2010**, *76*, 128 – 132.

[31] a) D. Chen, K. G. Daniel, M. S. Chen, D. J. Kuhn, K. R. Landis-Piwowar, Q. P. Dou, *Biochem. Pharmacol.* **2005**, *69*, 1421 – 1432; b) D. Chen, M. S. Chen, Q. C. Cui, H. J. Yang, Q. P. Dou, *Front. Biosci.* **2007**, *12*, 1935 – 1945; c) K. Plochmann, G. Korte, E. Koutsilieri, E. Richling, P. Riederer, A. Rethwilm, P. Schreier, C. Scheller, *Arch. Biochem. Biophys.* **2007**, *460*, 1 – 9.

[32] A. Kazi, K. G. Daniel, D. M. Smith, N. B. Kumar, Q. P. Dou, *Biochem. Pharmacol.* **2003**, *66*, 965 – 976.

[33] A. Dreiseitel, P. Schreier, A. Oehme, S. Locher, G. Rogler, H. Piberger, G. Hajak, P. G. Sand, *Biochem. Biophys. Res. Commun.* **2008**, *372*, 57 – 61.

[34] a) M. Kroll, F. Arenzana-Seisdedos, F. Bachelerie, D. Thomas, B. Friguet, M. Conconi, *Chem. Biol.* **1999**, *6*, 689 – 698; b) A. Paugam, C. Creuzet, J. Dupouy-Camet, M. P. Roisin, *Parasitol. Res.* **2002**, *88*, 785 – 787; c) T. Hatabu, M. Hagiwara, N. Taguchi, M. Kiyozawa, M. Suzuki, S. Kano, K. Sato, *Exp. Parasitol.* **2006**, *112*, 179 – 183.

[35] a) T. Isoe, M. Naito, A. Shirai, R. Hirai, T. Tsuruo, *Biochim. Biophys. Acta* **1992**, *1117*, 131 – 135; b) T. Oki, Y. Matsuzawa, A. Yoshimoto, K. Numata, I. Kitamura, S. Hori, A. Takamatsu, H. Umezawa, M. Ishizuka, H. Naganawa, H. Suda, M. Hamada, T. Takeuchi, *J. Antibiot.* **1975**, *28*, 830 – 834; c) S. Hori, M. Shirai, S. Hirano, T. Oki, T. Inui, S. Tsukagoshi, M. Ishizuka, T. Takeuchi, H. Umezawa, *Gann* **1977**, *68*, 685 – 690.

[36] a) M. E. Figueiredo-Pereira, W. E. Chen, J. R. Li, O. Johdo, *J. Biol. Chem.* **1996**, *271*, 23602; b) M. E. Figueiredo-Pereira, W. E. Chen, J. R. Li, O. Johdo, *J. Biol. Chem.* **1996**, *271*, 16455 – 16459.

[37] L. Margarucci, M. C. Monti, A. Tosco, R. Riccio, A. Casapullo, *Angew. Chem.* **2010**, *122*, 4052 – 4055; *Angew. Chem. Int. Ed.* **2010**, *49*, 3960 – 3963.

[38] A. F. Kisselev, M. Garcia-Calvo, H. S. Overkleeft, E. Peterson, M. W. Pennington, H. L. Ploegh, N. A. Thornberry, A. L. Goldberg, *J. Biol. Chem.* **2003**, *278*, 35869 – 35877.

[39] a) B. Xu, B. Monsarrat, J. E. Gairin, E. Girbal-Neuhauser, *Fundam. Clin. Pharmacol.* **2004**, *18*, 171 – 180; b) J. Terrasson, B. Xu, M. Li, S. Allart, J. L. Davignon, L. H. Zhang, K. Wang, C. Davrinche, *Fundam. Clin. Pharmacol.* **2007**, *21*, 281 – 289.

[40] I. E. Mohamed, S. Kehraus, A. Krick, G. M. König, G. Kelter, A. Maier, H. H. Fiebig, M. Kalesse, N. P. Malek, H. Gross, *J. Nat. Prod.* **2010**, *73*, 2053 – 2056.


© 2013 Wiley-VCH Verlag GmbH & Co. KGaA, Weinheim

[41] A. M. Santoro, M. C. Lo Giudice, A. D'Urso, R. Lauceri, R. Purrello, D. Milardi, *J. Am. Chem. Soc.* **2012**, *134*, 10451 – 10457.

[42] a) S. Tsukamoto, R. Yamanokuchi, M. Yoshitomi, K. Sato, T. Ikeda, H. Rotinsulu, R. E. P. Mangindaan, N. J. de Voogd, R. W. M. van Soest, H. Yokosawa, *Bioorg. Med. Chem. Lett.* **2010**, *20*, 3341 – 3343; b) C. X. Liu, X. L. Tang, P. L. Li, G. Q. Li, *Org. Lett.* **2012**, *14*, 1994 – 1997; c) S. A. Dyshlovoy, I. Naeth, S. Venz, S. N. Fedorov, L. K. Shubina, V. A. Stonik, S. Balabanov, F. Honecker, *Ann. Oncol.* **2012**, *23*, 28; d) S. A. Dyshlovoy, I. Naeth, S. Venz, L. K. Shubina, S. N. Fedorov, V. A. Stonik, S. Balabanov, F. Honecker, *Ann. Oncol.* **2012**, *23*, 32; e) S. A. Dyshlovoy, I. Naeth, S. Venz, M. Preukschas, H. Sievert, C. Jacobsen, L. K. Shubina, M. G. Salazar, C. Scharf, R. Walther, M. Krepstakies, P. Priyadarshini, J. Hauber, S. N. Fedorov, C. Bokemeyer, V. A. Stonik, S. Balabanov, F. Honecker, *J. Proteome Res.* **2012**, *11*, 2316 – 2330.

[43] T. H. Pham, A. Hovhannisyan, D. Bouvier, L. Tian, M. Reboud-Ravaux, G. Melikyan, M. Bouvier-Durand, *Bioorg. Med. Chem. Lett.* **2012**, *22*, 3822 – 3827.

[44] N. Gallastegui, P. Beck, M. Arciniega, R. Huber, S. Hillebrand, M. Groll, *Angew. Chem.* **2012**, *124*, 251 – 254; *Angew. Chem. Int. Ed.* **2012**, *51*, 247 – 249.

[45] D. Dunn, M. Iqbal, J. Husten, M. A. Ator, S. Chatterjee, *Bioorg. Med. Chem. Lett.* **2012**, *22*, 3503 – 3505.

[46] R. Z. Orlowski, D. J. Kuhn, *Clin. Cancer Res.* **2008**, *14*, 1649 – 1657.

[47] a) Millennium is owned by Takeda Oncology which is a subsidiary of Takeda Pharmaceutical Company; b) J. Adams, *Oncologist* **2002**, *7*, 9 – 16.

[48] a) D. Chauhan, L. Catley, G. L. Li, K. Podar, T. Hideshima, M. Velankar, C. Mitsiades, N. Mitsiades, H. Yasui, A. Letai, H. Ovaa, C. Berkers, B. Nicholson, T. H. Chao, S. T. C. Neuteboom, P. Richardson, M. A. Palladino, K. C. Anderson, *Cancer Cell* **2005**, *8*, 407 – 419; b) M. Cavo, *Curr. Hematol. Malig Rep.* **2007**, *2*, 128 – 137.

[49] P. G. Richardson, C. Mitsiades, R. Schlossman, I. Ghobrial, T. Hideshima, N. Munshi, K. C. Anderson, *Expert Rev. Anticancer Ther.* **2008**, *8*, 1053 – 1072.

[50] E. B. Golden, P. Y. Lam, A. Kardosh, K. J. Gaffney, E. Cadenas, S. G. Louie, N. A. Petasis, T. C. Chen, A. H. Schönthal, *Blood* **2009**, *113*, 5927 – 5937.

[51] E. Kupperman, E. C. Lee, Y. Y. Cao, B. Bannerman, M. Fitzgerald, A. Berger, J. Yu, Y. Yang, P. Hales, F. Bruzzese, J. Liu, J. Blank, K. Garcia, C. Tsu, L. Dick, P. Fleming, L. Yu, M. Manfredi, M. Rolfe, J. Bolen, *Cancer Res.* **2010**, *70*, 1970 – 1980.

[52] a) M. M. Seavey, L. D. Lu, K. L. Stump, N. H. Wallace, B. A. Ruggeri, *Int. Immunopharmacol.* **2012**, *12*, 257 – 270; b) R. Piva, B. Ruggeri, M. Williams, G. Costa, I. Tamagno, D. Ferrero, V. Giai, M. Coscia, S. Peola, M. Massaia, G. Pezzoni, C. Allievi, N. Pescalli, M. Cassin, S. di Giovine, P. Nicoli, P. de Feudis, I. Strepponi, I. Roato, R. Ferracini, B. Bussolati, G. Camussi, S. Jones-Bolin, K. Hunter, H. Zhao, A. Neri, A. Palumbo, C. Berkers, H. Ovaa, A. Bernareggi, G. Inghirami, *Blood* **2008**, *111*, 2765 – 2775; c) E. Sanchez, M. J. Li, J. A. Steinberg, C. Wang, J. Shen, B. Bonavida, Z. W. Li, H. M. Chen, J. R. Berenson, *Br. J. Haematol.* **2010**, *148*, 569 – 581; d) C. R. Berkers, M. Verdoes, E. Lichtman, E. Fiebiger, B. M. Kessler, K. C. Anderson, H. L. Ploegh, H. Ovaa, P. J. Galardy, *Nat. Methods* **2005**, *2*, 357 – 362.

[53] S. D. Demo, C. J. Kirk, M. A. Aujay, T. J. Buchholz, M. Dajee, M. N. Ho, J. Jiang, G. J. Laidig, E. R. Lewis, F. Parlati, K. D. Shenk, M. S. Smyth, C. M. Sun, M. K. Vallone, T. M. Woo, C. J. Molineaux, M. K. Bennett, *Cancer Res.* **2007**, *67*, 6383 – 6391.

[54] a) D. Chauhan, A. V. Singh, M. Aujay, C. J. Kirk, M. Bandi, B. Ciccarelli, N. Raje, P. Richardson, K. C. Anderson, *Blood* **2010**, *116*, 4906 – 4915; b) M. A. Hurchla, A. Garcia-Gomez, M. C. Hornick, E. M. Ocio, A. Li, J. F. Blanco, L. Collins, C. J. Kirk, D. Piwnica-Worms, R. Vij, M. H. Tomasson, A. Pandiella, J. F. San Miguel, M. Garayoa, K. N. Weilbaecher, *Leukemia* **2012**, *27*, 430 – 440.

[55] For reviews on proteasome inhibitors see: a) A. F. Kisselev, A. L. Goldberg, *Chem. Biol.* **2001**, *8*, 739 – 758; b) J. Myung, K. B. Kim, C. M. Crews, *Med. Res. Rev.* **2001**, *21*, 245 – 273; c) J. Adams, *Proteasome Inhibitors in Cancer Therapy*, Humana Press, New York, **2004**.

[56] H. A. Braun, S. Umbreen, M. Groll, U. Kuckelkorn, I. Mlynarczuk, M. E. Wigand, I. Drung, P. M. Kloetzel, B. Schmidt, *J. Biol. Chem.* **2005**, *280*, 28394 – 28401.

[57] a) J. Hines, M. Groll, M. Fahnestock, C. M. Crews, *Chem. Biol.* **2008**, *15*, 501 – 512; b) G. Lin, D. Y. Li, T. Chidawanyika, C. Nathan, H. L. Li, *Arch. Biochem. Biophys.* **2010**, *501*, 214 – 220; c) H. Shigemori, S. Wakuri, K. Yazawa, T. Nakamura, T. Sasaki, J. Kobayashi, *Tetrahedron* **1991**, *47*, 8529 – 8534.

[58] a) S. Momose, R. Sekizawa, H. Hashizume, N. Kinoshita, Y. Homma, M. Hamada, H. Iinuma, T. Takeuchi, *J. Antibiot.* **2001**, *54*, 997 – 1003; b) I. Momose, R. Sekizawa, H. Iinuma, T. Takeuchi, *Biosci. Biotechnol. Biochem.* **2002**, *66*, 2256 – 2258.

[59] a) I. Momose, Y. Umezawa, S. Hirosawa, H. Iinuma, D. Ikeda, *Bioorg. Med. Chem. Lett.* **2005**, *15*, 1867 – 1871; b) I. Momose, Y. Umezawa, S. Hirosawa, M. Iijima, H. Iinuma, D. Ikeda, *Biosci. Biotechnol. Biochem.* **2005**, *69*, 1733 – 1742.

[60] a) I. Momose, M. Iijima, M. Kawada, D. Ikeda, *Biosci. Biotechnol. Biochem.* **2007**, *71*, 1036 – 1043; b) M. Iijima, I. Momose, D. Ikeda, *Anticancer Res.* **2009**, *29*, 977 – 985.

[61] a) P. Baumann, K. Muller, S. Mandl-Weber, J. Leban, R. Doblhofer, A. Ammendola, R. Baumgartner, F. Oduncu, R. Schmidmaier, *Br. J. Haematol.* **2009**, *144*, 875 – 886; b) P. Baumann, K. Mueller, S. Mandl-Weber, H. Ostermann, R. Schmidmaier, F. Oduncu, J. Leban, R. Doblhofer, A. Ammendola, R. Baumgartner, *Blood* **2007**, *110*, 453A.

[62] M. Groll, L. Ditzel, J. Löwe, D. Stock, M. Bochtler, H. Bartunik, R. Huber, *Nature* **1997**, *386*, 463 – 471.

[63] J. F. Lynas, P. Harriott, A. Healy, M. A. McKervey, B. Walker, *Bioorg. Med. Chem. Lett.* **1998**, *8*, 373 – 378.

[64] For reviews on peptide coupling see: C. A. Montalbetti, V. Falque, *Tetrahedron* **2005**, *61*, 10827 – 10852.

[65] For reviews on peptide aldehydes see: a) A. Moulin, J. Martinez, J. Fehrentz, *J. Pept. Sci.* **2007**, *13*, 1 – 15; b) J. V. Potetinova, E. I. Milgotina, V. A. Makarov, T. L. Voyushina, *Russ. J. Bioorg. Chem.* **2001**, *27*, 141 – 150.

[66] C. Pothion, M. Paris, A. Heitz, L. Rocheblave, F. Rouch, J. A. Fehrentz, J. Martinez, *Tetrahedron Lett.* **1997**, *38*, 7749 – 7752.

[67] J. S. Schneekloth, J. L. Sanders, J. Hines, C. M. Crews, *Bioorg. Med. Chem. Lett.* **2006**, *16*, 3855 – 3858.

[68] M. Verdoes, B. Florea, W. A. van der Linden, D. Renou, A. M. C. van den Nieuwendijk, G. A. van der Marel, H. S. Overkleeft, *Org. Biomol. Chem.* **2007**, *5*, 1416 – 1426.

[69] H. Braun, Dissertation, Universität Darmstadt, **2007**.

[70] K. L. Rock, C. Gramm, L. Rothstein, K. Clark, R. Stein, L. Dick, D. Hwang, A. L. Goldberg, *Cell* **1994**, *78*, 761 – 771.

[71] J. Adams, M. Behnke, S. Chen, A. Cruickshank, L. R. Dick, L. Grenier, J. M. Klunder, Y. Ma, L. Plamondon, R. L. Stei, *Bioorg. Med. Chem. Lett.* **1998**, *8*, 333 – 338.

[72] S. Tsubuki, Y. Saito, M. Tomioka, H. Ito, S. Kawashima, *J. Biochem.* **1996**, *119*, 572 – 576.

[73] M. Groll, C. R. Berkers, H. L. Ploegh, H. Ovaa, *Structure* **2006**, *14*, 451 – 456.

[74] D. S. Matteson, K. M. Sadhu, *J. Am. Chem. Soc.* **1981**, *103*, 5241 – 5241.

[75] D. S. Matteson, D. Majumdar, *J. Am. Chem. Soc.* **1980**, *102*, 7590 – 7591.

[76] a) A. B. Shenvi, C. A. Kettner, U. S. Patent No. 4499082, February 12, **1985**. *Chem. Abstr.* **1985**, *103*, 71709; b) A. B.

 © 2013 Wiley-VCH Verlag GmbH & Co. KGaA, Weinheim 

Shenvi, U. S. Patent No. 4537773, August 27, **1985**. *Chem. Abstr.* **1986**, *104*, 19668.

[77] I. F. Pickersgill, J. Bishop, C. Koellner, J. Gomez, A. Geiser, R. Hett, V. Ammoscato, S. Munk, Y. Lo, F. Chui, V. Kulkarni, PCT Int. Appl., 2005097809, 20 Oct, **2005**.

[78] M. Janca, P. Dobrovolny, PCT Int. Appl., 2009004350, 08 Jan, **2009**.

[79] B. D. Dorsey, M. Iqbal, S. Chatterjee, E. Menta, R. Bernadini, A. Bernareggi, P. G. Cassarà, G. D'Arasmo, E. Ferretti, S. De Munari, A. Oliva, G. Pezzoni, C. Allievi, I. Strepponi, B. Ruggeri, M. A. Ator, M. Williams, J. P. Mallamo, *J. Med. Chem.* **2008**, *51*, 1068 – 1072.

[80] M. A. Beenen, C. An, J. A. Ellman, *J. Am. Chem. Soc.* **2008**, *130*, 6910 – 6911.

[81] F. A. Davis, P. Zhou, B. Chen, *Chem. Soc. Rev.* **1998**, *27*, 13 – 18.

[82] K. B. Kim, J. Myung, N. Sin, C. M. Crews, *Bioorg. Med. Chem. Lett.* **1999**, *9*, 3335 – 3340.

[83] a) Y. Iwabuchi, T. Sugihara, T. Esumi, S. Hatakeyama, *Tetrahedron Lett.* **2001**, *42*, 7867 – 7871; b) M. R. Dobler, *Tetrahedron Lett.* **2001**, *42*, 215 – 218.

[84] A. R. Pereira, A. J. Kale, A. T. Fenley, T. Byrum, H. M. Debonsi, M. K. Gilson, F. A. Valeriote, B. S. Moore, W. H. Gerwick, *ChemBioChem* **2012**, *13*, 810 – 817.

[85] E. M. Huber, M. Basler, R. Schwab, W. Heinemeyer, C. J. Kirk, M. Groettrup, M. Groll, *Cell* **2012**, *148*, 727 – 738.

[86] T. Muchamuel, M. Basler, M. A. Aujay, E. Suzuki, K. W. Kalim, C. Lauer, C. Sylvain, E. R. Ring, J. Shields, J. Jiang, P. Shwonek, F. Parlati, S. D. Demo, M. K. Bennett, C. J. Kirk, M. Groettrup, *Nat. Med.* **2009**, *15*, 781 – U12.

[87] L. H. Meng, R. Mohan, B. H. B. Kwok, M. Elofsson, N. Sin, C. M. Crews, *Proc. Natl. Acad. Sci. USA* **1999**, *96*, 10403 – 10408.

[88] M. Groll, K. B. Kim, N. Kairies, R. Huber, C. M. Crews, *J. Am. Chem. Soc.* **2000**, *122*, 1237 – 1238.

[89] N. Sin, K. B. Kim, M. Elofsson, L. H. Meng, H. Auth, B. H. B. Kwok, C. M. Crews, *Bioorg. Med. Chem. Lett.* **1999**, *9*, 2283 – 2288.

[90] D. H. Wei, B. L. Lei, M. S. Tang, C. G. Zhan, *J. Am. Chem. Soc.* **2012**, *134*, 10436 – 10450.

[91] a) S. Katukojvala, K. N. Barlett, S. D. Lotesta, L. J. Williams, *J. Am. Chem. Soc.* **2004**, *126*, 15348 – 15349; b) Z. Yue, J. R. Cusick, P. Ghosh, S. G. Ning, S. Katukojvala, J. Inghrim, T. J. Emge, L. J. Williams, *J. Org. Chem.* **2009**, *74*, 7707 – 7714.

[92] R. Sekizawa, I. Momose, N. Kinoshita, H. Naganawa, M. Hamada, Y. Muraoka, H. Iinuma, T. Takeuchi, *J. Antibiot.* **2001**, *54*, 874 – 881.

[93] H. D. Arndt, S. Schoof, J. Y. Lu, *Angew. Chem.* **2009**, *121*, 6900 – 6904; *Angew. Chem. Int. Ed.* **2009**, *48*, 6770 – 6773.

[94] M. N. Aminake, S. Schoof, L. Sologub, M. Leubner, M. Kirschner, H. D. Arndt, G. Pradel, *Antimicrob. Agents Chemother.* **2011**, *55*, 1338 – 1348.

[95] S. Schoof, G. Pradel, M. N. Aminake, B. Ellinger, S. Baumann, M. Potowski, Y. Najajreh, M. Kirschner, H. D. Arndt, *Angew. Chem.* **2010**, *122*, 3389 – 3393; *Angew. Chem. Int. Ed.* **2010**, *49*, 3317 – 3321.

[96] a) S. V. Ley, A. Priour, C. Heusser, *Org. Lett.* **2002**, *4*, 711 – 714; b) S. V. Ley, A. Priour, *Eur. J. Org. Chem.* **2002**, 3995 – 4004.

[97] a) L. Bülow, I. Nickeleit, A. K. Girbig, T. Brodmann, A. Rentsch, U. Eggert, F. Sasse, H. Steinmetz, R. Frank, T. Carlomagno, N. P. Malek, M. Kalesse, *ChemMedChem* **2010**, *5*, 832 – 836; b) B. Stauch, B. Simon, T. Basile, G. Schneider, N. P. Malek, M. Kalesse, T. Carlomagno, *Angew. Chem.* **2010**, *122*, 4026 – 4030; *Angew. Chem. Int. Ed.* **2010**, *49*, 3934 – 3938.

[98] V. R. Pattabiraman, J. L. Stymiest, D. J. Derksen, N. I. Martin, J. C. Vederas, *Org. Lett.* **2007**, *9*, 699 – 702.

[99] a) M. Hasegawa, K. Kinoshita, C. Nishimura, U. Matsumura, M. Shionyu, S. Ikeda, T. Mizukami, *Bioorg. Med. Chem. Lett.* **2008**, *18*, 5668 – 5671; b) K. Yoshida, K. Yamaguchi, A. Mizuno, Y. Unno, A. Asai, T. Sone, H. Yokosawa, A. Matsuda, M. Arisawa, S. Shuto, *Org. Biomol. Chem.* **2009**, *7*, 1868 – 1877; c) S. F. Vanier, G. Larouche, R. P. Wurz, A. B. Charette, *Org. Lett.* **2010**, *12*, 672 – 675.

[100] a) V. S. Korotkov, A. Ludwig, O. V. Larionov, A. V. Lygin, M. Groll, A. de Meijere, *Org. Biomol. Chem.* **2011**, *9*, 7791 – 7798; b) A. de Meijere, V. S. Korotkov, A. V. Lygin, O. V. Larionov, V. V. Sokolov, T. Graef, M. Es-Sayed, *Org. Biomol. Chem.* **2012**, *10*, 6363 – 6374.

[101] R. H. Feling, G. O. Buchanan, T. J. Mincer, C. A. Kauffman, P. R. Jensen, W. Fenical, *Angew. Chem.* **2003**, *115*, 369 – 371; *Angew. Chem. Int. Ed.* **2003**, *42*, 355 – 357.

[102] a) D. Chauhan, L. Catley, G. Li, K. Podar, T. Hideshima, C. Mitsiades, H. Ovaa, C. Berkers, N. Munshi, T. Chao, B. Nicholson, S. T. Neuteboom, P. Richardson, M. Palladino, K. C. Anderson, *Cancer Cell* **2005**, *8*, 407 – 419; b) V. R. Macherla, S. S. Mitchell, R. R. Manam, K. A. Reed, T.-H. Chao, B. Nicholson, G. Deyanat-Yazdi, B. Mai, P. R. Jensen, W. Fenical, S. T. C. Neuteboom, K. S. Lam, M. A. Palladino, B. C. M. Potts, *J. Med. Chem.* **2005**, *48*, 3684 – 3687; c) J. C. Cusack Jr., R. Liu, L. Xia, T.-H. Chao, C. Pien, W. Niu, V. J. Palombella, S. T. Neuteboom, M. A. Palldino, *Clin. Cancer Res.* **2006**, *12*, 6758 – 6764; d) S. Ruiz, Y. Krupnik, M. Keating, J. Chandra, M. Palladino, D. McConkey, *Mol. Cancer Ther.* **2006**, *5*, 1836 – 1843; e) K. S. Ahn, G. Sethi, T.-H. Chao, S. T. C. Neuteboom, M. M. Chaturvedi, M. A. Palladino, A. Younes, B. B. Aggarwall, *Blood* **2007**, *110*, 2286 – 2295.

[103] a) E. J. Corey, G. A. Reichard, *J. Am. Chem. Soc.* **1992**, *114*, 10677 – 10678; b) E. J. Corey, G. A. Reichard, R. Kania, *Tetrahedron Lett.* **1993**, *34*, 6977 – 6980; c) G. Fenteany, R. F. Standaert, G. A. Reichard, E. J. Corey, S. L. Schreiber, *Proc. Natl. Acad. Sci. USA* **1994**, *91*, 3358 – 3362; d) E. J. Corey, W.-D. Z. Li, *Chem. Pharm. Bull.* **1999**, *47*, 1 – 10.

[104] a) S. Omura, T. Fujimoto, K. Otogura, K. Matsuzaki, R. Moriguchi, H. Tanaka, Y. Sasaki, *J. Antibiot.* **1991**, *44*, 113 – 116; b) S. Omura, K. Matsuzaki, T. Fujimoto, K. Kosuge, T. Furuya, S. Fujita, A. Nakagawa, *J. Antibiot.* **1991**, *44*, 117 – 118.

[105] M. Groll, R. Hubert, B. C. M. Potts, *J. Am. Chem. Soc.* **2006**, *128*, 5136 – 5141.

[106] R. R. Manam, K. A. McArthur, T.-H. Chao, J. Weiss, J. A. Ali, V. J. Palombella, M. Groll, G. K. Lloyd, M. A. Palladino, S. T. C. Neuteboom, V. R. Macherla, B. C. M. Potts, *J. Med. Chem.* **2008**, *51*, 6711 – 6724.

[107] M. Groll, E. P. Balskus, E. N. Jacobsen, *J. Am. Chem. Soc.* **2008**, *130*, 14981 – 14983.

[108] a) P. G. Williams, G. O. Buchanan, R. H. Feling, C. A. Kauffman, P. R. Jensen, W. Fenical, *J. Org. Chem.* **2005**, *70*, 6196 – 6203; b) K. A. Reed, R. R. Manam, S. S. Mitchell, J. Xu, S. Teisan, T.-H. Chao, G. Deyanat-Yazdi, S. T. C. Neuteboom, K. S. Lam, B. C. M. Potts, *J. Nat. Prod.* **2007**, *70*, 269 – 276; c) A. S. Eustáquio, B. S. Moore, *Angew. Chem.* **2008**, *120*, 4000 – 4002; *Angew. Chem. Int. Ed.* **2008**, *47*, 3936 – 3938.

[109] L. R. Reddy, P. Saravanan, E. J. Corey, *J. Am. Chem. Soc.* **2004**, *126*, 6230 – 6231.

[110] a) S. A. Frank, D. J. Mergott, W. R. Roush, *J. Am. Chem. Soc.* **2002**, *124*, 2404 – 2405; b) D. J. Mergott, S. A. Frank, W. R. Roush, *Org. Lett.* **2002**, *4*, 3157 – 3160; c) V. K. Aggarwal, I. Emme, S. Y. Fulford, *J. Org. Chem.* **2003**, *68*, 692 – 700; d) J. E. Yeo, X. Yang, H. J. Kim, S. Koo, *J. Chem. Soc. Chem. Commun.* **2004**, 236 – 237.

[111] a) I. Fleming, *Chemtracts: Org. Chem.* **1996**, *9*, 1 – 64; b) G. R. Jones, Y. Landais, *Tetrahedron* **1996**, *52*, 7599 – 7662.

[112] Reviews: a) O. G. Kulinkovich, *Chem. Rev.* **2003**, *103*, 2597 – 2632; b) F. Sato, S. Okamoto, *Adv. Synth. Catal.* **2001**, *343*, 759 – 784.


© 2013 Wiley-VCH Verlag GmbH & Co. KGaA, Weinheim

[113] a) L. R. Reddy, J.-F. Fournier, B. V. S. Reddy, E. J. Corey, *J. Am. Chem. Soc.* **2005**, *127*, 8974 – 8976; b) L. R. Reddy, J.-F. Fournier, B. V. S. Reddy, E. J. Corey, *Org. Lett.* **2005**, *7*, 2699 – 2701.
[114] B. V. S. Reddy, L. R. Reddy, E. J. Corey, *Tetrahedron Lett.* **2005**, *46*, 4589.
[115] A. Endo, S. J. Danishefsky, *J. Am. Chem. Soc.* **2005**, *127*, 8298 – 8299.
[116] T. Ling, V. R. Macherla, R. R. Manam, K. A. McArthur, B. C. M. Potts, *Org. Lett.* **2007**, *9*, 2289 – 2292.
[117] a) E. C. Minnihan, S. L. Colleti, F. D. Toste, H. C. Shen, *J. Org. Chem.* **2007**, *72*, 6287 – 6289; b) C.-Y. Zhou, C.-M. Che, *J. Am. Chem. Soc.* **2007**, *129*, 5828 – 5829.
[118] K. Takahashi, M. Midori, K. Kawano, J. Ishihara, S. Hatakeyama, *Angew. Chem.* **2008**, *120*, 6340 – 6342; *Angew. Chem. Int. Ed.* **2008**, *47*, 6244 – 6246.
[119] T. Fukuda, K. Sugiyama, S. Arima, Y. Harigaya, T. Nagamitsu, S. Omura, *Org. Lett.* **2008**, *10*, 4239 – 4242.
[120] H. Ooi, N. Ishibashi, Y. Iwabuchi, J. Ishihara, S. Hatakeyama, *J. Org. Chem.* **2004**, *69*, 7765 – 7768.
[121] a) P. Garner, J. M. Park, *J. Org. Chem.* **1987**, *52*, 2361 – 2364; b) A. McKillop, R. J. K. Taylor, R. J. Watson, N. Lewis, *Synthesis* **1994**, 31 – 33.
[122] Y. Sato, H. Fukuda, M. Tomizawa, T. Masaki, M. Shibuya, N. Kanoh, Y. Iwabuchi, *Heterocycles* **2010**, *81*, 2239 – 2246.
[123] N. Satoh, S. Yokoshima, T. Fukuyama, *Org. Lett.* **2011**, *13*, 3028 – 3031.
[124] N. P. Mulholland, G. Pattenden, I. A. S. Walters, *Org. Biomol. Chem.* **2006**, *4*, 2845 – 2846.
[125] M. Lee, D. H. Kim, *Bioorg. Med. Chem.* **2002**, *10*, 913 – 922.
[126] G. Ma, H. Nguyen, D. Romo, *Org. Lett.* **2007**, *9*, 2143 – 2146.
[127] a) V. Caubert, N. Langlois, *Tetrahedron Lett.* **2006**, *47*, 4473 – 4475; b) V. Caubert, J. Massé, P. Retailleau, N. Langlois, *Tetrahedron Lett.* **2007**, *48*, 381 – 384.
[128] I. V. Margalef, L. Rupnicki, H. W. Lam, *Tetrahedron* **2008**, *64*, 7896 – 7901.
[129] R. A. Mosey, J. J. Tepe, *Tetrahedron Lett.* **2009**, *50*, 295 – 297.
[130] B. Li, M. Berliner, R. Buzon, C. K.-F. Chiu, S. T. Colgan, T. Kaneko, N. Keene, W. Kissel, T. Le, K. R. Leeman, B. Marquez, R. Morris, L. Newell, S. Wunderwald, M, Witt, J. Weaver, Z. Zhang, Z. Zhang, *J. Org. Chem.* **2006**, *71*, 9045 – 9050.
[131] J. R. Struble, J. W. Bode, *Tetrahedron* **2009**, *65*, 4957 – 4967.
[132] Y. Kaiya, J. Hasegawa, T. Momose, T. Sato, N. Chida, *Chem. Asian J.* **2011**, *6*, 209 – 219.
[133] a) A. Rosenthal, L. B. Nguyen, *J. Org. Chem.* **1969**, *34*, 1029 – 1034; b) G. W. J. Fleet, K. James, R. J. Lunn, C. J. Mathews, *Tetrahedron Lett.* **1986**, *27*, 3057 – 3058.
[134] T. Ling, B. C. Potts, V. R. Macherla, *J. Org. Chem.* **2010**, *75*, 3882 – 3885.
[135] H. Kamisaki, Y. Kobayashi, T. Kimachi, Y. Yasui, Y. Takemoto, *J. Organomet. Chem.* **2011**, *696*, 42 – 45.
[136] a) J. Deska, S. Hähn, U. Kazmaier, *Org. Lett.* **2011**, *13*, 3210 – 3213; b) P. Barbie, L. Huo, R. Müller, U. Kazmaier, *Org. Lett.* **2012**, *14*, 6064 – 6067.
[137] L. L. Beer, B. S. Moore, *Org. Lett.* **2007**, *9*, 845 – 848.
[138] J. Barbion, G. Sorin, M. Selkti, E. Kellenberger, R. Baati, S. Santoro, F. Himo, A. Pancrazi, M.-I. Lannou, J. Ardisson, *Tetrahedron* **2012**, *68*, 6504 – 6512.
[139] a) M. Bogyo, J. S. McMaster, M. Gaczynska, D. Tortorella, A. L. Goldberg, H. Ploegh, *Proc. Natl. Acad. Sci. USA* **1997**, *94*, 6629; b) T. Nazif, M. Bogyo, *Proc. Natl. Acad. Sci. USA* **2001**, *98*, 2967 – 2972.
[140] H. S. Overkleeft, P. R. Bos, B. G. Hekking, E. J. Gordon, H. L. Ploegh, B. M. Kessler, *Tetrahedron Lett.* **2000**, *41*, 6005 – 6009.
[141] a) B. I. Florea, M. Verdoes, N. Li, W. A. van der Linden, P. P. Geurink, H. van den Elst, T. Hofmann, A. de Ru, P. A. van Veelen, K. Tanaka, K. Sasaki, S. Murata, H. den Dulk, J. Brouwer, F. A. Ossendorp, A. F. Kisselev, H. S. Overkleeft, *Chem. Biol.* **2010**, *17*, 795 – 801; b) A. C. Mirabella, A. A. Pletnev, S. L. Downey, B. I. Florea, T. B. Shabaneh, M. Britton, M. Verdoes, D. V. Filippov, H. S. Overkleeft, A. F. Kisselev, *Chem. Biol.* **2011**, *18*, 608 – 618; c) M. Britton, M. M. Lucas, S. L. Downey, M. Screen, A. A. Pletnev, M. Verdoes, R. A. Tokhunts, O. Amir, A. L. Goddard, P. M. Pelphrey, D. L. Wright, H. S. Overkleeft, A. F. Kisselev, *Chem. Biol.* **2009**, *16*, 1278 – 1289; d) M. Verdoes, B. I. Florea, V. Menendez-Benito, C. J. Maynard, M. D. Witte, W. A. van der Linden, A. van den Nieuwendijk, T. Hofmann, C. R. Berkers, F. W. B. van Leeuwen, T. A. Groothuis, M. A. Leeuwenburgh, H. Ovaa, J. J. Neefjes, D. V. Filippov, G. A. van der Marel, N. P. Dantuma, H. S. Overkleeft, *Chem. Biol.* **2006**, *13*, 1217 – 1226; e) B. M. Kessler, D. Tortorella, M. Altun, A. F. Kisselev, E. Fiebiger, B. G. Hekking, H. L. Ploegh, H. S. Overkleeft, *Chem. Biol.* **2001**, *8*, 913 – 929.
[142] a) D. Krahn, C. Ottmann, M. Kaiser, *Nat. Prod. Rep.* **2011**, *28*, 1854 – 1867; b) A. S. Bachmann, M. Pirrung, R. Dudler, C. Archer, J. Opoku-Ansah, *Pharm. Biol.* **2012**, *50*, 651 – 651.
[143] M. Groll, B. Schellenberg, A. S. Bachmann, C. R. Archer, R. Huber, T. K. Powell, S. Lindow, M. Kaiser, R. Dudler, *Nature* **2008**, *452*, 755 – 757.
[144] a) U. Wäspi, D. Blanc, T. Winkler, P. Rüedi, R. Dudler, *Mol. Plant-Microbe Interact.* **1998**, *11*, 727 – 733; b) U. Waspi, P. Hassa, A. A. Staempfli, L. P. Molleyres, T. Winkler, R. Dudler, *Microbiol. Res.* **1999**, *154*, 89 – 93.
[145] a) T. Ohnuma, R. Obata, T. Yamasaki, H. Kamei, T. Naito, *J. Pharm. Sci.* **1987**, *76*, S167; b) M. Oka, Y. Nishiyama, S. Ohta, H. Kamei, M. Konishi, T. Miyaki, T. Oki, H. Kawaguchi, *J. Antibiot.* **1988**, *41*, 1331 – 1337; c) M. Oka, H. Ohkuma, H. Kamei, M. Konishi, T. Oki, H. Kawaguchi, *J. Antibiot.* **1988**, *41*, 1906 – 1909; d) M. Oka, K. Yaginuma, K. Numata, M. Konishi, T. Oki, H. Kawaguchi, *J. Antibiot.* **1988**, *41*, 1338 – 1350.
[146] a) J. Shoji, H. Hinoo, T. Kato, T. Hattori, K. Hirooka, K. Tawara, O. Shiratori, Y. Terui, *J. Antibiot.* **1990**, *43*, 783 – 787; b) Y. Terui, J. Nishikawa, H. Hinoo, T. Kato, J. Shoji, *J. Antibiot.* **1990**, *43*, 788 – 795.
[147] J. Clerc, M. Groll, D. J. Illich, A. S. Bachmann, R. Huber, B. Schellenberg, R. Dudler, M. Kaiser, *Proc. Natl. Acad. Sci. USA* **2009**, *106*, 6507 – 6512.
[148] a) K. Numata, M. Oka, Y. Nakakita, T. Murakami, T. Miyaki, M. Konishi, T. Oki, H. Kawaguchi, *J. Antibiot.* **1988**, *41*, 1351 – 1357; b) M. Oka, Y. Nishiyama, S. Ohta, H. Kamei, M. Konishi, T. Miyaki, T. Oki, H. Kawaguchi, *J. Antibiot.* **1988**, *41*, 1331 – 1337; c) M. Oka, K. Numata, Y. Nishiyama, H. Kamei, M. Konishi, T. Oki, H. Kawaguchi, *J. Antibiot.* **1988**, *41*, 1812 – 1822; d) M. Oka, H. Ohkuma, H. Kamei, M. Konishi, T. Oki, H. Kawaguchi, *J. Antibiot.* **1988**, *41*, 1906 – 1909; e) M. Oka, K. Yaginuma, K. Numata, M. Konishi, T. Oki, H. Kawaguchi, *J. Antibiot.* **1988**, *41*, 1338 – 1350.
[149] U. Schmidt, A. Kleefeldt, R. Mangold, *J. Chem. Soc. Chem. Commun.* **1992**, 1687 – 1689.
[150] C. H. Dai, C. R. J. Stephenson, *Org. Lett.* **2010**, *12*, 3453 – 3455.
[151] J. Clerc, B. Schellenberg, M. Groll, A. S. Bachmann, R. Huber, R. Dudler, M. Kaiser, *Eur. J. Org. Chem.* **2010**, 3991 – 4003.
[152] M. C. Pirrung, G. Biswas, T. R. Ibarra-Rivera, *Org. Lett.* **2010**, *12*, 2402 – 2405.
[153] T. R. Ibarra-Rivera, J. Opoku-Ansah, S. Ambadi, A. S. Bachmann, M. C. Pirrung, *Tetrahedron* **2011**, *67*, 9950 – 9956.
[154] J. Clerc, N. Li, D. Krahn, M. Groll, A. S. Bachmann, B. I. Florea, H. S. Overkleeft, M. Kaiser, *Chem. Commun.* **2011**, *47*, 385 – 387.
[155] J. Opoku-Ansah, T. R. Ibarra-Rivera, M. C. Pirrung, A. S. Bachmann, *Pharm. Biol.* **2012**, *50*, 25 – 29.
[156] W. A. van der Linden, L. I. Willems, T. B. Shabaneh, N. Li, M. Ruben, B. I. Florea, G. A. van der Marel, M. Kaiser, A. F.

 © 2013 Wiley-VCH Verlag GmbH & Co. KGaA, Weinheim 

Kisselev, H. S. Overkleeft, *Org. Biomol. Chem.* **2012**, *10*, 181 – 194.

[157] a) Y. Koguchi, J. Kohno, M. Nishio, K. Takahashi, T. Okuda, T. Ohnuki, S. Komatsubara, *J. Antibiot.* **2000**, *53*, 105 – 109; b) J. Kohno, Y. Koguchi, M. Nishio, K. Nakao, M. Kuroda, R. Shimizu, T. Ohnuki, S. Komatsubara, *J. Org. Chem.* **2000**, *65*, 990 – 995.

[158] M. Kaiser, A. G. Milbradt, C. Siciliano, I. Assfalg-Machleidt, W. Machleidt, M. Groll, C. Renner, L. Moroder, *Chem. Biodiversity* **2004**, *1*, 161 – 173.

[159] M. Groll, Y. Koguchi, R. Huber, J. Kohno, *J. Mol. Biol.* **2001**, *311*, 543 – 548.

[160] S. Lin, S. J. Danishefsky, *Angew. Chem.* **2002**, *114*, 530 – 533; *Angew. Chem. Int. Ed.* **2002**, *41*, 512 – 515.

[161] S. Lin, S. J. Danishefsky, *Angew. Chem.* **2001**, *113*, 2021 – 2024; *Angew. Chem. Int. Ed.* **2001**, *40*, 1967 – 1970.

[162] Review on Suzuki coupling: N. Miyaura, A. Suzuki, *Chem. Rev.* **1995**, *95*, 2457 – 2483.

[163] M. Inoue, H. Sakazaki, H. Furuyama, M. Hirama, *Angew. Chem.* **2003**, *115*, 2758 – 2761; *Angew. Chem. Int. Ed.* **2003**, *42*, 2654 – 2657.

[164] M. Inoue, H. Furuyama, H. Sakazaki, M. Hirama, *Org. Lett.* **2001**, *3*, 2863 – 2865.

[165] a) P. G. Gassman, W. N. Schenk, *J. Org. Chem.* **1977**, *42*, 918 – 920; b) P. G. Gassman, P. K. G. Hodgson, R. J. Balchunis, *J. Am. Chem. Soc.* **1976**, *98*, 1275 – 1276.

[166] B. K. Albrecht, R. M. Williams, *Org. Lett.* **2003**, *5*, 197 – 200.

[167] B. K. Albrecht, R. M. Williams, *Proc. Natl. Acad. Sci. USA* **2004**, *101*, 11949 – 11954.

[168] P. Liu, E. N. Jacobsen, *J. Am. Chem. Soc.* **2001**, *123*, 10772 – 10773.

[169] T. Ishiyama, M. Murata, N. Miyaura, *J. Org. Chem.* **1995**, *60*, 7508 – 7510.

[170] a) M. Kaiser, M. Groll, C. Renner, R. Huber, L. Moroder, *Angew. Chem.* **2002**, *114*, 817 – 820; *Angew. Chem. Int. Ed.* **2002**, *41*, 780 – 783; b) M. Kaiser, M. Groll, C. Siciliano, I. Assfalg-Machleidt, E. Weyher, J. Kohno, A. G. Milbradt, C. Renner, R. Huber, L. Moroder, *ChemBioChem* **2004**, *5*, 1256 – 1266.

[171] M. Groll, M. Götz, M. Kaiser, E. Weyher, L. Moroder, *Chem. Biol.* **2006**, *13*, 607 – 614.

[172] Z.-Q. Yang, B. H. B. Kwok, S. Lin, M. A. Koldobskiy, C. M. Crews, S. J. Danishefsky, *ChemBioChem* **2003**, *4*, 508 – 513.

[173] S. Lin, Z.-Q. Yang, B. H. B. Kwok, M. Koldobskiy, C. M. Crews, S. J. Danishefsky, *J. Am. Chem. Soc.* **2004**, *126*, 6347 – 6355.

[174] A. Berthelot, S. Piguel, G. Le Dour, J. Vidal, *J. Org. Chem.* **2003**, *68*, 9835 – 9838.

[175] N. Basse, S. Piguel, D. Papapostolou, A. Ferrier-Berthelot, N. Richy, M. Pagano, P. Sarthou, J. Sobczak-Thépot, M. Reboud-Ravaux, J. Vidal, *J. Med. Chem.* **2007**, *50*, 2842 – 2850.


© 2013 Wiley-VCH Verlag GmbH & Co. KGaA, Weinheim